Dissertation zur Erlangung des Doktorgrades der Fakultät für Chemie und Pharmazie der Ludwigs-Maximilians-Universität München

Ctk1 function is crucial for efficient translation initiation and interacts with the mRNP processing factor Npl3

Britta Coordes
aus
Bremen

2011

Erklärung

Diese Dissertation wurde im Sinne von § 13 Abs. 3 bzw. 4 der Promotionsordnung vom 29. Januar 1998 (in der Fassung der sechsten Änderungssatzung vom 16. August 2010) von Herrn Prof. Dr. Roland Beckmann betreut.

Ehrenwörtliche Versicherung

Diese Dissertation wurde selbständig, ohne unerlaubte Hilfe erarbeitet.

München, den 30.04.11

Britta Coordes

Dissertation eingereicht am 03.05.11

1. Gutachter: Prof. Dr. Roland Beckmann
2. Gutachter: Prof. Dr. Klaus Förstemann

Mündliche Prüfung am 27.06.11

Parts of the present thesis are submitted for publication:

Coordes B., Brünger K.M., Burger K., Soufi B., Horenk J., Eick D., Olsen J.V., Sträßer K.: "Ctk1 function is crucial for efficient translation initiation", under revision.

As a collaboration with the laboratory of Prof. Karl-Peter Hopfner, the following manuscript will be submitted for publication:

Schiller C., Lammens K., Guerini I., **Coordes B**., Schlauderer F., Möckel C., Schele A., Sträßer K., Jackson S. P., Hopfner K.-P.:
"Insights into DNA double-strand break repair and ataxia-telangiectasia like disease from the structure of an Mre11-Nbs1 complex", manuscript in preparation.

TABLE OF CONTENTS

SUMMARY

The expression of genes into proteins encompasses the transcription of the DNA into mRNA by RNA Polymerase II (PolII), mRNA processing within the nucleus, mRNA export to the cytoplasm and the translation of the mRNA into the encoded proteins by the ribosomes. In recent studies, it became increasingly clear that these steps are intertwined and rely on a subset of proteins that often function not only in one, but in a variety of these processes.

One of these proteins is Ctk1, a kinase which phosphorylates PolII on the C-terminal domain of its largest subunit Rpb1 during transcription elongation. This is important for the transcription rate as well as for proper recruitment of mRNA processing factors. Furthermore, Ctk1 is involved in translation by phosphorylating Rps2, a component of the small ribosomal subunit, thereby increasing the decoding fidelity during translation elongation.

In this study, an additional function of Ctk1 in translation initiation was identified. Translation active extracts of Ctk1 depleted cells showed a dramatic reduction in translation activity of a capped luciferase mRNA, but not of an Internal Ribosome Entry Site (IRES) containing reporter mRNA when compared to wild-type extracts. Since translation of this IRES containing reporter follows a distinct mode of initiation independent of any initiation factors, a translation initiation defect was suggested for Ctk1 depleted cells. Consistently, Ctk1 depleted cells showed a decreased formation of 80S initiation complexes *in vitro* as shown by incorporation of radiolabeled mRNA into translation initiation complexes. Toeprint experiments revealed that Ctk1 is needed for efficient joining of the ribosomal subunits at the start codon. Importantly, the kinase activity of Ctk1 was essential for its function in translation initiation. In an attempt to identify a substrate, which needs to be phosphorylated by Ctk1 for efficient translation initiation, a proteomic SILAC (Stable Isotope Labeling by Amino acids in Cell culture) approach with ribosomes and ribosome associated factors was applied. This experiment showed that in the absence of Ctk1, the phosphorylation of various proteins involved in ribosome biogenesis or translation itself is decreased. However, no direct substrate of Ctk1 could be identified.

In addition, the interaction of Ctk1 with Npl3 - a nucleo-cytoplasmic shuttling serine arginine rich (SR) protein, which functions in mRNA processing and mRNA export, was analyzed. Mutants of both either Ctk1 or Npl3 have similar defects in gene expression and thus it was investigated whether they interact. It was shown that Ctk1 and Npl3 interact genetically and that Ctk1 phosphorylates Npl3 on three residues *in vitro*. However, an influence of this interaction on translation could not be determined.

1. INTRODUCTION

1.1. The mechanism of cap dependent translation initiation

Eukaryotic translation initiation is a very intricate and highly dynamic process leading to the formation of an elongation competent 80S ribosomal complex located at the start codon of the mRNA. Translation initiation starts with the association of the methionyl initiator tRNA (Met-$tRNA_i$) to the GTP-bound eukaryotic initiation factor (eIF) 2 to form a ternary complex (TC). In yeast, this TC is thought to bind the initiation factors eIF1, eIF3 and eIF5 thus forming the multifactor complex (MFC) (Asano et al., 2000). The MFC then associates with the 40S ribosomal subunit and eIF1A resulting in the formation of the 43S initiation complex. The mRNA enters the process of translation initiation by binding to the eIF4F complex and the poly(A) binding protein (Pab1). eIF4F itself is comprised of the cap-binding protein eIF4E, the RNA helicase eIF4A, its auxiliary protein eIF4B, and the scaffold protein eIF4G, which connects all eIF4F complex members as well as eIF3 and Pab1. The eIF4F complex associates with the mRNA at its 5' 7-methylguanosine (m^7GpppG) cap and enables the formation of an mRNA loop due to the binding of Pab1, which is associated with the poly(A) tail of the mRNA. In a process facilitated by eIF5, eIF4F, and Pab1, the 43S complex assembles at the eIF4F bound mRNA at its 5' end, generating the 48S initiation complex. Next, as part of the 48 initiation complex, the 40S subunit with its associated initiation factors is thought to scan along the mRNA with the help of the RNA helicase activity of eIF4A and its auxiliary factor eIF4B. The latter two factors unwind secondary structures in the 5' untranslated region (UTR). When the small subunit reaches the start codon, correct base pairing of the Met-$tRNA_i$ with the AUG located at the ribosomal P-site triggers eIF1 release and eIF5 promoted hydrolysis of eIF2-bound GTP. This leads to the dissociation of eIF2•GDP and P_i, eIF3, and eIF4F. The initiation factor eIF5B is also a GTPase and functions directly in 60S subunit joining. The hydrolysis of eIF5B-bound GTP at the start codon mediates the displacement of the remaining initiation factors, eIF5B itself as well as eIF1A. Joining of the 60S subunit then generates elongation competent 80S complexes. Subsequently, eIF2B mediates the GDP-exchange on eIF2 necessary for its recycling for the next round of initiation (reviewed in Lorsch & Dever, 2010; Sonenberg & Hinnebusch 2009; Jackson et al., 2010). The process of translation initiation is illustrated in FIGURE 1.

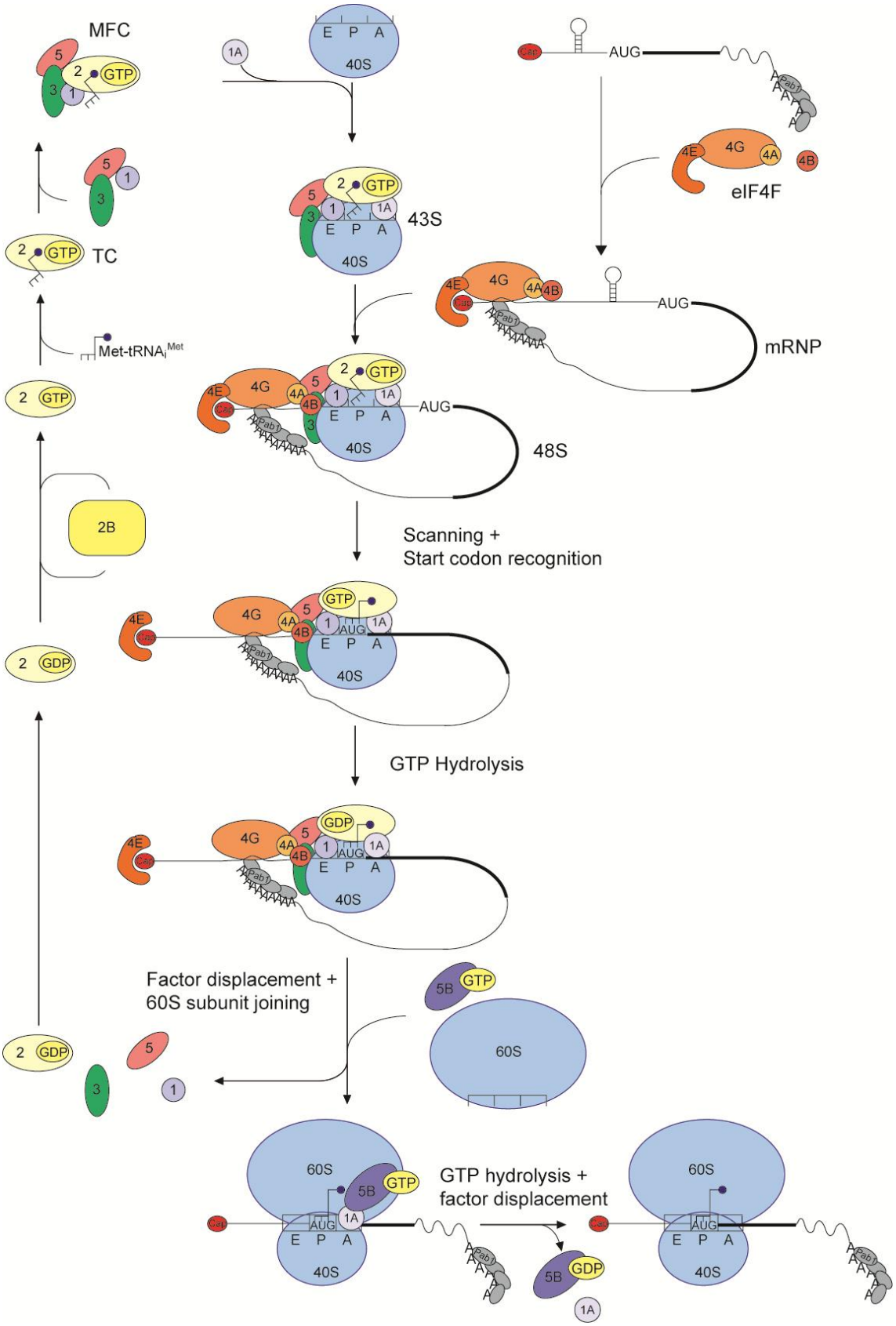

FIGURE 1: The mechanism of cap-dependent translation initiation (adapted from Preiss & Hentze 2003 and Jackson et al., 2010). Initiation comprises the recognition and recruitment of the mRNA and the tRNA to the 40S subunit, the process of 5'UTR scanning and 60S subunit joining and results in the formation of an elongation competent 80S ribosome at the start codon. For details see text. Initiation factors are labeled omitting eIF (eIF1A – 1A); TC – ternary complex; MFC: multi factor complex.

1.2. Translational control under stress conditions

Translation needs to be tightly controlled for cells to react rapidly and reversibly to environmental and intracellular changes. Upon stress, overall translation is shut down while the translation of only specific mRNAs, which are important for cell survival, continues or is even increased. This translational control mostly happens at the step of initiation. Upon amino acid starvation (reviewed in Hinnebusch, 2005) and some other stress conditions, *e.g.* peroxide stress (Mascarenhas et al., 2008; reviewed in Altmann & Linder, 2010), exposure to rapamycin and volatile anesthetics (Palmer et al., 2005; reviewed in Hinnebusch, 2005), the initiation factor eIF2α is phosphorylated at S51 by the kinase Gcn2 (general control non-derepressable 2). Gcn2 is the only eIF2α kinase in yeast (reviewed in Hinnebusch, 2005) and is activated upon binding of uncharged tRNAs, which accumulate in cells starved for amino acids. It is thought that also the other stress factors at least partly activate Gcn2 by affecting the pool of uncharged amino acids (Palmer et al., 2005, Yang et al., 2000). Phosphorylated eIF2α inhibits the recycling of eIF2-GDP to eIF2-GTP by guanine nucleotide exchange factor (GEF) eIF2B, which is necessary for a new round of initiation (FIGURE 1). Since eIF2-GDP cannot form the TC, TC levels are reduced and translation initiation of most mRNAs is repressed. The translation of the *GCN4* open reading frame (ORF), however, is increased upon stress. Gcn4 is a transcription factor stimulating the transcription of a variety of amino acid biosynthetic and other genes, which are important for growth in stress conditions. *GCN4* mRNA contains four upstream ORFs (uORFs), which repress *GCN4* translation under normal growth conditions. When TC levels are low, however, only uORF1 is translated, reinitiation occurs, but the 40S subunits increasingly scans past the other uORFs until the *GCN4* ORF. Hence *GCN4* translation is de-repressed (reviewed in Hinnebusch 2005).

Another well studied mechanism of translational control, which is important for regulating a specific subset of mRNAs (Cridge et al., 2010), and is induced upon stress (Deloche et al., 2004; Meier et al., 2006) involves the 4E-binding proteins (4EBPs). eIF4G and 4EBPs share a motif that is essential for the interaction with eIF4E. Therefore, 4EBP bound mRNAs exclude eIF4G and are translationally silenced (reviewed in Jackson et al., 2010 and in Richter & Sonenberg 2005). Only hypophosphorylated 4EBPs bind to eIF4E, thus their phosphorylation activates translation. (reviewed in Raught & Gingras, 2007 and Altmann & Linder 2010). This mode of translational control has been characterized mostly in mammals, but also in yeast there have been identified two 4EBPs: Caf20 and Eap1 (Altmann et al., 1997; Cosentino et al., 2000). Whereas Eap1 has been shown to be involved in translational attenuation of bulk

mRNA, the regulation via Caf20 has not yet been established (reviewed in Altmann & Linder, 2010). In yeast, the cleavage of eIF4G is also a mechanism to reduce translation initiation in certain unfavorable growth conditions (Berset et al., 1998; reviewed in Altmann & Linder, 2010).

All mechanisms presented, eIF2α phosphorylation, eIF4E inactivation by 4EBPs and eIF4G cleavage, lead to a decrease in translation initiation reducing the overall translation rate (reviewed in Hinnebusch et al., 2007 and in Raught & Gingras, 2007).

1.3. Translation initiation by Internal Ribosome Entry Sites

In eukaryotes, most mRNAs are translated following canonical cap-dependent translation initiation. Among viruses, however, a cap-independent mechanism of translation initiation is commonly used. This is achieved through initiation mediated by Internal Ribosome Entry Sites (IRESes), which are located upstram of the ORF to be translated. IRESes are defined as RNA elements which are highly structured and enable cap-independent translation. This non-canonical mechanism of translation initiation promotes translation of viral proteins even when translation initiation is shut down in the host cell due to the infection. There exist four different classes of IRESes, which are defined by the virus they are derived from, their distinct structure as well as their mode of ribosome recruitment (reviewed in Hellen, 2009 and in Doudna & Sarnow, 2007).

Initiation by type 1 and type 2 IRESes are similar. Type 1 IRESes are represented by the IRES of the poliovirus (Pelletier & Sonenberg, 1988). The prototype of type 2 IRESes is the encephalomyocarditis virus (EMCV) IRES (Jang et al., 1988). Both viruses belong to the family of picornaviruses. Initiation via these two types of IRESes requires the same group of eIFs as the canonical initiation mechanism, except for the cap binding protein eIF4E and the part of eIF4G that interacts with eIF4E. During IRES translation, eIF4G specifically binds to a domain of the IRES located next to the initiation codon, recruits eIF4A and promotes binding of the 43S initiation complex to the IRES (Pestova et al., 1996 a+b; deBreyne et al., 2009; reviewed in Hellen, 2009; FIGURE 2).

Type 3 IRESes are represented by the Hepatitis C virus (HCV) and type 4 IRESes by the Cricket paralysis virus (CrPV). Both types have their distinct sequences and structures and initiation occurs by different mechanisms, but in both cases a direct and translation factor independent recruitment of 40S is involved (FIGURE 2). For translation of type 3 IRESes, at least the Met-tRNA$_i$, eIF2, eIF3, eIF5, and eIF5B are required (Pestova et al., 1998; reviewed

in Fraser & Doudna, 2007, Kieft, 2008 and Hellen, 2009). The type 4 IRESes consist of the intergenic regions of the genomes of dicistroviruses, which are located between two large ORFs (Wilson et al., 2000; Jang et al., 2009; reviewed in Kieft, 2009). These IRESes do not require any initiation factors to assemble elongation-compentent 80S ribosomes at the start codon and thus use the simplest mechanism of initiation among the IRESes (Jan & Sarnow, 2002; Pestova & Hellen, 2003). They do so by binding directly either to 40S subunits (which can then join 60S subunits independently of eIF5B) or to 80S ribosomes. Initiation occurs with the IRES mimicking the base pairing interaction of the initiation codon and the anticodon of the Met-tRNA$_i$ at the ribosomal P-site of the 40S subunit. (Wilson et al., 2000; Pestova & Hellen, 2003; Jan et al., 2003; reviewed in Hellen, 2009). The CrPV IRES is one of very few viral IRESes that is translated in yeast (Thompson et al., 2001).

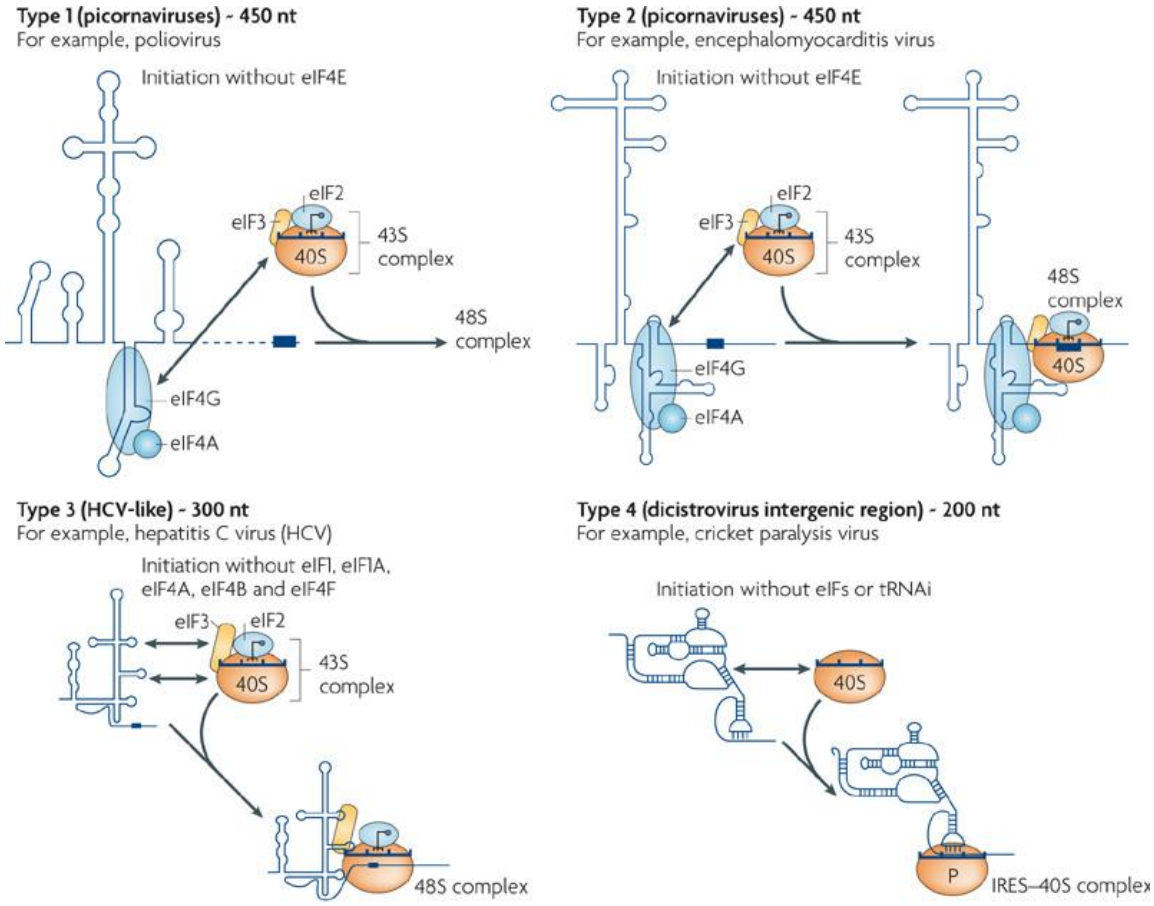

FIGURE 2: Structure of the four different types of viral IRESes and their mode of ribosome recruitment (Jackson et al., 2010). Type 1 and type 2 IRESes interact with eIF4G, which is enhanced by eIF1A. The IRES of the HCV virus (type 3 IRES) interacts with eIF3 and the 40S subunit during intitation and the type 4 IRESes do not need any translation initiation factor for their translation and directly bind to 40S or 80S ribosomes.

IRESes have been mainly studied in viruses, but they are also found in cellular mRNAs of eukaryotes including yeast (Gilbert et al., 2007, Wilker et al., 2007, Marr et al., 2007; reviewed in Komar & Hatzoglou 2005). It is still a matter of discussion how these IRESes are defined and to what extend they exist in the genome. Their structures as well as their mode of 80S recruitment remain largely unknown. It is assumed that – as in the case of the viral IRESes – their translation is favored when general translation is shut down, *e.g.* in stress conditions (Gilbert et al., 2007, reviewed in Gilbert, 2010).

1.4. The transcription cycle

Eukaryotic RNA Polymerase II (PolII) is a multisubunit enzyme that catalyzes the transcription of mRNA and most snRNAs. The C-terminal domain (CTD) of its largest subunit Rpb1 can be differentially phosphorylated and couples transcription to mRNA processing. Although the three eukaryotic polymerases (RNA Polymerase I, II, III) are similar in structure and subunit configuration, this CTD is unique to PolII. It mainly serves as a binding platform for proteins involved in transcription, histone modification and mRNA processing. The CTD consists of multiple repeats of the consensus heptapeptide $Y_1S_2P_3T_4S_5P_6S_7$ that are differentially phosphorylated on serine 2 (S2), serine 5 (S5), and – as discovered recently – on serine 7 (S7) (Chapman et al., 2007; Egloff et al., 2007; reviewed in Buratowski 2009 and in Phatnani & Greenleaf 2006). Different phosphorylation patterns are predominant at distinct stages of the transcription cycle, and transcription factors as well as messenger ribonucleoprotein (mRNP) processing factors bind to a specifically phosphorylated form of the CTD. Due to these dynamic interactions, the stages of transcription are coordinated with other events necessary for correct gene expression (FIGURE 3, reviewed in Buratowski 2009 and Phatnani & Greenleaf 2006).

During transcription initiation, hypophosphorylated PolII, general transcription factors (TF) and the mediator complex, which transmits signals from activators and repressors to the polymerase, are recruited to the promoter to form the pre-initiation complex (PIC). As soon as PolII is incorporated into the PIC, the Srb10 subunit of mediator stimulates the CTD S5 phosphorylation via the basal transcription factor TFIIH subunit Kin28. This modification disrupts the binding of mediator and TFs and leads to promoter clearance of PolII and transcription initiation (Max et al., 2007). S5 phosphorylation remains high during transcription of up to the first hundred nucleotides (nt), but decreases further downstream (Komarnitsky et al., 2000). The mRNA capping enzyme (Cho et al., 1997), the nuclear cap

binding complex (CBC) (Wong et al., 2007) as well as the H3K4 methyltransferase Set1, which is part of the COMPASS complex, are recruited to the transcription machinery through the S5 phosphorylated CTD (Ng et al., 2003).

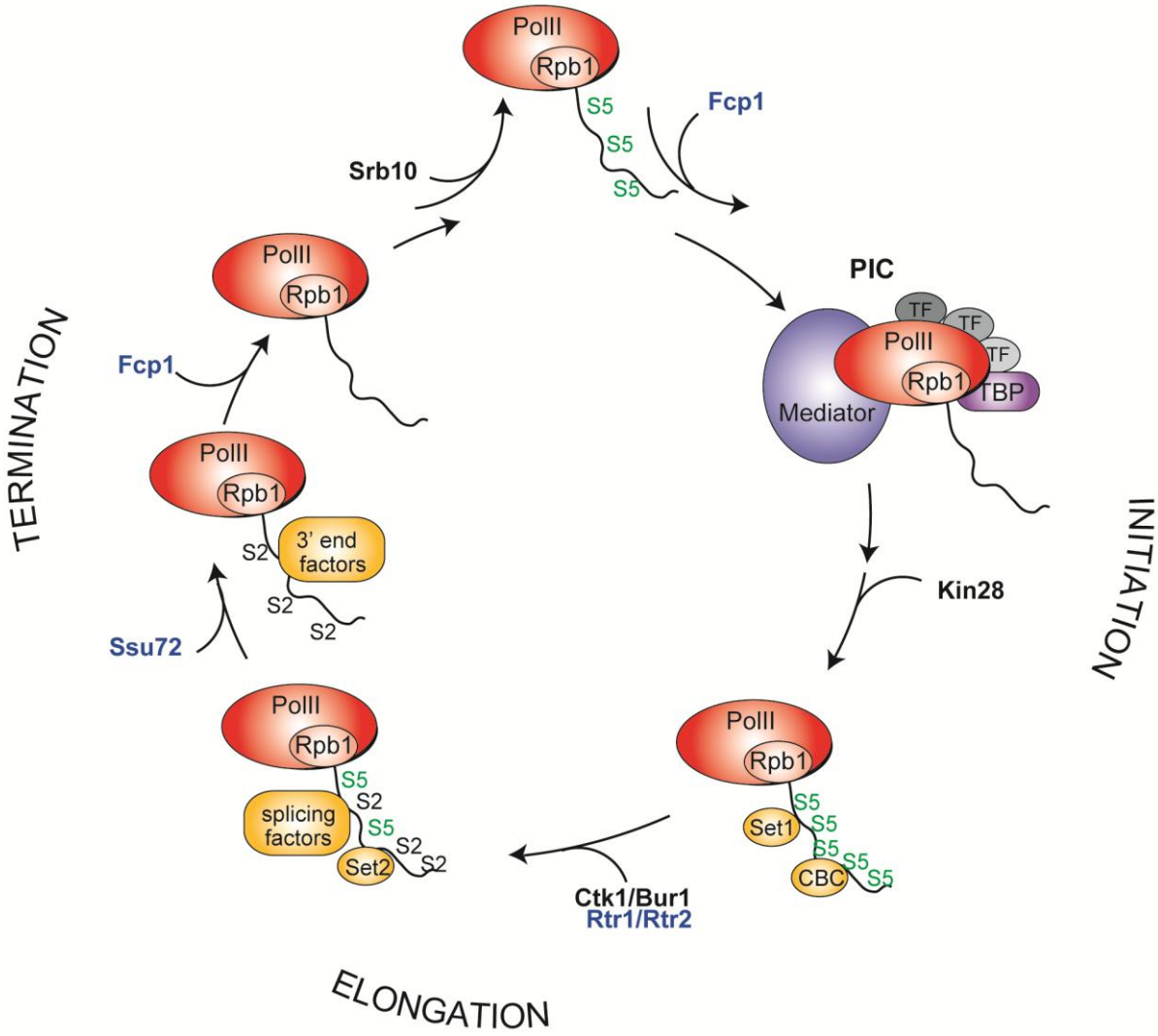

FIGURE 3: The transcription cycle (based on Prelich, 2002). Hypophosphorylated PolII is assembled into the pre-initiation complex (PIC) together with the TATA-box binding protein (TBP), general transcription factors (TF), and mediator. During initiation, the CTD is phosphorylated on S5 by Kin28. Phosphorylation on S2 by Ctk1 and Bur1 marks the elongation phase. At the same time S5 phosphorylation is reduced by Rtr1 (and maybe Rtr2). The phosphatases Ssu72 and Fcp1 dephosphorylate the CTD, thereby recycling PolII. Srb10 can repress transcription by phosphorylating the CTD on S5 prior to PIC formation. mRNA processing factors and methyltransferases are recruited depending on the CTD phosphorylation status. Kinases are shown in black and phosphatases in blue.

At the transition to processive transcription elongation, S5 phosphorylation is reduced by the S5 phosphatase Rtr1 (and presumably also by Rtr2) in yeast (Mosley et al., 2009) and probably later in the transcription cycle, also by Ssu72 (Krishnamurty et al., 2004). At the same time the CTD becomes predominantly and increasingly phosphorylated at S2 by the kinases Ctk1 and Bur1 (reviewed in Buratowski, 2009), thus marking the elongation phase.

PolII phosphorylated at S2 mediates the recruitment of the H3K36 methyltransferase Set2 (Kizer et al., 2005; reviewed in Hampsey & Reinberg, 2003) and of spliceosome components, which remove introns co-transciptionally (Du and Warren, 1997; Kim et al., 1997; Hirose et al., 1999). The CTD phosphorylated at S2 has also been implicated in the dissociation of the H3K4 methyltransferase and COMPASS subunit Set1 from transcribing PolII, thus confining methylation of H3K4 to the 5'-end of coding sequences (Xiao et al., 2007). The CTD is important for mRNA 3'-end processing, since S2 phosphorylated CTD recruits polyadenylation factors like Pcf11 (Barilla et al., 2001; Licatalosi et al., 2002; Ahn et al., 2004; Meinhart & Cramer, 2004). Polyadenylation of the mRNA is tightly linked to transcription termination (Kim et al., 2004a+b; West et al., 2004). The termination complex contains the protein Rtt103, which binds to the CTD phosphorylated at S2 and is involved in recruiting the Rat1 complex important for transcription termination (Kim et al, 2004b).

The regulation of the CTD also involves the phosphatases Fcp1 and Ssu72, which dephosphorylate S2 and S5, respectively (Cho et al., 2001; Krishnamurthy, 2004). This is crucial for transcription regulation and for the recycling of PolII for another round of transcription after its dissociation from the mRNA (Cho et al., 1999).

The recently discovered S7 phosphorylation of the CTD is mediated by the transcription factor TFIIH as well as Bur1-Bur2 and is found on the CTD during transcription along the entire gene. It has been reported to function in 3'-end processing of non-coding small RNAs, but also in transcription elongation of all PolII transcripts (Egloff et al., 2007; Chapman et al., 2007; Tietjen et al., 2010).

1.5. The CTDK-I complex and the related complex Bur1-Bur2

Ctk1 is the kinase subunit of the Carboxy Terminal Domain Kinase I (CTDK-I) complex, which phosphorylates RNA Polymerase II (PolII) on S2 of the CTD during transcription elongation (1.4). In addition to the kinase subunit Ctk1, the CTDK-I complex comprises the cyclin Ctk2 and Ctk3, a protein with unknown function (Sterner et al., 1995). *CTK1* deletion is not lethal, but leads to a severe growth defect (Lee & Greenleaf, 1991).

Through the S2 phosphorylation of the CTD, Ctk1 couples transcription with cotranscriptional splicing, histone methylation and mRNA polyadenylation. It was shown that Ctk1 is responsible for the recruitment of polyadenylation and cleavage factors to the 3'-end of transcribed genes and that Ctk1 deletion affects pre-mRNA 3'-end processing *in vivo*. (Ahn et al., 2004; Ni et al., 2004).

Ctk1 also helps to release basal transcription initiation factors from PolII including TFIIH, when PolII enters productive elongation. Interestingly, this function of Ctk1 is independent of its kinase activity (Ahn et al., 2009).

Additionally, a role of Ctk1 in damage-induced transcription has been reported. Mutations in *CTK* genes render yeast cells sensitive to the DNA damaging agents like UV irradiation and hydroxyurea. Ctk1 was shown to regulate genes that are required for DNA repair and environmental stress responses (Ostapenko & Solomon, 2003).

Interestingly, Ctk1 also plays a role in RNA Polymerase I (PolI) transcription (Bouchoux et al., 2004; Grenetier et al., 2006). However, its molecular function in this process remains unknown.

Apart from transcription-related functions, Ctk1 was shown to have an additional role in translation (Röther & Sträßer 2007). Ctk1 interacts specifically with ribosomes and is required for efficient translation *in vivo* and *in vitro*. Ctk1 function increases the correct decoding of the mRNA during translation elongation by phosphorylating residue S238 of Rps2, a protein of the small ribosomal subunit. Correspondingly, miscoding is increased in a non-phosphorylatable mutant of Rps2 (*rps2-S238A*). Phosphorylation of Rps2 by Ctk1, however, does not account for the immense translation defect observed in translation active extracts of Ctk1 depleted cells implicating a second role for Ctk1 in translation.

In yeast, there exists a second kinase/cyclin complex, which is similar to the CTDK-I complex and fulfils a related role in the cell: The essential Bur1 (kinase) and Bur2 (cyclin) complex. Bur1 is required for efficient transcription elongation (Keogh et al., 2003) and – as Ctk1 – was shown to phosphorylate the CTD of PolII on S2 (Murray et al., 2001; Qiu et al., 2009). Although Ctk1 is thought to be responsible for the bulk of S2 phoshorylation, recent evidence suggests that initial S2 phosphorylation by Bur1 might stimulate subsequent phosphorylation by Ctk1. Bur1 has also been shown to be responsible for the residual S2 phosphorylation observed in Δ*ctk1* cells (Qiu et al., 2009).

Besides this function, Bur1 is known to phosphorylate the transcription elongation factor subunit Spt5 (Zhou et al., 2009; Liu et al., 2009). This phosphorylation is important for recruitment of the PAF complex to the site of transcription, which consequently is reduced in Bur1 mutant strains (Laribee et al., 2005; Liu et al., 2009). The PAF complex functions in recruiting factors to the elongating PolII that are involved in chromatin modification like H3K4 methylation and in mRNA maturation. Thus histone modification and mRNA maturation are also affected by mutations of Bur1.

In addition, Bur1 phosphorylates and activates the E2 ubiquitin conjugating enzyme Rad6 involved in H2B ubiquitilation (Wood et al., 2005). This, again is required for H3K4 methylation by the COMPASS complex (Wood et al., 2003 + 2005; Lee et al., 2007).
Both, the CTDK-I and the Bur1-Bur2 complex have been suggested to be the homologues of the human positive transcription elongation factor b (P-TEFb) containing the kinase subunit CDK9 (reviewed in Wood & Shilatifard, 2006). P-TEFb was shown to phosphorylate both the human homologue of Spt5 (the mammalian DRB sensitivity inducing factor (DSIF)) and S2 on the CTD of PolII. However, this notion has been recently questioned and the Bur1-Bur2 complex is favored as a P-TEFb homologue, whereas for Ctk1 the homologues CDK12 or CDK13 presumably in complex with cyclin K have been newly identified. These two human kinases also phosphorylate the CTD of Rpb1 on S2 (Bartkowiak et al. 2010).

1.6. Ribosome biogenesis

Eukaryotic ribosomes consist of four highly modified rRNAs and around 80 ribosomal proteins, which have to be assembled in a complicated, multistep process, which occurs in the nucleus (mostly in the nucleolus) and the cytoplasm. More than 200 non-ribosomal proteins and snoRNAs are involved in this process (reviewed in Henras et al., 2008; Lempiäinen & Shore, 2009)
Ribosome synthesis starts with the transcription of a long precursor rRNA – the 35S rRNA – and the 5S rRNA from rDNA tandem repeats by Polymerase I (PolI) and Polymerase III (PolIII), respectively. The 35S rRNA contains the 18S, 5.8S and 25S rRNA, which are flanked and separated by interspersed spacer regions. Cotranscriptionally, a subset of small subunit ribosomal proteins (rps) and non-ribosomal factors associate with the pre-rRNA to form the 90S pre-ribosome. The nascent 35S rRNA is modified by about 75 different small nucleolar (sno) RNAs, which mediate 2'-O-ribose methylation of nucleotides and the formation of pseudouridines (reviewed in Henras et al., 2008 and Kressler et al., 2010). The rRNA of the 90S pre-ribosome gets cleaved in the spacer region between the sequences of the 18S and the 5.8S rRNA. This leads to the separation of the early 40S pre-ribosome containing the 20S pre-rRNA from the remaining 27S pre-rRNA. The resulting 40S precursor with the 20S pre-rRNA is changed in composition due to the displacement of non-ribosomal factors and association of a small set of novel biogenesis factors and further rps proteins (Schäfer et al., 2003; reviewed in Granneman & Baserga, 2004 and Kressler et al., 2010). This particle is transported out of the nucleolus to the cytoplasm. Here, the 40S pre-ribosome is further rearranged and the last

rps proteins are bound. Finally, the 20S pre-RNA is dimethylated and cleaved yielding the 18S rRNA, thus completing 40S subunit assembly (reviewed Zemp & Kutay, 2007 and Kressler et al., 2010; FIGURE 4).

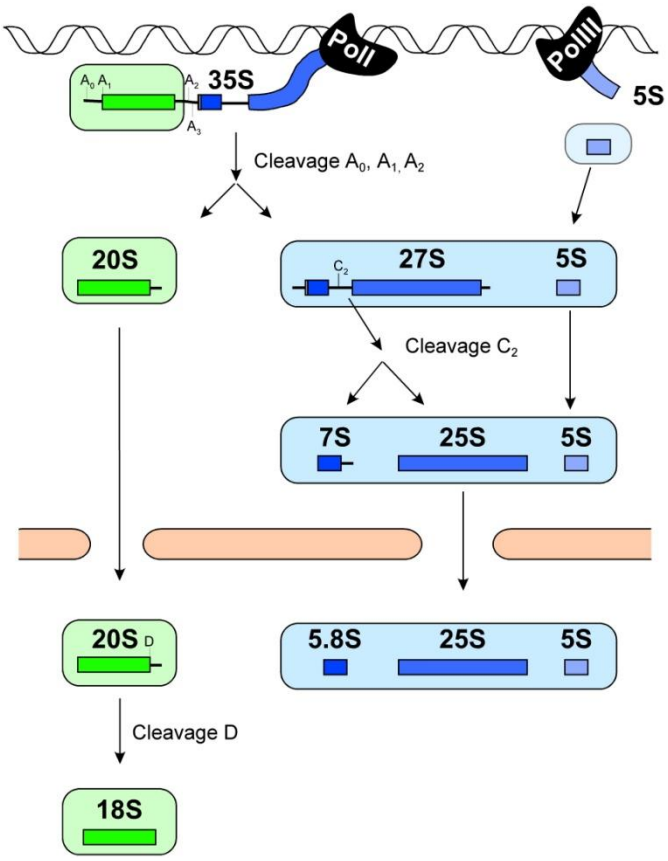

FIGURE 4: Simplified overview of the major steps in pre-rRNA processing (Kressler et al., 2010). Ribosome assembly starts with the transcription of the 35S rRNA precursor. RNA cleavage at site A2 seperates the two branches into the 40S (green) and the 60 S pre-ribosomes (blue). Inside the cytoplasmic 40S precursor, the 20S pre-rRNA is cleaved at site D to generate the mature 18S rRNA. 27S pre-rRNA, 5S RNP, ribosomal proteins, and non-ribosomal factors form the first 60S precursor. Within pre-60S particles, the 27S pre-rRNA is further processed to generate mature 5.8S and 25S rRNA.

After cleavage of the 35S pre-rRNA, the 27S pre-rRNA assembles with large subunit ribosomal proteins and non-ribosomal factors to generate the earliest pre-60S ribosomes (reviewed in Henras et al., 2008; Granneman & Baserga 2004). Further rearrangement of this pre-60S complex involves the dissociation and association of distinct non-ribosomal factors and rRNA modifications. In addition, the 5S RNP complex, consisting of the 5S rRNA and Rpl5 is incorporated into the complex (Zhang et al., 2007; reviewed in Kressler et al., 2010). The pre-60S particle undergoes further compositional changes during its transition from the nucleolus to the nucleoplasm (Milkereit et al., 2001; Kressler et al., 2008). During this step, the 27S pre-rRNA is processed into 25S and 5.8S rRNA (Nissan et al., 2002) and an export

competent particle is formed. After transport to the cytoplasm, the pre-60S particle undergoes further rearrangements and probably the final 5.8 rRNA processing takes place here (Ansel et al., 2008; Gabel & Ruvkun 2008; reviewed in Zemp & Kutay, 2007). The last modifications of the pre-60S subunit which lead to a mature 60S that can bind to the 40S subunit include dissociation of non-ribosomal factors, incorporation of Rpl10 and release of the anti 40S/60S association factor Tif6 (Senger et al., 2001; Lo et al., 2010; reviewed in Kressler et al., 2010 and Zemp & Kutay, 2007; FIGURE 4).

1.7. The SR protein Npl3

Npl3 is - together with the related proteins Hrb1 and Gbp2 - one of three heterogeneous nuclear ribonucleoproteins (hnRNPs) with serine arginine (SR) repeats at their C-termini. Like Ctk1, Npl3 is involved in multiple steps of gene expression (FIGURE 5). Npl3 is nuclear at steady state, shuttles between the nucleus and the cytoplasm (Wilson et al., 1994) and interacts with PolII phosphorylated at S2 in order to stimulate its transcription elongation activity *in vitro* (Dermody et al, 2008). It binds to pre-mRNA, recruits RNA splicing factors (Kress et al., 2008) and is involved in mRNA 3'-end processing. More specifically, it has been suggested to prevent transcription termination at cryptic termination sites. Npl3 is thought to fulfill this function by competing with RNA cleavage factors (such as Hrp1 and Rna15) for binding the nascent transcripts (Bucheli & Buratowski, 2005; Bucheli et al., 2007; Deka et al., 2007). Npl3 has a higher affinitiy to RNA than Hrp1 and Rna15, but the cleavage factors bind more strongly to AU-rich sequences – a characteristic of strong transcription termination sites – than Npl3. Thus, at these sites they can displace Npl3 for proper RNA cleavage (Bucheli et al., 2007). Hence, the competition between Npl3 and Hrp1 determines the choice of transcription termination sites (Bucheli & Buratowsky, 2005).

After transcription termination, Npl3 remains bound to the mRNA and promotes mRNA export (Lee et al., 1996; Kadowaki et al., 1994). Like the shuttling mRNA binding proteins Gbp2, Hrb1 and Pab1, it is part of the exported mRNP. Recent studies suggest that Npl3 also functions in translation while remaining bound to the mRNA during its first round of translation. The prolonged association of Npl3 with ribosomes leads to reduced translation efficiency (Windgassen et al., 2004). Furthermore, Npl3 has a role in translation termination (Estrella et al., 2009). Npl3 is transported back into the nucleus by its import receptor Mtr10 (FIGURE 5; Senger et al., 1998).

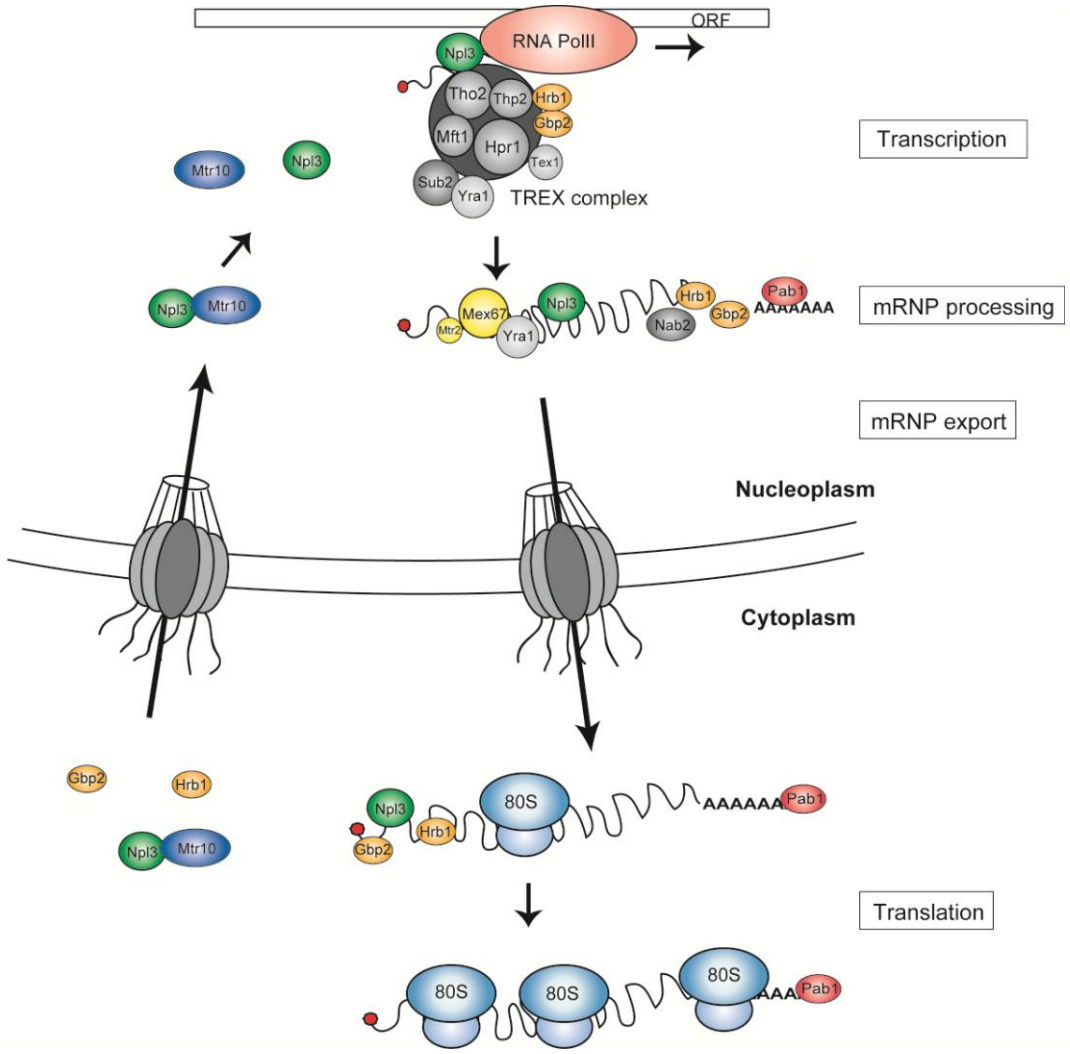

FIGURE 5: Npl3 functions in multiple steps of gene expression. Npl3 promotes transcription, associates with the mRNA cotranscriptionally, functions in mRNA 3'-end processing, mRNA export and translation. It is imported into the nucleus via its import receptor Mtr10.

Npl3 can be post-translationally modified through arginine methylation and serine phosphorylation. Methylation by the arginine methyltransferase Hmt1 occurs in the nucleus and is important for splicing (Kress et al., 2008) and for the nuclear export of the mRNP (Xu & Henry, 2004; McBride et al., 2005). Additionally, arginine methylation weakens the association of Npl3 with Tho2, a subunit of the THO and TREX (TRanscription and EXport) complexes, which stimulate elongation and mRNA nuclear export (McBride et al., 2005; Sträßer et al., 2002). Hence it was postulated by Wong et al. (2010) that arginine methylation of Npl3 leads to an increased pool of recycled THO, which can again be recruited to the site of transcription, thus enhancing transcription efficiency.

Npl3 is phosphorylated on S411 in the cytoplasm by Sky1, which is important for proper nuclear localization of Npl3. In the absence of this phosphorylation, the association of Npl3 with its nuclear import factor Mtr10 is decreased (Gilbert et al., 2001; Yun & Fu 2000). In the nucleus, Npl3 is dephosphorylated by Glc7 leading to increased association of Npl3 with the mRNA and enabling the recruitment of the Mex67 export factor (Gilbert & Guthrie, 2004). Phosphorylation of Npl3 by casein kinase II (CK2) in the nucleus was suggested to contribute to the dissociation of Npl3 from the nascent transcript and hence to promote the recruitment of the RNA cleavage factor Rna15 (Dermody et al., 2008).

Recently, a function in translation initiation has been suggested for Npl3. Npl3 was shown to bind to both the mRNP and pre-60S ribosomes. Additionally, Npl3 was evidenced to positively influence subunit joining at the start codon – a function that was dependent upon Npl3's ability to form homodimers. Hence, it was hypothesized that the Npl3 molecule located at the mRNP forms a homodimer with the Npl3 molecule that is bound to the 60S subunit. Thus, the recruitment of the 60S subunit could be enhanced by Npl3 homodimer formation resulting in efficient translation initiation (Thomas Gross, PhD thesis, 2009).

In summary, like Ctk1 (1.5), Npl3 has multiple functions in gene expression ranging from transcription to translation. It would be interesting to investigate whether the two proteins interact with each other to fulfil these functions.

1.8. Aim of this work

As reported previously, the kinase subunit of the CTDK-I complex besides its well known role in transcription also functions in translation (Röther & Sträßer, 2007). It enhances translation fidelity by phosphorylating Rps2, a protein of the small ribosomal subunit, on serine 238. However, the non-phosphorylatable *rps2*-S238A mutant did not show a translation defect as strong as observed in cells depleted of Ctk1. This result lead to the hypothesis that Ctk1 has an additional role in translation which accounts for the dramatic drop of translation efficiency upon Ctk1 depletion. The aim of this work was to reveal this additional role of Ctk1 in translation.

It could be elucidated in this study that Ctk1 has a function in translation initiation. Thus, the following task was to determine the role of Ctk1 in this process on a molecular level. This included the identification of the specific step within translation initiation, which is affected upon loss of Ctk1. In addition, the aim of this thesis was to investigate whether the kinase activity of Ctk1 is important for its function in translation initiation and to identify a possible

substrate of Ctk1, whose phosphorylation is important for efficient translation initiation.

As a second aspect, the interaction of Ctk1 with the nucleocytoplasmic shuttling mRNP processing factor and SR protein Npl3 was to be analyzed. Both Ctk1 and Npl3 function in similar processes during gene expression and preliminary experiments have shown that the two proteins interact genetically. In addition, Npl3 is known to be regulated in part via its phosphorylation. Thus it would be interesting to investigate whether the kinase Ctk1 phosphorylates Npl3 and what function this phosphorylation might have.

2. RESULTS

2.1 Ctk1 function is crucial for translation initiation

2.1.1. Ctk1 is needed for efficient translation initiation

Ctk1 is a transcription factor that was previously reported to phosphorylate Rps2 on S238 and thus increases translational accuracy (1.5, Röther & Sträßer, 2007). The translation defect of an *rps2-S238A* mutant, however, is not as severe as the translation defect observed in Ctk1 depleted cells (Röther & Sträßer 2007, FIGURE 6C). This indicates that Ctk1 has an additional role in translation. In order to identify this potential novel function of Ctk1 in translation it was first assessed whether Ctk1 functions in translation initiation. To do this, Ctk1 was depleted from cells by expressing Ctk1 under control of the *GAL1* promoter and growth for 18 h in glucose containing medium (4.2.2.5). As shown previously, this leads to almost complete depletion of Ctk1, but only to a minor growth defect (FIGURE 6A, Röther & Sträßer 2007). The activity of translation active extracts of Ctk1 depleted cells to translate a capped mRNA versus different Internal Ribosome Entry Site (IRES) containing mRNAs (4.2.4) was compared. The CrPV IRES, which does not require any translation initiation factors for 80S recruitment to the start codon (Wilson et al., 2000; reviewed in Hellen, 2009; 1.3), was used in this assay. In addition, two yeast IRESes derived from genes required for invasive growth upon nutrient limitation, *NCE102* and *GPR1*, were taken. In contrast to the CrPV IRES, the mechanism for cap-independent translation of these yeast mRNAs is still enigmatic, but was shown to depend at least on the initiation factor eIF4G (Gilbert et al., 2007). All IRES containing mRNAs were constructed with an unphysiological ApppG cap analogue followed by an inhibitory stem loop to almost completely inhibit any residual cap-dependent translation (Gilbert et al., 2007). The respective IRESes were inserted upstream of the firefly luciferase (F-luc) reporter gene. As control for canonical translation a corresponding reporter was used that carried an m^7GpppG-cap but lacked the inhibitory stem loop and the IRES (FIGURE 6B).

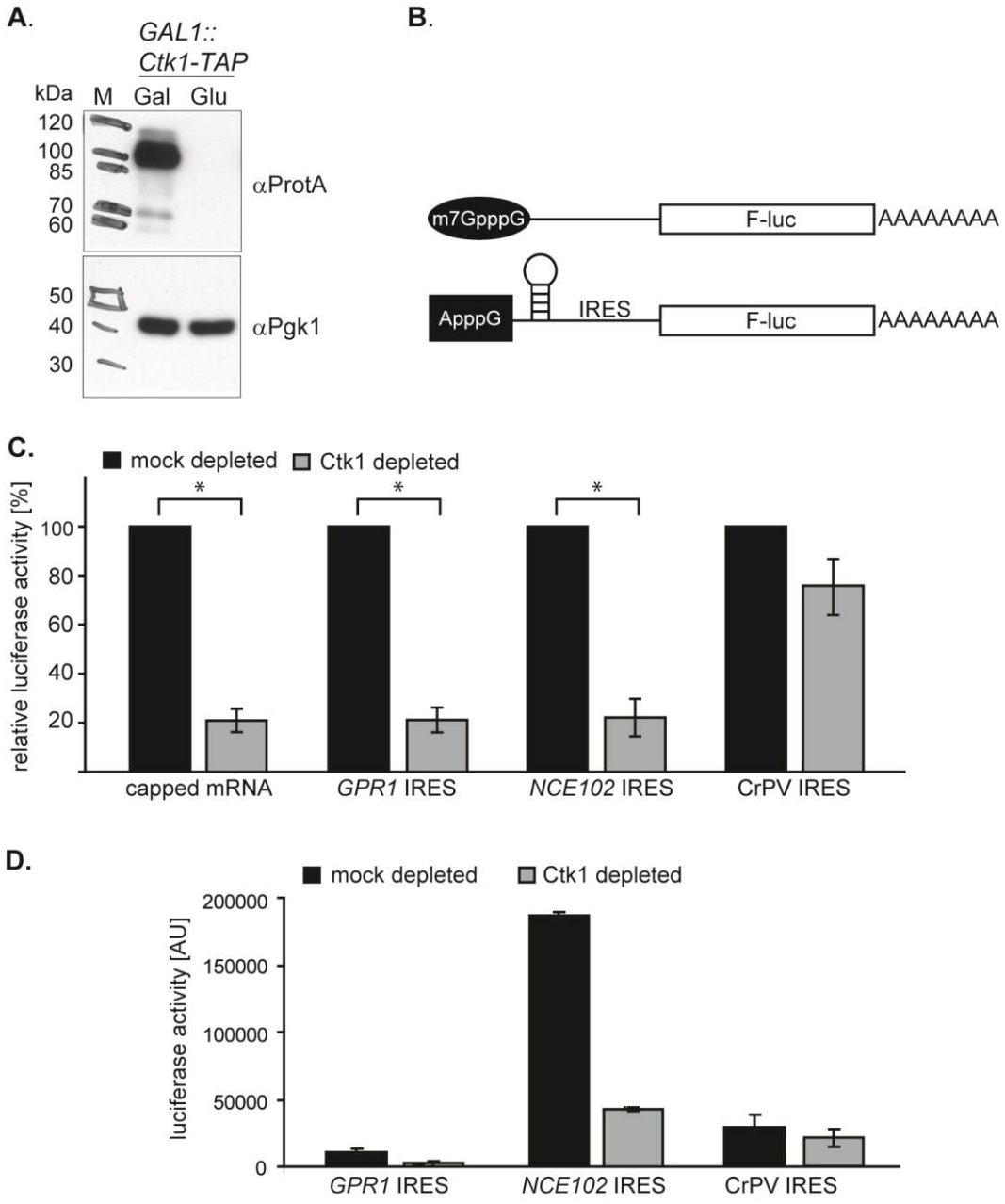

FIGURE 6: Ctk1 function is essential for efficient translation initiation. *A*, After 18 h growth of *GAL1::Ctk1-TAP* in glucose containing media (Glu), Ctk1 cannot be detected by western blotting. *B*, Luciferase (F-luc) reporter constructs used to assess initiation independent translation contain either an m^7GpppG-cap or an unphysiological ApppG-cap followed by an inhibitory stem loop and an IRES. IRESes used correspond to the CrPV IRES or yeast IRESes of the *GPR1* or the *NCE102* gene. *C*, Loss of Ctk1 causes decreased translation activity of capped but not of CrPV IRES-containing RNA. The translation activity of translation active extracts from mock and Ctk1 depleted cells for the reporters shown in *B* was analyzed. For each RNA construct the activity of the mock depleted extracts was set to 100. *D*, Absolute values of luciferase activity of mock and Ctk1 depleted extracts for the three IRES containing reporters. The error bars represent the standard deviation of at least three independent experiments. AU: arbitrary units; Gal: galactose containing media; Glu: glucose containing media.

In agreement with previous studies, the translation of the capped mRNA was reduced to 20% in extracts of Ctk1 depleted compared to mock depleted wt cells (FIGURE 6C and Röther & Sträßer, 2007). Translation of the *GPR1* and the *NCE102* IRES containing RNAs was decreased to the same extent as translation of capped mRNA. Importantly, translation of the CrPV IRES-containing mRNA was reduced only to 80% in Ctk1 depleted extracts reflecting the fact that the translation defect of these extracts is circumvented by the initiation mechanism of this IRES (FIGURE 6C). The fact that translation of the IRES-containing mRNA was 20% lower than in mock depleted extracts is probably due to the elongation defect in Ctk1 depleted extracts (Röther & Sträßer, 2007).

All three IRES containing mRNAs used were translated less efficiently than the capped mRNA (0.2% - 4% of the capped construct), but were still around 100x more efficiently translated than the negative control containing an ApppG cap and a stem loop but no IRES (data not shown). The three different IRES containing mRNAs were translated with similar efficiency with the *NCE102* IRES containing mRNA being translated best and the *GPR1* IRES containing mRNA being translated least (FIGURE 6D).

Since translation initiation mediated by the CrPV IRES is independent of any translation initiation factors, this result suggests that Ctk1 is required for the correct interplay of translation initiation factors necessary to recruit translation competent 80S ribosomes to the start codon. Thus, in extracts depleted of Ctk1 not only translation elongation, but also translation initiation is impaired.

2.1.2. Loss of Ctk1 causes a decrease of 80S initiation complex formation and inefficient subunit joining at the start codon

The next aim was to corroborate that Ctk1 is indeed necessary for efficient translation initiation and moreover to specify the step in translation initiation that it functions in. Therefore, the incorporation of radiolabeled mRNA into translation initiation complexes was evaluated in extracts of Ctk1 and mock depleted cells.

To do this, the initiation assay described by Beckmann et al. (2005) was adapted to yeast (4.2.5). Four yeast transcripts were used for this analysis: *RPL38* mRNA, *RPL41* mRNA with two different lengths of 5'UTR (22 bp and 80 bp), and *PGK1* mRNA with a shortened open reading frame (ORF). These mRNAs were selected with respect to a high expression level, lack of introns and – in the case of the mRNAs coding for the ribosomal proteins – for a short ORF necessary for a good resolution of the initiation complexes on sucrose density gradients.

These four mRNAs were incubated with Ctk1 and mock depleted extracts under conditions in which translation initiation occurs but elongation is blocked by the addition of cycloheximide. The resulting translation initiation complexes were separated on a sucrose density gradient followed by scintillation counting of the gradient fractions in order to assess the distribution of the radioactively labeled mRNA. During translation initiation, the mRNA is first bound by a subset of translation initiation factors and mRNA binding proteins forming an mRNP. This mRNP then binds to the 43S subunit (40S subunit plus initiation factors) to generate a 48S initiation complex. After scanning of the 40S subunit along the 5'UTR, the 60S subunit joins the 40S subunit at the start codon forming the 80S initiation complex. In this initiation assay the three mRNA containing initiation complexes – mRNPs, 48S, and 80S complexes – were separated and visualized.

To characterize the four novel reporter mRNAs, their incorporation into initiation complexes was first analyzed in mock depleted wild-type (wt) extracts. FIGURE 7A shows the distribution of each radiolabeled mRNA on a sucrose density gradient. All four mRNAs were mostly incorporated into 80S initiation complexes with a smaller portion being part of 48S initiation complexes or present in the light, ribosome free fraction. The incorporation into 80S ribosomes was highest for the *RPL38* and the *RPL41* (22 bp 5'UTR) mRNA, intermediate for the *PGK1* mRNA, and lowest for the *RPL41* (80 bp 5'UTR) mRNA.

Strikingly, the incorporation of the four different mRNAs into 80S ribosomes was reduced in Ctk1 depleted compared to mock depleted extracts, whereas the fraction of mRNA in mRNPs and 48S initiation complexes was increased (FIGURE 7B-E). This implies that the formation of 80S initiation complexes is impaired in Ctk1 depleted extracts. This defect does not seem to be specific for a certain mRNA since it occurred with all four reporters. The peak for labeled 48S initiation complexes was increased in Ctk1 compared to mock depleted extracts indicating that Ctk1 functions in translation initiation after formation of 48S and before formation of 80S initiation complexes.

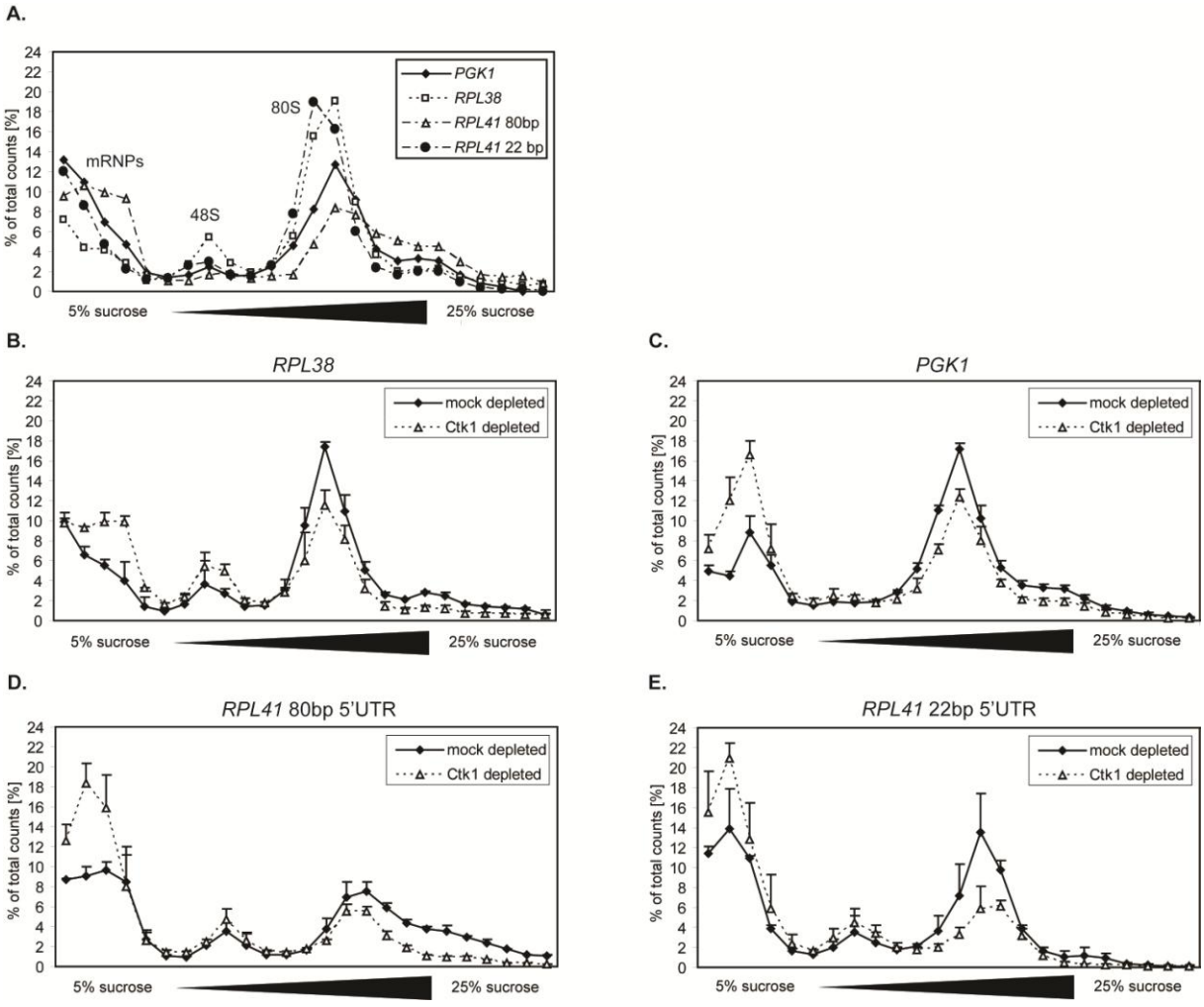

FIGURE 7: In Ctk1 depleted extracts formation of 80S initiation complexes is decreased while 48S initiation complexes and mRNPs are increased. *A*, Incorporation of *PGK1* (♦), *RPL38* (□), *RPL41* with 80 bp 5'UTR (Δ), and *RPL41* with 22 bp 5'UTR (•) into initiation complexes was analyzed in initiation reactions of translation active extracts. The fractions containing mRNPs, 48S, and 80S complexes are indicated. *B-E*, In comparison to mock depleted extracts (♦) Ctk1 depletion (Δ) caused a decrease in the incorporation of *RPL38* mRNA (*B*), *PGK1* mRNA (*C*), *RPL41* mRNA with 80 bp 5'UTR (*D*), and *RPL41* mRNA with 22 bp 5'UTR (*E*) into 80S initiation complexes. Free mRNPs and, to a lesser extent, mRNAs bound to 48S initiation complexes are increased upon Ctk1 depletion with all mRNAs tested. The error bars represent the standard deviation of each fraction of at least three independent experiments.

The most likely scenarios are that Ctk1 function is needed for scanning of the 5'UTR by the small ribosomal subunit or for 60S subunit joining at the start codon. In order to distinguish between these two possibilities, the position of the 40S subunit on the *RPL38* mRNA in Ctk1 depleted extracts was determined by a toeprint assay (4.2.6). Translation reactions were performed as described above except that the reporter mRNA was not radiolabeled. Subsequently, the reactions were subjected to sucrose density centrifugation and fractions containing 48S initiation complexes pooled (FIGURE 8).

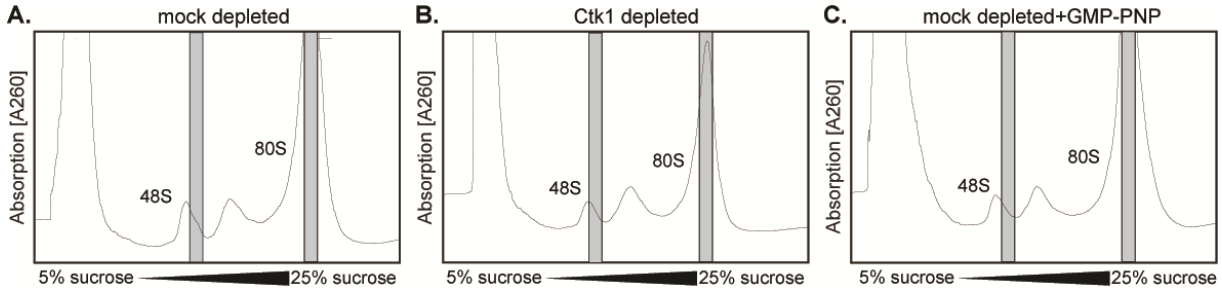

FIGURE 8: Gradients used for isolating 48S and 80S initiation complexes needed for toeprint analysis. Gradient fractions (in grey) of 48S and 80S initiation complexes were taken from mock depleted (*A*), Ctk1 depleted (*B*), and GMP-PNP treated mock depleted extracts (*C*). The RNA of these fractions was extracted and subjected to reverse transcription.

Reverse transcription with a primer annealing to the ORF in the direction of the cap renders transcription products whose lengths depend on the position of the 40S subunit on the mRNA ("toeprint"). 40S subunits positioned at the start codon yield a distinct short transcription product, whereas 40S subunits located at the cap as well as scanning 40S subunits yield a long transcription product. In FIGURE 9A these two toeprints are indicated.

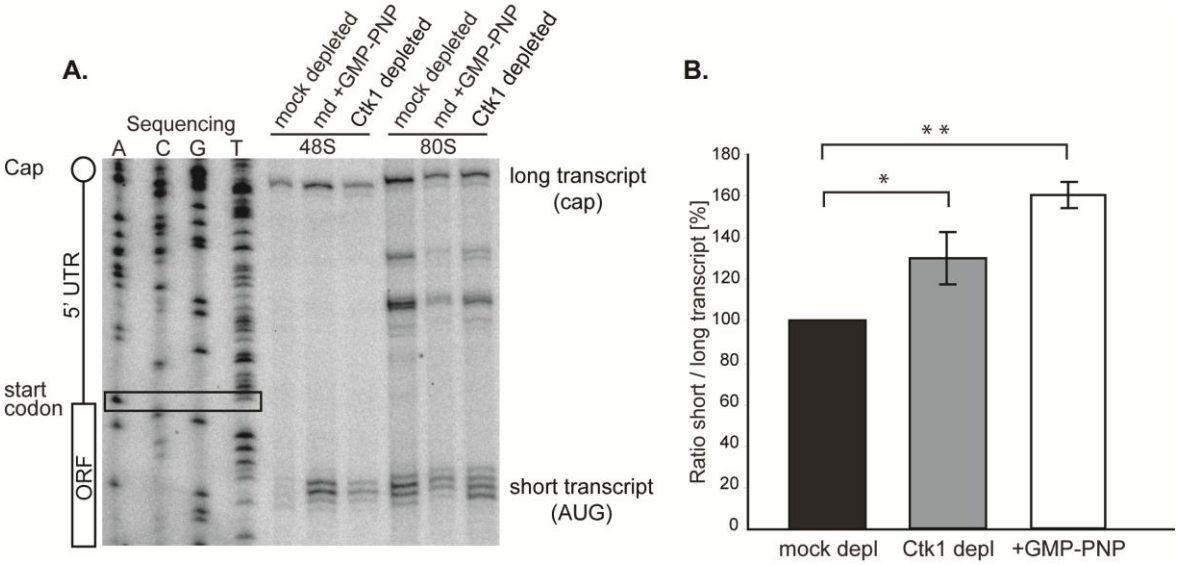

FIGURE 9: The 40S subunit is located at the start codon in 48S initiation complexes accumulating in Ctk1 depleted extracts. *A,* Toeprints of fractions shown in FIGURE 8 were analyzed on a sequencing gel. The short toeprint is produced when the 40S subunit is located at the start codon whereas the long transcript is generated when the 40S is in the process of scanning or bound to the very 5-'end of the mRNA. *B,* Quantification of the ratios of the short transcript versus the long transcripts of the 48S initiation complexes shown in *A.* The signal for the short transcript is significantly increased in Ctk1 depleted extracts in comparison to mock depleted extracts. The error bars represent the standard deviation of three independent experiments. md: mock depleted.

Importantly, there was a clear toeprint signal for 40S subunits positioned at the start codon in Ctk1 depleted extracts in contrast to mock depleted extracts. The toeprint for the long transcript, on the other hand, was about the same in both extracts. The increased toeprint

signal for 40S subunits at the start codon in Ctk1 depleted extracts indicates a defect in subunit joining rather than scanning. As a positive control for a subunit joining defect, non-hydrolysable GTP was added to the mock depleted reaction. As expected, this treatment lead – as in the case of Ctk1 depleted cells – to an increased toeprint signal for the short transcripts corresponding to 40S positioned at the start codon. The ratio of short and long transcripts in mock depleted, Ctk1 depleted, and GMP-PNP treated extracts (FIGURE 9B) indicates that 40S initiation complexes accumulated to a significant degree at the start codon in Ctk1depleted extracts. These results strongly suggest that Ctk1 function is required for subunit joining at the start codon.

2.1.3 The translation defect in Ctk1 depleted cells is not caused by stress

Translation is mostly controlled at the step of initiation. Upon different stress conditions, eIF2α is phosphorylated which leads to a decrease in TC formation and thus inhibits translation initiation. In addition, translation initiation can be shut down in stress conditions via the 4EBPs or eIF4G cleavage (1.2; FIGURE 1).

In order to exclude a possible unspecific stress-induced inhibition of translation initiation upon loss of Ctk1 function, eIF2α phosphorylation as well as the incorporation of radiolabeled mRNA into translation initiation complexes was assessed in Ctk1 depleted cells. The level of eIF2α phosphorylation was compared in whole cell protein extracts obtained from mock and Ctk1 depleted, *Δctk1*, and 3-amino-1,2,4-triazole (3AT) treated wt cells, which served as a positive control. 3AT is a drug that induces amino acid starvation by being a competitive inhibitor of an enzyme involved in histidine production. As previously reported, depletion of Ctk1 under control of the *GAL1* promoter for 18 hours lead to an almost complete loss of Ctk1, but not to the severe growth defect of *Δctk1* cells (FIGURE 6A; Röther & Sträßer 2007). As shown in FIGURE 10A, eIF2α phosphorylation was increased in *Δctk1* but not in Ctk1 depleted cells compared to wt indicating that the translation defect in Ctk1 depleted extracts is not caused by eIF2α phosphorylation.

To assess formation of 48S complexes in extracts of *Δctk1* cells, a translation initiation assay was performed in the presence of GMP-PNP (4.2.5). This non-hydrolysable GTP analogue prevents subunit joining and therefore increases the amount of 48S complexes. In contrast to Ctk1 depleted extracts, the peak for mRNA in 48S initiation complexes was decreased in extracts of *Δctk1* cells (FIGURE 10B,C). Thus, the translation defect in Ctk1 depleted extracts

is not caused by stress and slow growth of the cells.

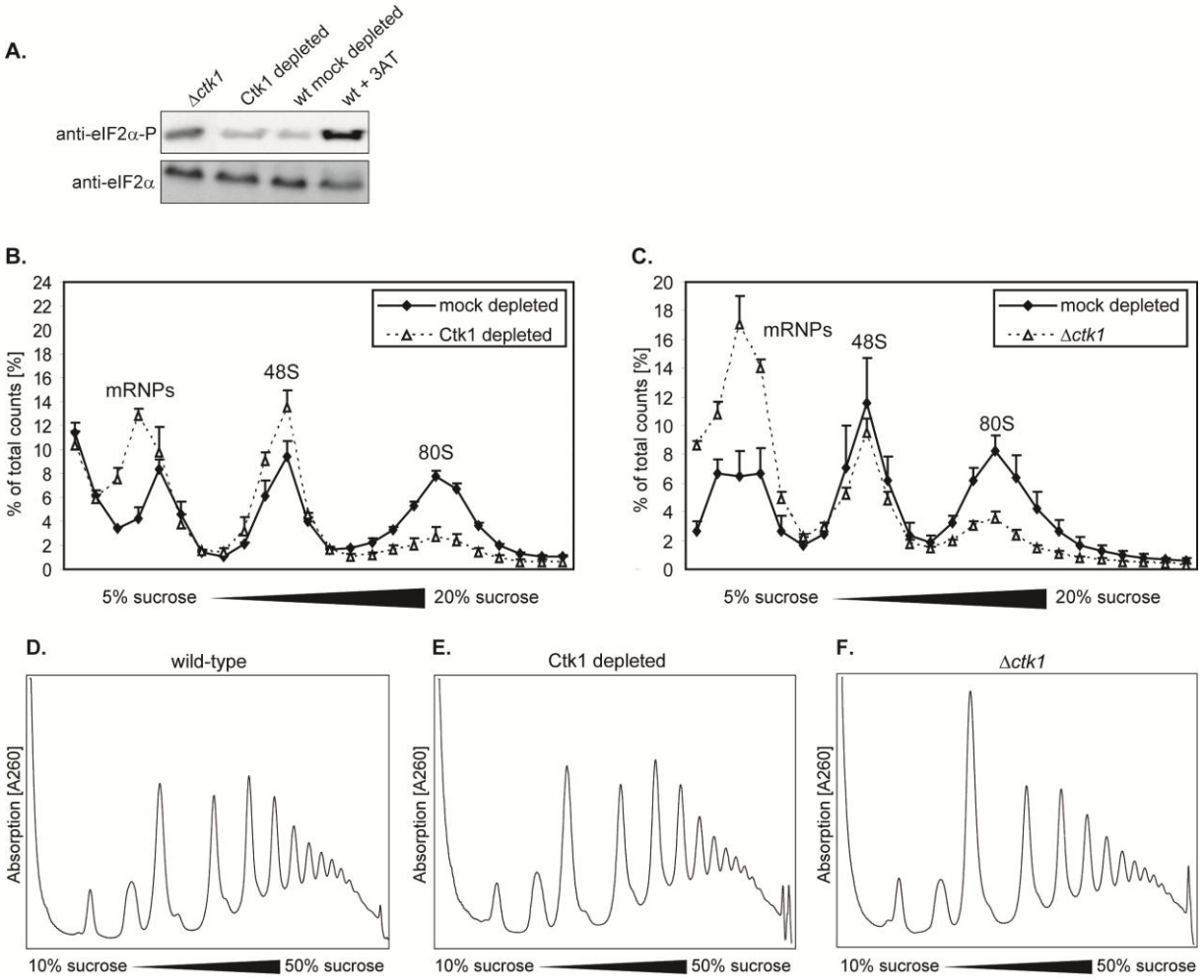

FIGURE 10: Impaired translation in Ctk1 depleted cells is not due to an overall stress response. *A*, Western blotting of *Δctk1*, Ctk1, and mock depleted extracts against total eIF2α and phosphorylated eIF2α (eIF2α-P) reveals that the phosphorylated form of eIF2α is increased in *Δctk1* cells as well as in cells treated with 3-amino-1,2,4-triazole (3AT), which served as positive control. *B* and *C*, The incorporation of *RPL38* mRNA into 48S initiation complexes analyzed by an initiation assay is increased in Ctk1 depleted extracts (*B*), but rather decreased in *Δctk1* extracts (*C*). GMP-PNP was added to the initiation assay for better analysis of 48S initiation complexes. *D-F*, The polysome profiles of wt (*D*) and Ctk1 depleted (*E*) cells were similar whereas in the polysome profile of *Δctk1* (*F*) cells the 80S peak was increased and polysomes were decreased. The error bars represent the standard deviation of each fraction of at least three independent experiments.

According to the results above, the polysome profile of Ctk1 depleted cells resembled the wt profile, whereas the profile of *Δctk1* cells showed an increased 80S peak with a concomitant decrease of polysomes (FIGURE 10D-F). Taken together, these data revealed that, unlike *Δctk1* cells, Ctk1 depleted cells do not have a stress induced translation initiation defect. Since the specific function of Ctk1 in translation was to be analyzed, all experiments were carried out with Ctk1 depleted cells in order to exclude a stress induced unspecific shut down of translation in the mutant strain.

Ctk1 depleted cells exhibited the same polysome profiles as wt cells (FIGURE 10D+E) despite the significant defect in translation initiation of Ctk1 depleted translation active extracts observed *in vitro* (FIGURE 6C; FIGURE. 7B-E; FIGURE 9D+E). This is probably due to the fact that *in vitro* translation experiments are more sensitive than polysome gradients – that show the *in vivo* distribution of ribosomal complexes – rendering the significant, but small translation initiation defect of Ctk1 depleted cells undetectable *in vivo*.

2.1.4. The kinase activity of Ctk1 is important for its function in translation initiation

Ctk1 is a serine/threonine kinase known to phosphorylate the C-terminal domain of Rpb1, the largest subunit of PolII, and S238 of Rps2, a protein of the small ribosomal subunit. These phosphorylation events are necessary for efficient transcription elongation, mRNA 3'-end processing, and translation elongation. In addition, Ctk1 plays a structural role in transcription: It is involved in the release of basal transcription factors from PolII independently of its kinase activity as PolII enters productive elongation (Ahn et al., 2009; 1.5).

Thus, it was determined whether the Ctk1 kinase activity is needed for efficient translation initiation. For this, translation active extracts were prepared (4.2.4.1) of cells expressing *CTK1* from the *GAL1* promoter and containing a plasmid encoding either wt Ctk1, the kinase dead Ctk1 mutant Ctk1-D324N (Ahn et al., 2009), or an empty plasmid. After shifting the cells to glucose-containing medium, only the *CTK1* copy located on the plasmid was expressed. As Ctk1 is a non-essential protein, and the *ctk1-D324N* mutant shows a similar slow growth phenotype as the complete deletion, cells were grown in minimal media to ensure the presence of the respective plasmid. The expression of the *CTK1* mutant was the same as the wt protein (FIGURE 11A). Measuring translation activity of these extracts with a luciferase reporter mRNA (FIGURE 11B; 4.2.4.2), the same reduction in the Ctk1 depleted cells compared to mock depleted cells (Ctk1 depleted cells expressing *CTK1* from the additional plasmid) was observed as in FIGURE 6C (2.1.1.). Consequently, the growth in minimal versus YPD medium did not affect the decrease in translation efficiency of Ctk1 depleted cells. Crucially, the Ctk1 mutant *ctk1-D324N* showed the same reduction in overall translation efficiency as the depletion (FIGURE 11B). Thus, the kinase activity of Ctk1 is indispensable for Ckt1's function in translation initiation. In order to confirm that the kinase activity is necessary for translation initiation and to assess whether it is needed for efficient

80S complex formation, initiation assays (4.2.5) with extracts depleted of wt Ctk1, but expressing either wt *CTK1*, *ctk1-D324N*, or no *CTK1* from a plasmid were performed. FIGURE 11C shows that the migration of radiolabeled mRNA differed when the cells were grown in minimal media compared to full media (FIGURE 7). The peak for unbound mRNAs increased whereas 48S intermediates were not visible. This was also the case when different markers for the plasmid, *i.e.* different minimal media, were used (data not shown). Nonetheless and importantly, a reduction in 80S formation was observed in both Ctk1 depleted and in the *ctk1-D324N* expressing extracts. In agreement with the results shown in FIGURE 7, the amount of mRNPs was increased. FIGURE 11D shows that even though the reduction in 80S formation is small in Ctk1 depleted cells as well as in cells only expressing the kinase dead mutant of Ctk1, the reduction is still significant when the area of the 80S peak is measured. This result suggests that the kinase activity of Ctk1 is essential for efficient translation initiation.

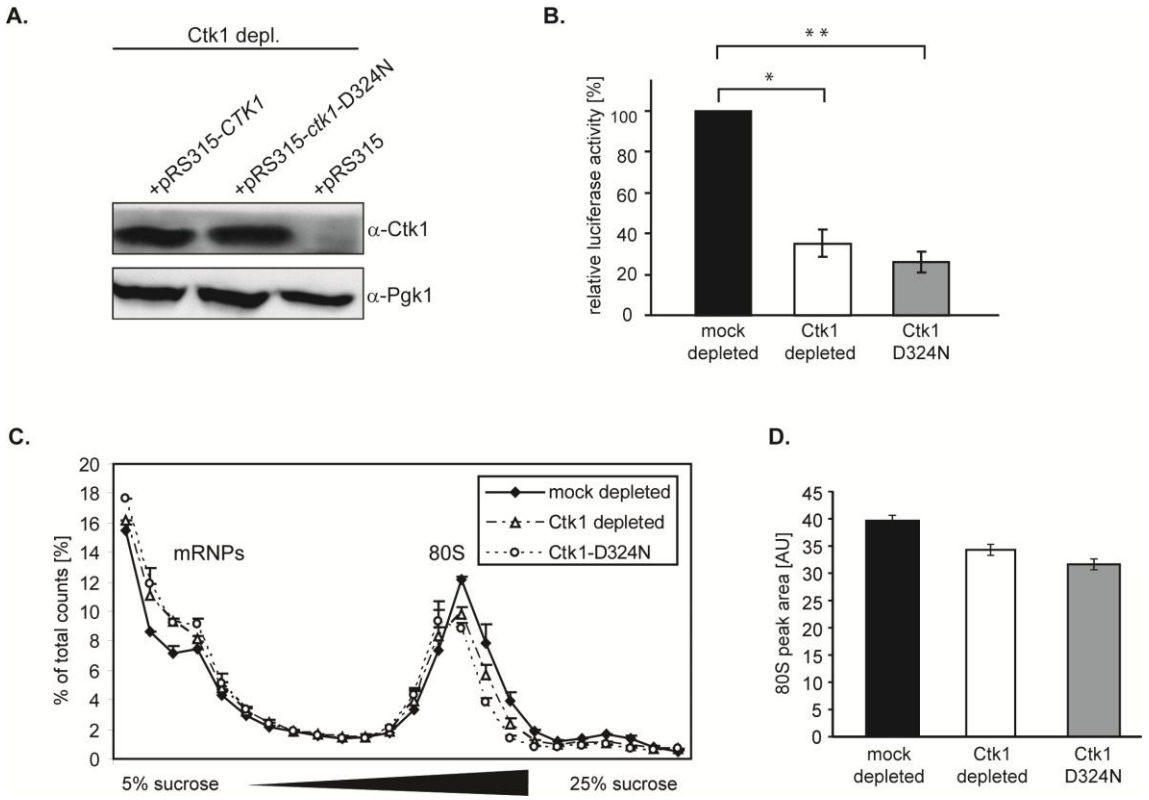

FIGURE 11: The kinase activity of Ctk1 is essential for efficient translation initiation. *A*, Cellular levels of the Ctk1 wt protein and the Ctk1 D324N mutant were similar as determined by western blotting. *B*, Translation of a luciferase reporter mRNA is reduced to 30% in Ctk1 depleted extracts as well as in extracts expressing *ctk1-D324N* after Ctk1 depletion. *C*, In comparison to mock depleted extracts (♦), Ctk1 depletion with (o) or without (Δ) additional expression of the kinase dead mutant *ctk1-D324N* lead to a decrease of mRNA incorporation into 80S initiation complexes and an increase in mRNPs. *D*, The area of the 80S peak of the gradients shown in (*C*) is reduced in Ctk1 depleted extract with or without the expression of *ctk1-D324N* compared to mock depleted extracts. The error bars represent the standard deviation of of at least three independent experiments in (*B*) and the standard deviation of at least two independent experiments in (*C* and *D*). AU: arbitrary units.

2.1.5. The translation initiation defect in Ctk1 depleted extracts is not due to the missing phosphorylation of Rps2

As phosphorylation of Rps2 on S238 is important for translation fidelity, it was analyzed whether this phosphorylation event is also important for translation initiation. To this end, extracts of cells expressing either wt *RPS2* or the non-phosphorylatable *rps2-S238A* mutant were prepared (4.2.4.1) and assessed for their general translation activity (4.2.4.2; FIGURE 12A) as well as for the formation of translation initiation intermediates (4.2.5, FIGURE 12B). In contrast to translation fidelity (Röther & Sträßer, 2007) the overall translation rate and, importantly, the formation of 48S and 80S complexes was not impaired by the *RPS2* mutation. This shows that the missing phosphorylation of Rps2 on S238 in Ctk1 depleted cells is not responsible for the translation initiation defect in Ctk1 depleted cells. Taken together, these results indicate that phosphorylation of (a) substrate(s) by Ctk1 other than Rps2 is required for efficient translation initiation.

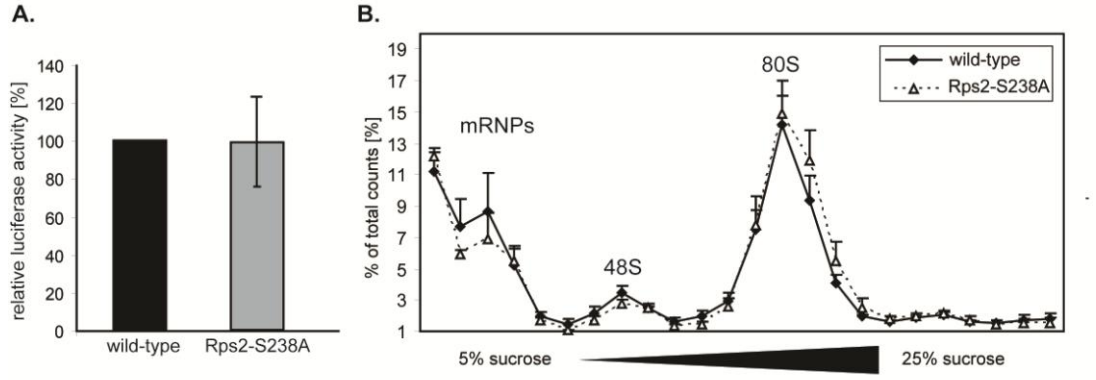

FIGURE 12: An Rps2 mutant that cannot be phosphorylated by Ctk1, Rps2-S238A, does not show a translation initiation defect. *A*, The translation of a luciferase reporter is the same in extracts of cells expressing a wt or a mutant copy of *RPS2*. *B*, Incorporation of *RPL38* mRNA into translation initiation complexes is similar in translative active extracts expressing either wt *RPS2* (♦) or *rps2-S238A* (Δ) as shown by translation initiation assays. The error bars represent the standard deviation of three independent experiments.

2.2. Ctk1 phosphorylates distinct translation initiation factors *in vitro*, but *in vivo* no substrate of Ctk1 could be identified

2.2.1. Ctk1 phosphorylates distinct translation initiation factors *in vitro*

As the Ctk1 kinase activity is important for its function in translation initiation, a candidate approach was taken to identify a substrate of Ctk1 involved in this process. For this, different translation initiation factors were tagged with a TAP tag (4.2.2.4) and initiation complexes

purified by tandem affinity (TAP) purification (4.2.8). In order to cover as many initiation factors as possible, at least one subunit of the different initiation complexes was tagged. Subsequently, either the complexes (applying a low salt wash) or single proteins (applying a high salt wash) were purified for analysis of *in vitro* phosphorylation by Ctk1 (4.2.11). The TAP purified candidate substrate(s) (complexes) are shown on an SDS-PAGE in FIGURE 13.

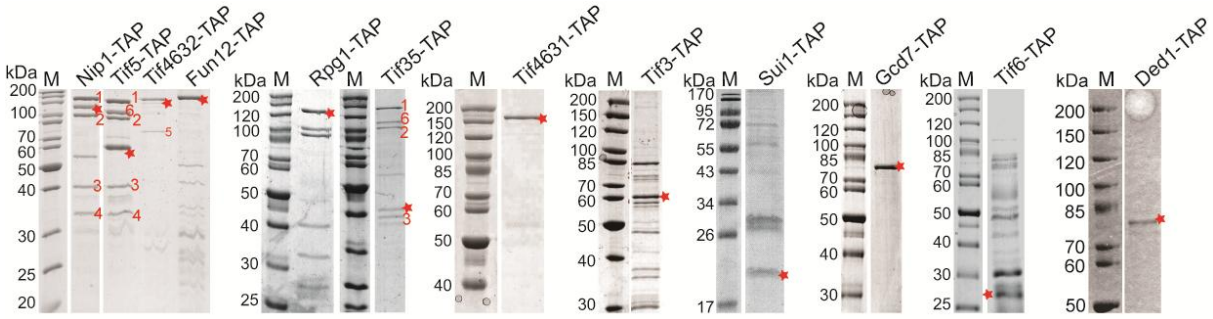

FIGURE 13: SDS-PAGE of purified translation initiation factors and complexes. The indicated TAP tagged proteins were purified by TAP purification. 10 µl concentrated calmodulin eluates were loaded in each lane and the protein carrying the CBP tag marked with an asterisk. Identified copurifiers are numbered: 1 – Rpg1; 2 – Prt1; 3 - Tif34; 4 – Tif35; 5 – Pab1; 6 – Nip1.

All purified proteins were analyzed for phosphorylation by Ctk1 in *in vitro* kinase assays. The eIF3 initiation factors Rpg1 and Nip1 (FIGURE 14A), the eIF5 member Tif5 (FIGURE 14B), the eIF4G proteins Tif4631 and Tif4632 (FIGURE 14C+D) as well as the helicase Ded1 (FIGURE 14C) were phosphorylated by Ctk1 *in vitro*.

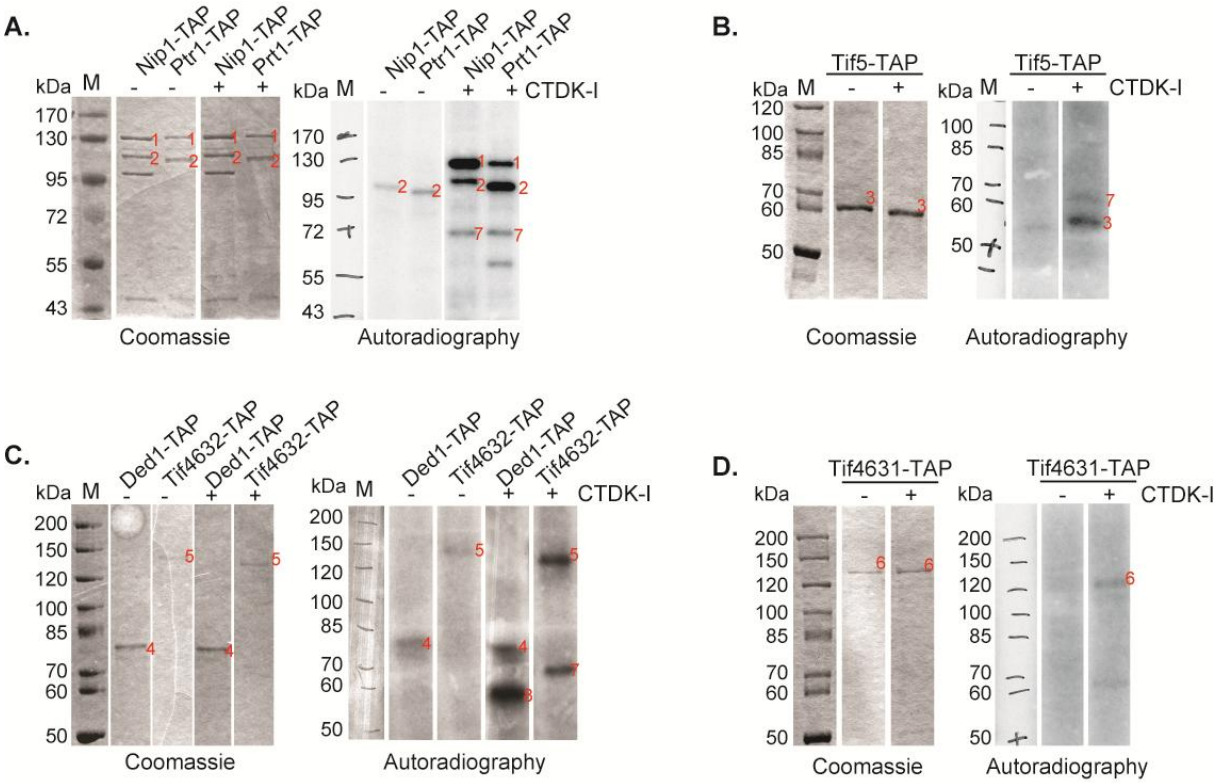

FIGURE 14: *In vitro* kinase assay of initiation factors phosphorylated by Ctk1 *in vitro*. Rpg1, Nip1 (*A*), Tif5 (*B*), Ded1, Tif4632 (*C*) and Tif4631(*D*) are phosphorylated by Ctk1 *in vitro*. Identified bands are numbered: 1 – Rpg1; 2 – Nip1; 3 – Tif5; 4 – Ded1; 5 -5 Tif4632; 6 – Tif4631; 7 – Ctk1-CBP; 8 – Ctk1; CBP – calmodulin binding protein.

2.2.2. *In vivo*, no phosphorylation by Ctk1 of the identified *in vitro* substrates of Ctk1 can be detected

The initiation factors, which were phosphorylated by Ctk1 *in vitro*, were further tested for *in vivo* phosphorylation by Ctk1. Cultures with tagged candidate proteins were grown in phosphate depleted media followed by growth in media containing radioactively labeled orthophosphate for labeling of newly phosphorylated proteins. Then, candidate proteins were purified with IgG beads in a mock depleted and Ctk1 depleted background and directly eluted from the beads with SDS containing buffer (4.2.12.1). As can be seen in FIGURE 15, Nip1 is the only candidate protein that is a phosphoprotein *in vivo*. However, there was no reduction in phosphorylation of Nip1 visible upon Ctk1 depletion (FIGURE 15A). In the case of Tif5, only the copurifier Gcd11 (eIF2γ), which has approximately the same size as Tif5, was a phosphoprotein *in vivo*. Tif5 itself was not phosphorylated (FIGURE 15B).

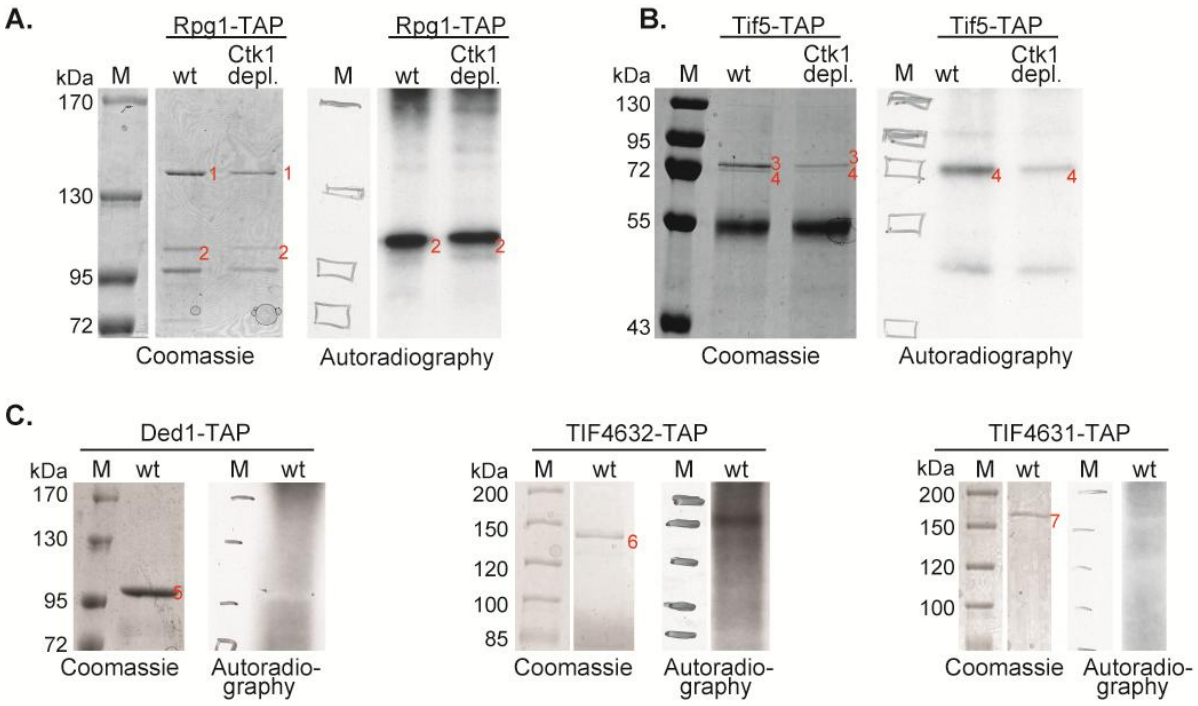

FIGURE 15: *In vivo* kinase assay of translation initiation factors that are phosphorylated by Ctk1 *in vitro*. *A*, Nip1 is a phosphoprotein *in vivo*, but the phosphorylation is not reduced upon Ctk1 depletion. *B*, Not Tif5, but a copurifier is phosphoprotein *in vivo*. *C*, Ded1, Tif4632 and Tif4631 are no phosphoproteins *in vivo*. Identified bands are numbered: 1 – Rpg1-TAP; 2 -2 Nip1; 3 – Tif5-TAP; 4 – Gcd11; 5 -5 Ded1-TAP; 6 – Tif4632-TAP; 7 – Tif4631-TAP.

TABLE 1 summarizes the candidate approach of finding a substrate of Ctk1 that is involved in translation initiation. For none of the six proteins phosphorylated by Ctk1 *in vitro*, a reduction in phosphorylation could be detected *in vivo* upon Ctk1 depletion. In the case of Nip1, the phosphorylation was also compared *in vivo* between a wt and a *Δctk1* background, but here as well, no reduction was detectable (data not shown). Part of the *in vitro* and *in vivo* kinase assays shown here were carried out by Katharina Brünger (Sträßer lab).

TABLE 1: Analysis of candidate translation initiation factors for phosphorylation by Ctk1.

Proteins analyzed	complex	*In vitro* kinase	*In vivo* kinase
Sui1	eIF1	probably negative	not assessed
Gcd11	eIF2	probably negative	phosphorylated in *vivo*, but phosporylation does not change upon Ctk1 depletion
Gcd7	eIF2B	negative	
Rpg1	eIF3	positive	not phosphorylated *in vivo*
Prt1	eIF3	negative	
Nip1	eIF3	positive	phosphorylated in *vivo*, but phosporylation does not change upon Ctk1 depletion
Tif34	eIF3	negative	
Tif35	eIF3	negative	
Tif3	eIF4B	negative	
Tif4631	eIF4G	weakly phosphorylated	not phosphorylated *in vivo*
Tif4632	eIF4G	weakly phosphorylated	not phosphorylated *in vivo*
Tif5	eIF5	positive	not phosphorylated *in vivo*
Fun12	eIF5B	negative	
Tif6	eIF6	probably negative	not assessed
Ded1		weakly phosphorylated	not phosphorylated *in vivo*

2.3. Ctk1 depletion causes reduced phosphorylation of proteins involved in ribosome biogenesis and translation, but Ctk1 is not involved in rRNA processing

2.3.1. Ctk1 depletion causes reduced phosphorylation of proteins involved in ribosome biogenesis and translation

As a second, unbiased approach to identify a possible substrate of Ctk1 that accounts for the translation initiation defect of Ctk1 depleted cells, a proteomic method was employed. The phosphorylation status of ribosomes and ribosome associated proteins in mock and Ctk1 depleted cells was analyzed using stable isotope labeling with amino acids in cell culture (SILAC) and subsequent mass spectrometry. To compare the phosphorylation status of proteins derived from mock and Ctk1 depleted cells, one culture was grown in media containing light lysine and the other in media containing heavy lysine. After cell lysis, the extracts of the two strains were combined for the purification, which reduces unspecific variations in the phosphorylation patterns of wt and mutant strain caused by differences in the

preparation. 40S, 60S, and 80S ribosomes were prepared by subsequent centrifugation steps with a sucrose density gradient as a final purification step. A high salt wash was omitted in this assay to allow more loosely associated proteins to remain bound to the ribosome. Fractions of the sucrose gradient containing 40S, 60S, and 80S ribosomes were pooled and digested with LysC. The phosphopeptides were enriched and analyzed by LC-MS/MS. The amino acids with a different phosphorylation level were determined and the phosphorylation ratio between mock and Ctk1 depleted samples calculated (FIGURE 16; 4.2.13). The sample preparation was done by Katharina Brünger (Sträßer lab) and the mass spectrometric and computational analysis carried out by Boumediene Soufi (present address: Genentech Inc., San Francisco, USA) and Jesper V. Olsen (NNF Center for Protein Research, Copenhagen, Denmark).

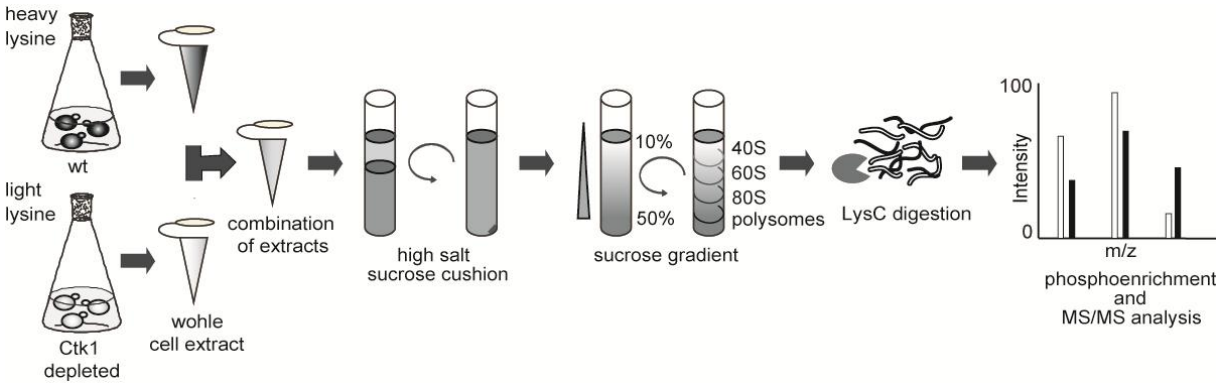

FIGURE 16: Flow scheme of the preparation of a ribosome enriched fraction for SILAC mass spectrometry.

The LC-MS/MS analysis of these samples showed that a multitude of proteins changed their phosphorylation pattern upon Ctk1 depletion (SUPPLEMENTAL TABLE 1). Interestingly, a number of ribosomal proteins and proteins involved in ribosome biogenesis contained phosphorylation sites that were less phosphorylated in Ctk1 depleted cells (TABLE 2). Importantly, the reduction in phosphorylated peptides of these proteins should not be caused by a diminished association of these proteins with the ribosome, because the phosphorylation of other residues of the same proteins remained unchanged (SUPPLEMENTAL TABLE 1). Furthermore, these data verify that ribosomes and translation initiation factors of Ctk1 depleted cells do not exhibit the phosphorylation pattern typical for stressed cells, such as eIF2α (Hinnebusch, 2005) and decreased Rps6 phosphorylation (Urban et al., 2007; reviewed in Meyuhas, 2008), corroborating that the initiation defect is specific to the loss of Ctk1 and not to a general stress response triggered by depletion of Ctk1.

The proteins listed in TABLE 2 represent proteins, which cover the entire process of ribosome biogenesis – rDNA transcription, rRNA modification, subunit maturation in the nucleus, export, and maturation in the cytoplasm (1.6). Additionally, some proteins with functions implicated directly in translation were less phosphorylated upon Ctk1 depletion (TABLE 2).

TABLE 2: List of proteins involved in ribosome biogenesis or translation that contain phosphosites that are less phosphorylated upon Ctk1 depletion and analyzed as candidate substrates.

Protein	Function	Site	Phosphorylation compared to wt*
Cbf5	pseudouridine synthase subunit of H/ACA snoRNP	T423	0.55 +/-0.15
Pop1	cleavage of pre-rRNA and tRNA	T524	0.45 +/-0.06
Nop13	nucleolar protein found in preribosomal complexes	S2	0.56 +/-0.17
Nop53	nucleolar protein involved in 60S biogenesis	S31	0.64 +/-0.18
Srp40	nucleolar protein, role in preribosome assembly or transport	S133	0.71 +/-0.15
Nop16	constituent of 66S pre-ribosomal subunits	T152	0.58 +/-0.28
		S176	0.52 +/-0.13
Cic1	copurifies with 66S pre-ribosomal particles	T11	0.70 +/-0.13
		S17	0.63 +/-0.05
		S359	0.66 +/-0.19
		S366	0.77 +/-0.25
Sda1	actin skeleton organization, involved in 60S ribosome biogenesis	S591	0.65 +/-0.15
Jjj1	co-chaperone required for a late step in ribosome biogenesis	S393	0.83 +/-0.08
		T504	0.77 +/-0.07
Rei1	cytoplasmic pre-60S factor	T111	0.64 +/-0.10
Mrs6	regulates the transcription factor Sfp1 controlling genes involved in ribosome biogenesis	S470	0.35 +/-0.09
Ltv1	required for 40S export from nucleus	S281	0.63 +/-0.19
Stm1	required for translation under nutrient stress	S55	0.55 +/-0.07
Rps16a/b	ribosomal protein	S2	0.57 +/-0.01
Rps17a/b	ribosomal protein	S70	0.59 +/-0.05
Rps18a/b	ribosomal protein	S107	0.82 +/-0.12
Rps24a/b	ribosomal protein	S14	0.73 +/-0.13
Rps1a/b	ribosomal protein	S36	0.70 +/-0.05
		S/T245	0.87 +/-0.05
		T254	0.75 +/-0.07
Rps5	ribosomal protein	T4	0.85 +/-0.09
Rps6a/b	ribosomal protein	T163	0.57 +/-0.02
Rps8a/b	ribosomal protein	T132	0.58 +/-0.29
Rps9a/b	ribosomal protein	S9	0.61 +/-0.05
Rps11a/b	ribosomal protein	S9	0.86 +/-0.11
		T44	0.62 +/-0.07

*Error values represent the standard deviation of 2-6 experiments.

Since the aim was to identify a substrate of Ctk1 important for efficient translation initiation, all proteins listed in TABLE 2 were considered possible candidates. Proteins of the large ribosomal subunit were not considered since *in vitro* Ctk1 only phosphorylates proteins of the small ribosomal subunit (data not shown). Cbf5, Nop13, Rei1, Cic1, Sda1, Nop53, Stm1 and Ltv1 were C-terminally TAP tagged (4.2.2.4) and purified under control of their endogenous promoter in a TAP purification until TEV cleavage (4.2.10). Pop1 was N-terminally tagged and overexpressed via a *GAL1* promoter (4.2.2.4). Nop16 and Srp40 were purified from *E.coli*, Nop16 with a C-terminal His-tag and Srp40 with an N-terminal GST-tag (4.2.10). The ribosomal proteins were purified via a sucrose cushion (4.2.9.). Each of the purified protein (complex) is shown on an SDS-PAGE in FIGURE 17.

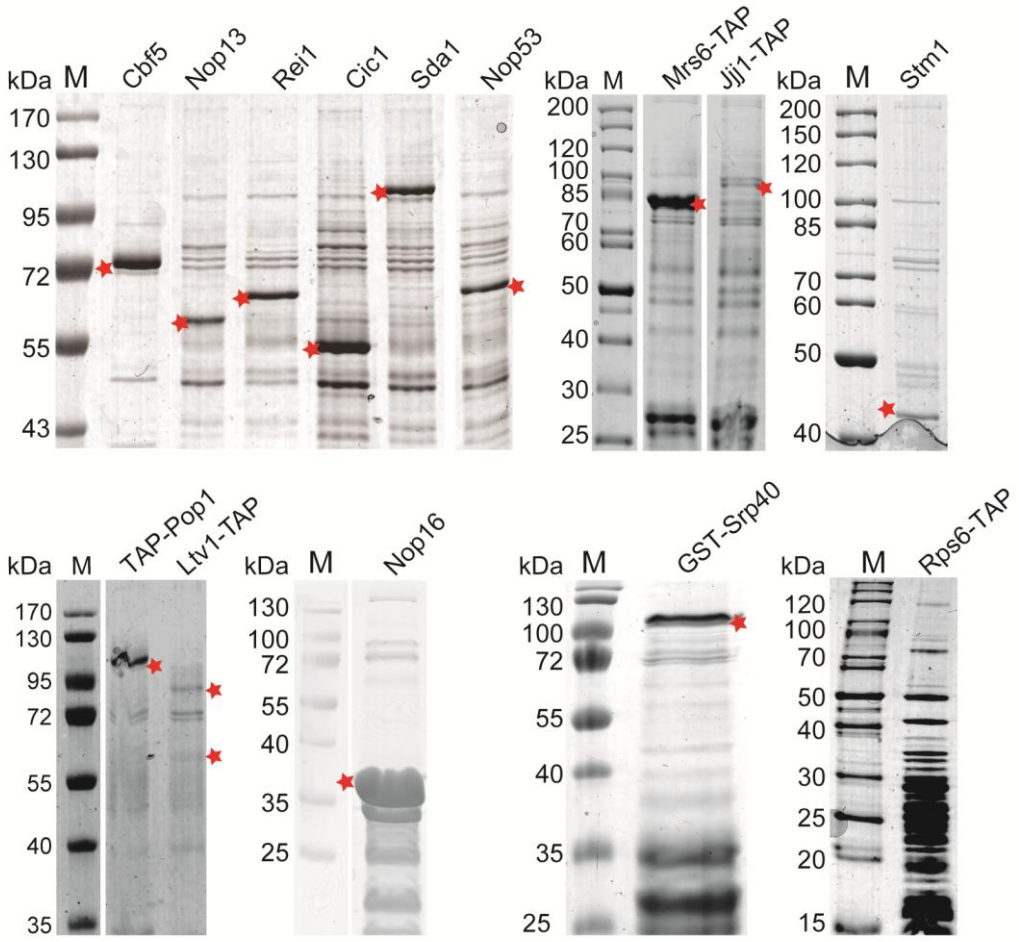

FIGURE 17: SDS-PAGE of purified candidate substrates of Ctk1 derived from the SILAC screen. The tagged proteins are marked with an asterisk. As an example of ribosome purification via a sucrose cushion, an Rps6-TAP strain was taken.

All proteins were tested for direct phosphorylation by Ctk1 in *in vitro* kinase assays with purified CTDK-I complex and the candidate substrate (4.2.11). Three of the 25 candidate

substrates tested were directly phosphorylated by Ctk1 – namely Sda1, Mrs6 and Ltv1 (FIGURE 18). Next, it was assessed whether these three proteins were phosphorylated by Ctk1 on the site identified by the mass spectrometric analysis.

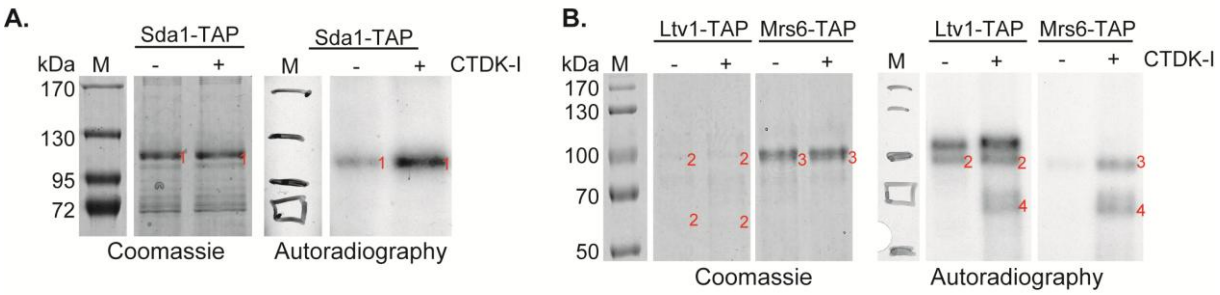

FIGURE 18: Positive *in vitro* kinase assay of candidate substrates of Ctk1 derived from the SILAC screen. Sda1 (*A*), Ltv1, Mrs6 (*B*) are phosphorylated by Ctk1 in *in vitro* kinase assays. Identified bands are numbered: 1 – Sda1; 2 – Ltv1; 3 – Mrs6; 4 – Ctk1.

Therefore, serine to alanine mutants of the three proteins phosphorylated by Ctk1 *in vitro* were created and tested for *in vitro* phosphorylation by Ctk1. However, all three mutants showed unchanged phosphorylation by Ctk1 (FIGURE 19). This indicates that the decreased *in vivo* phosphorylation of the site upon Ctk1 loss as determined by the SILAC analysis is likely not due to a direct phosphorylation by Ctk1.

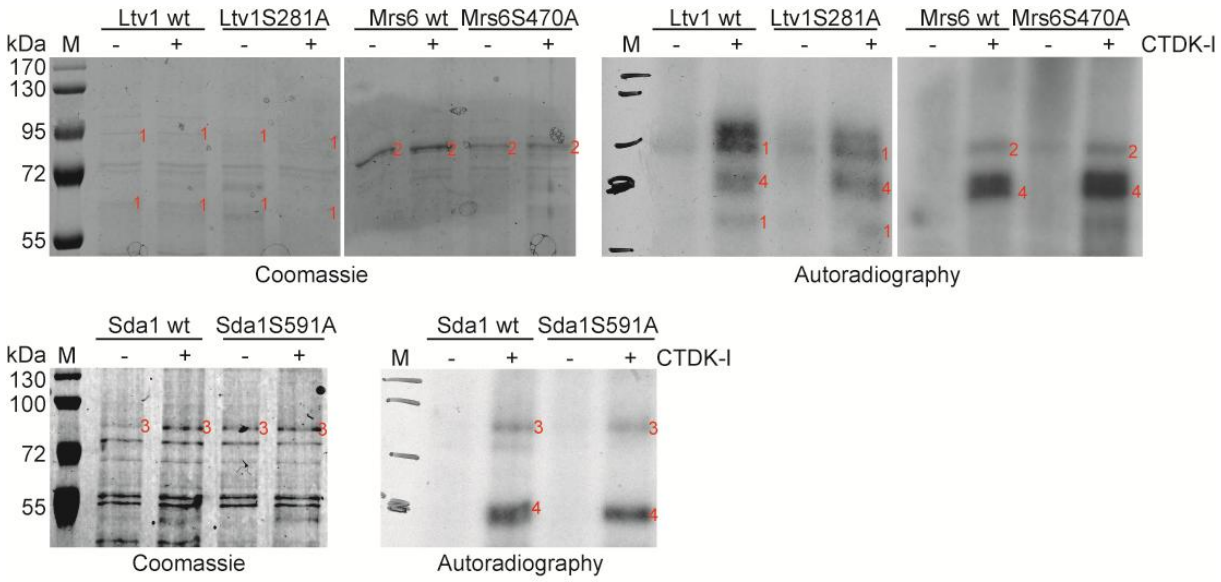

FIGURE 19: **Candidate substrates of Ctk1 derived from the SILAC screen, which are directly phosphorylated by *Ctk1 in vitro*, are not phosphorylated by Ctk1 on the phosphosite identified in the SILAC screen**. *In vitro* kinase assay of serine to alanine mutants of candidate proteins on the phosphosites determined by SILAC analysis. Identified bands are numbered: 1 – Ltv1; 2 – Mrs6; 3 – Sda1; 4 – Ctk1.

The results of the purification and the *in vitro* kinase assays are summarized in TABLE 3. None of the candidate substrates of Ctk1 identified by SILAC that have a function in ribosome biogenesis or translation are phosphorylated by Ctk1 on the phosphosite derived from the SILAC screen.

TABLE 3: Proteins analyzed, that contain phosphosites that are less phosphorylated upon Ctk1 depletion. The proteins are involved in ribosome biogenesis or translation. If not indicated differently, the proteins were purified via TAP-purification.

Protein	Purification	*In vitro* kinase assay	Does Ctk1 phosphorylate the candidate on the phosphosite determined by SILAC?
Cbf5	Cbf5-TAP	negative	
Pop1	Overexpression *GAL1*::Pop1-TAP	negative	
Nop13	Nop13-TAP	negative	
Nop53	Nop53-TAP	negative	
Srp40	Overexpression in *E.coli* with pGEX4T-2-Srp40	negative	
Nop16	Nop16-TAP	negative	
Cic1	Cic1-TAP	negative	
Sda1	**Sda1-TAP**	**positive**	**no**
Jjj1	Jjji1-TAP	negative	
Rei1	Rei1-TAP	negative	
Mrs6	**Mrs6-TAP**	**positive**	**no**
Ltv1	**Ltv1-TAP**	**positive**	**no**
Stm1	Stm1-TAP	negative	
Rps16a/b	Rps16a-TAP, purification with sucrose cushion	negative	
Rps17a/b	Rps17b-TAP, purification with sucrose cushion	negative	
Rps18a/b	Rps18a-TAP, purification with sucrose cushion	negative	
Rps24a/b	Rps24a-TAP, purification with sucrose cushion	negative	
Rps1a/b	Rps1a-TAP, Rps1b-TAP, purification with sucrose cushion	negative	
Rps5	Rps5-TAP, purification with sucrose cushion	negative	
Rps6a/b	Rps6a-TAP, purification with sucrose cushion	negative	
Rps8a/b	Rps8a-TAP, Rps8b-TAP	negative	
Rps9a/b	Rps9b-TAP	negative	
Rps11a/b	Rps11a-TAP	negative	

2.3.2. In contrast to the depletion of Bur2, Ctk1 depletion does not cause rRNA processing defects

Since the phosphorylation status of many proteins involved in ribosome biogenesis changed due to Ctk1 depletion (TABLE 2), it was analyzed whether defective ribosome biogenesis could be the cause of the translation initiation defect in Ctk1 depleted extracts. To test whether rRNA processing is affected upon Ctk1 depletion, pulse chase experiments with mock and Ctk1 depleted cells were performed (4.2.14). Cells were grown in phosphate depleted media and labeled for 5 minutes with radioactive phosphate. As a control, cells depleted of Bur2 were analyzed. FIGURE 20A shows that, as in the case of Ctk1, depletion of Bur2 for 18 h lead to complete loss of the protein. Newly formed rRNA intermediates were resolved on a gel and the intensity of the different bands measured (FIGURE 20B+C).

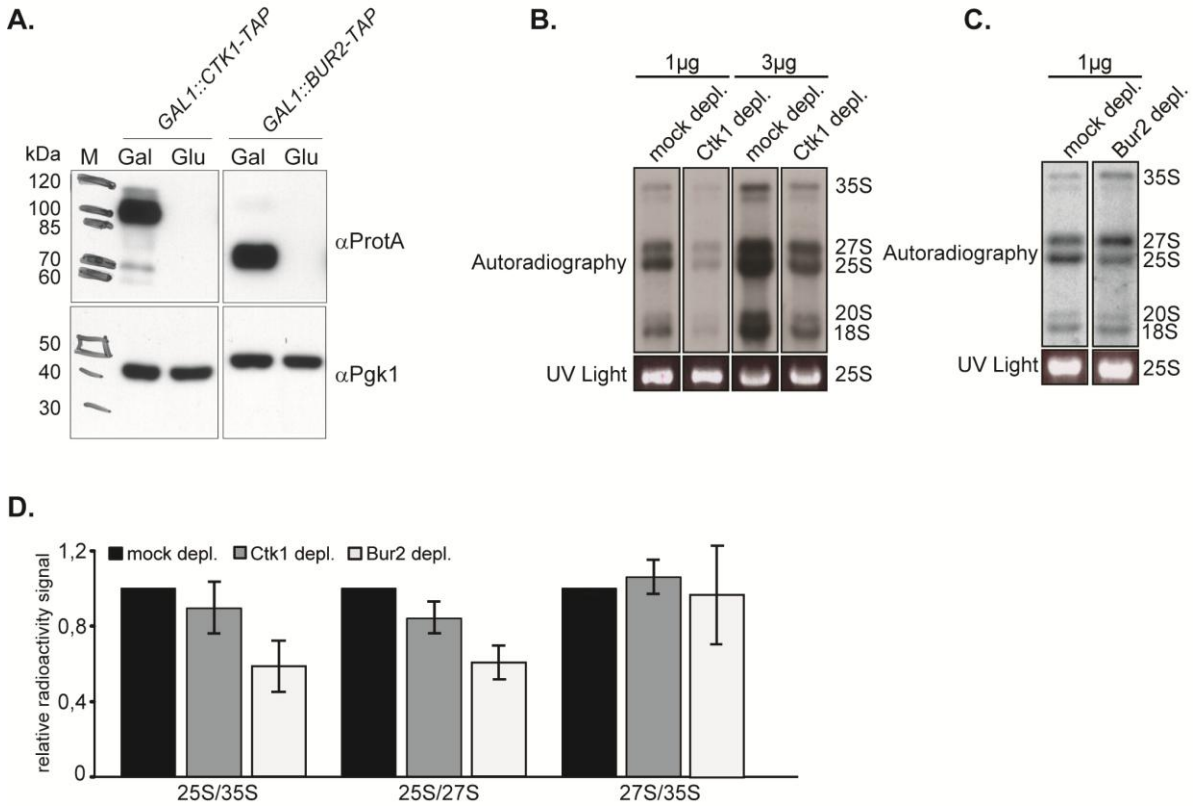

FIGURE 20: Bur2 depleted, but not Ctk1 depleted cells have an rRNA processing defect. Upon 18 hours of glucose depletion of *GAL1* driven expression of *BUR2* or *CTK1*, no protein can be detected on western blot level (*A*). The amount of PolI transcript is reduced, but the ratio of the different rRNA intermediates is similar in Ctk1 depleted cells (*B*) whereas in Bur2 depleted cells, overall PolI transcription stays the same and the ratio of the different rRNA intermediates was changed (*C*) as shown by autoradiography after radioactive labeling of newly formed rRNA . *D*, Quantification of the ratio of rRNA intensities shown in (*B*) and (*C*).

Consistent with previous studies (Bouchoux et al., 2004; Grenetier et al., 2006), the PolI transcription rate was decreased in cells lacking Ctk1 as can be seen by the decreased level of 35S RNA and all further processing products (FIGURE 20B). Importantly, however, the ratios of RNA intermediates (25S/35S, 25S/27S, and 27S/35S) did not change significantly upon Ctk1 depletion (FIGURE 20D). Thus, the different phosphorylation pattern of proteins involved in ribosome biogenesis did not cause a major defect in rRNA processing. Surprisingly, however, depletion of Bur2 resulted in a decrease of 25S rRNA compared to the other rRNA intermediates, indicating that the Bur1-2 complex is involved in rRNA processing. Unlike in the case of Ctk1 depletion, Bur2 depletion did not cause a PolI transcription defect.

The radioactive labeling and the analysis of the radioactive signals were done by Kaspar Burger (Eick lab, Helmholtz Center Munich).

2.4. Ctk1 depleted extracts have an increased sensitivity to RNAse compared to mock depleted extracts

In order to obtain a hint whether the different phosphorylation pattern of proteins involved in ribosome biogenesis and the ribosome itself results in an alteration of the ribosome integrity, the RNAse sensitivity of translation active extracts of mock depleted and Ctk1 depleted was measured. The extracts were treated with micrococcal nuclease for 15 min and the reaction was stopped with the addition of EGTA. Subsequently, the translation activity of the extracts was assessed by the translation of *in vitro* transcribed luciferase mRNA (4.2.4.2).

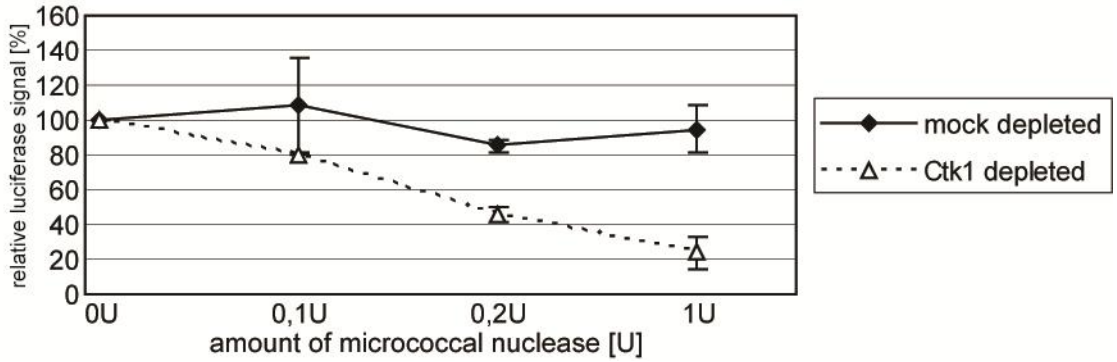

FIGURE 21: Translation active extracts of Ctk1 depleted cells are more sensitive to micrococcal nuclease than mock depleted extracts. Extracts were treated with micrococcal nuclease prior to *in vitro* translation of *in vitro* transcribed luciferase mRNA.

As shown in FIGURE 21, Ctk1 depleted extracts are more sensitive to micrococcal nuclease treatment than mock depleted extracts. Their ability to translate luciferase mRNA is reduced after treatment with the nuclease. This could have several reasons, but indicates that the ribosome is more prone to RNA degradation in Ctk1 depleted compared to wt extracts.

2.5. Depletion of the Bur1-Bur2 complex leads to a similar translation initiation defect as CTDK-I depletion

The CTDK-I complex and the Bur1-Bur2 complex have similar, but not identical functions and were thought to possess the same homologue in higher eukaryotes (1.5). It is a matter of current research how their functions in yeast differ. To test whether the function in translation initiation is the same for Bur1-Bur2 and CTDK-I, translation active extracts of a Bur2 depleted strain were prepared and tested for *in vitro* translation of a luciferase reporter and for translation initiation in a translation initiation assay (4.2.4, 4.2.5).

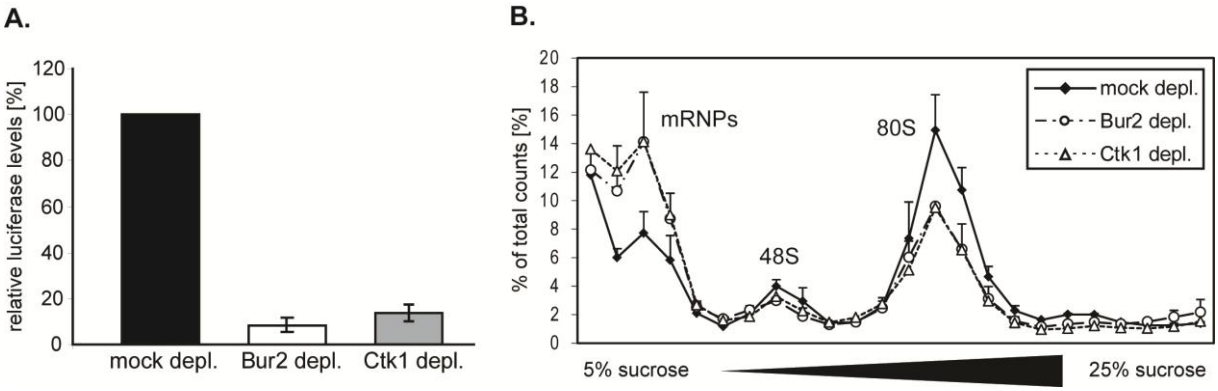

FIGURE 22: Depletion of Bur2 leads to reduced translation activity of translation active extracts. *A*, Luciferase assay of Bur2 and Ctk1 depleted compared to mock depleted translation active extracts. *B*, Initiation assay of Bur2 and Ctk1 depleted compared to mock depleted extracts. Error bars represent the standard deviation of two independent experiments.

As can be seen in FIGURE 22, translation active extracts of Bur2 depleted cells had a reduced translation rate of a luciferase reporter similar to Ctk1 depleted extracts (FIGURE 22A) and, as Ctk1 depleted translation active extracts, showed reduced 80S formation in an initiation assay (FIGURE 22B). In this assay, an RS453 wt background strain was used and not, as in all former experiments with Ctk1 depleted extracts, a W303 genetic background. Apparently, this lead to a rather reduced 48S formation in Ctk1 depleted and Bur2 depleted extracts (FIGURE 22B) compared to mock depleted and not to an increased 48S formation as observed before (FIGURE 7). In summary, Ctk1 depletion and Bur2 depletion most likely cause the same phenotype in translation initiation.

2.6. Ctk1 and Npl3 most likely have antagonistic functions in the nucleus and Npl3 is an *in vitro* substrate of Ctk1

2.6.1. *CTK1* and *NPL3* interact genetically

Npl3 is a nucleo-cytoplasmic shuttling protein known to function in transcription termination and nuclear mRNP processing and was implicated to have an additional role in translation (1.7). Since it has similar functions in gene expression as Ctk1, Npl3 might be an interaction partner or a direct substrate of Ctk1, which is involved in translation or in another process in gene expression. It could also be that the two proteins interact in another way than being kinase and substrate and still be important for a specific step in gene expression.

To test a possible interaction of Npl3 and Ctk1, a genetic approach was employed. There are several methods to assess a genetic interaction between two genes. In the case of synthetic lethality or synthetic sickness, both genes of interest are mutated leading to their reduced function. If the combination of the mutations in the candidate genes results in a more pronounced growth defect than the single mutations, the two genes are synthetic sick. If cells with single mutations are viable but cells containing both mutations die, the two genes are synthetic lethal. A synthetic lethality or sickness phenotype is an indication that the gene products interact with each other also physically or function in the same or in redundant pathways. Cells with a deletion of either *CTK1* or *NPL3* are already very sick so that a combination of the two mutants could not be generated. In order to nonetheless analyze a potential genetic interaction between *CTK1* and *NPL3*, Npl3 was overexpressed in *Δctk1* cells to assess whether this rescues the *Δctk1* slow growth phenotype by performing dot spots (4.2.15). Unexpectedly, the opposite was the case. As shown in FIGURE 23A, plasmid-based overexpression of Npl3 under control of the *GAL1* promoter (YCplac plasmid) in galactose containing media (SGC-Trp) is lethal in combination with a deletion of *CTK1*. It can also be seen, however, that the overexpression of Npl3 in the wt background already leads to reduced growth.

It is already known that Ctk1 and Npl3 interact physically (Tardiff et al., 2007) and in order to assess this interaction in more detail, a genomically TAP tagged strain of Npl3 was generated. Strikingly, it was observed that the introduction of a C-terminal TAP tag on Npl3 rescues the Δ*ctk1* phenotype (FIGURE 23B). As a control, the TAP tag was also introduced at the N-

terminus of Npl3. However, this did not influence the growth of Δ*ctk1* cells. Thus, the C-terminal TAP tag introduces a characteristic to Npl3 that causes a rescue of the Δ*ctk1* phenotype.

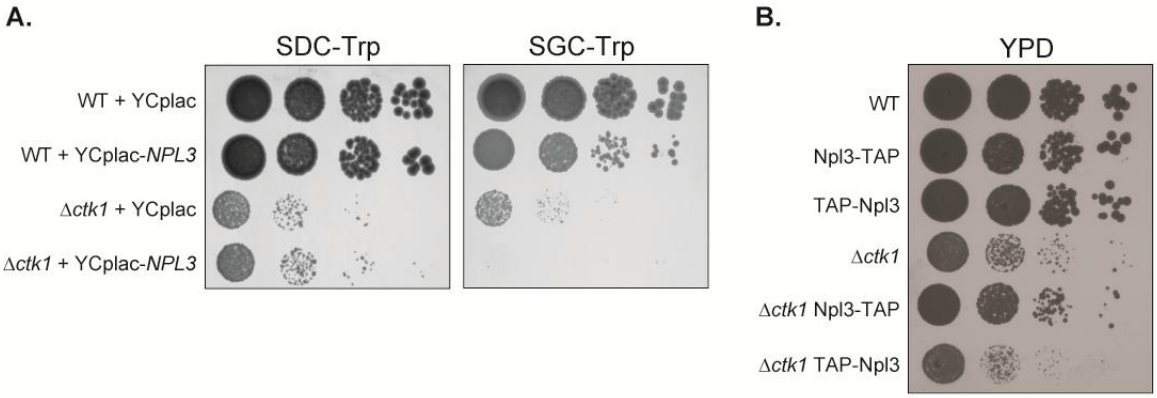

FIGURE 23: Overexpression of Npl3 is synthetic lethal with the deletion of *CTK1* and a C-terminal TAP tag on Npl3 rescues the Δ*ctk1* slow growth phenotype. *A,* Npl3 expressed under control of a *GAL1* promoter (YCplac plasmid) is synthetic lethal with a *CTK1* deletion when grown on galactose containing media (SGC-Trp). *B,* A C-terminal, but not an N-terminal TAP tag rescues the slow growth phenotype of *Δctk1* cells.

2.6.2. A C-terminal TAP tag leads to the mislocalization of Npl3 to the cytoplasm

Npl3 shuttles between the nucleus and the cytoplasm, but is mainly nuclear at steady state. Its reimport to the nucleus is mediated by the import factor Mtr10, which binds to the C-terminus of Npl3 (1.7). In order to assess whether the TAP tag on the C-terminus of Npl3 inhibits Mtr10 binding and thus also its nuclear reimport, the localization of wt Npl3, Npl3-TAP and TAP-Npl3 was analyzed.

Strikingly, the C-terminal TAP Tag on Npl3 indeed leads to mislocalization of Npl3 to the cytoplasm whereas Npl3 is still nuclear when expressed with an N-terminal TAP tag (FIGURE 24). Thus, only the Npl3 mutant mislocalized to the cytoplasm is able to suppress the Δ*ctk1* slow growth phenotype (FIGURE 23B). Consequently, it could be that Npl3 and Ctk1 have antagonistic functions in the nucleus, meaning that it is important to maintain a certain ratio of Npl3 and Ctk1 molecules in the nucleus. This is in agreement with the notion that overexpression of Npl3 is toxic in a Δ*ctk1* background (FIGURE 23A). On the other hand, increased Npl3 levels in the cytoplasm might rescue loss of Ctk1 function in translation. If the two proteins have synergistic functions in this compartment, the suppression of Δ*ctk1* slow growth by cytoplasmic Npl3 could also be explained.

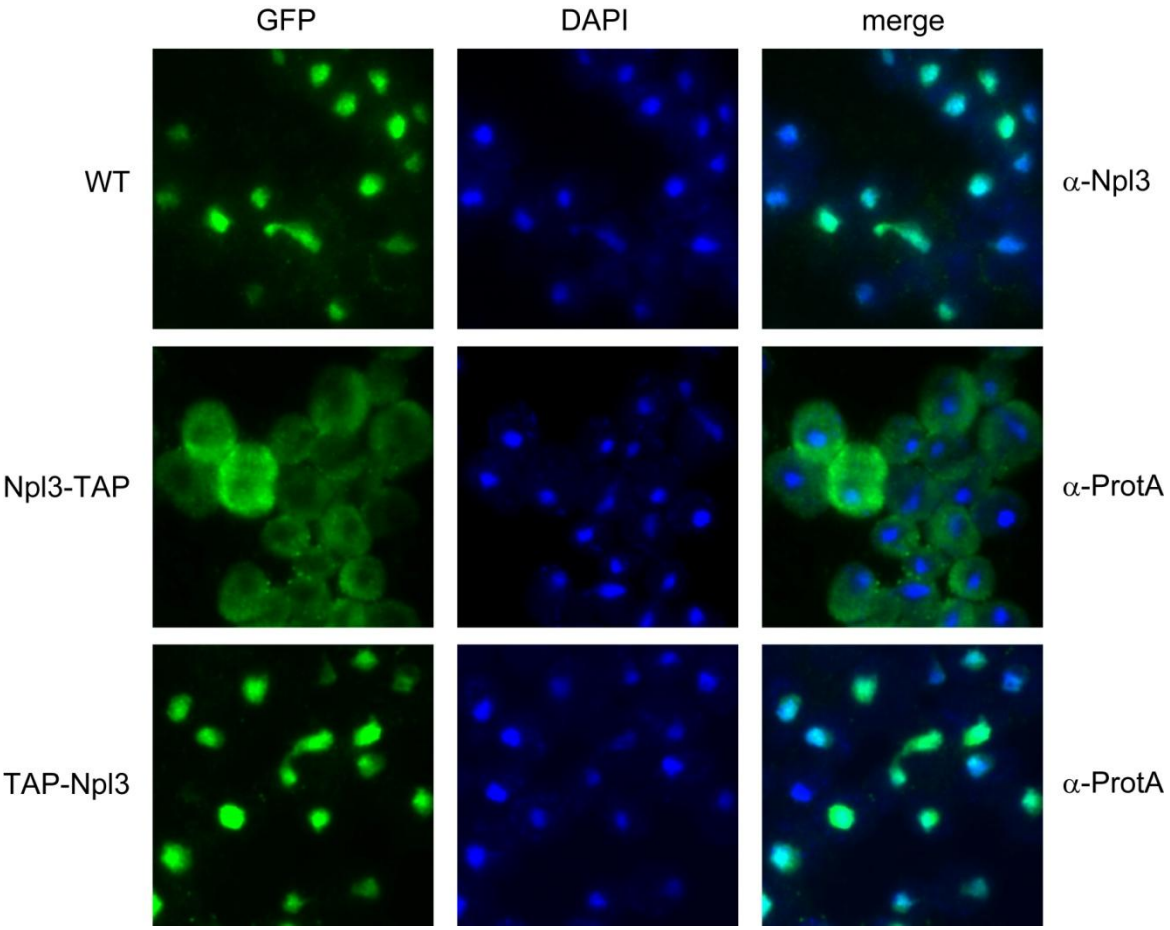

FIGURE 24: In contrast to an N-terminal TAP tag, a C-terminal TAP tag on Npl3 leads to its mislocalization to the cytoplasm. Indirect immunofluorescence with an antibody against Npl3 or the ProteinA tag on Npl3. The nucleus is stained with DAPI (4',6-Diamidine-2'-phenylindole Dihydrochloride). GFP: green fluorescence protein;

2.6.3. Ctk1 phosphorylates Npl3 on S349, S356 and S411

As Ctk1 and Npl3 interact physically and genetically, they might also interact functionally. To test this, Npl3 was analyzed as a possible substrate of the Ctk1 kinase. FIGURE 25B shows that *in vitro*, Npl3 is a substrate of Ctk1 (4.2.11).

There has been reported a role for Npl3 in translation and especially in subunit joining during translation initiation depending on its C-terminus. According to Gross, PhD thesis 2009, the homodimerization of Npl3 is necessary for its function in subunit joining (1.7). The amino acids (AA) important for this function are localized between C-terminal AA50 and AA75 as assessed by C-terminal truncations of Npl3 (Gross, PhD thesis, 2009). It could be that the phosphorylation of Npl3 by Ctk1 is crucial for this function of Npl3 in translation initiation. In order to analyze whether the phosphosite(s) of Npl3 phosphorylated by Ctk1 are localized

within the amino acids important for Npl3 homodimerization, C-terminal truncations of Npl3 were tested as substrates of Ctk1 (FIGURE 25A, marked in color).

A.

```
1   MSEAQETHVE QLPESVVDAP VEEQHQEPPQ APDAPQEPQV PQESAPQESA
51  PQEPPAPQEQ NDVPPPSNAP IYEGEESHSV QDYQEAHQHH QPPEPQPYYP
101 PPPPGEHMHG RPPMHHRQEG ELSNTRLFVR PFPLDVQESE LNEIFGPFGP
151 MKEVKILNGF AFVEFEEAES AAKAIEEVHG KSFANQPLEV VYSKLPAKRY
201 RITMKNLPEG CSWQDLKDLA RENSLETTFS SVNTRDFDGT GALEFPSEEI
251 LVEALERLNN IEFRGSVITV ERDDNPPPIR RSNRGGFRGR GGFRGGFRGG
301 FRGGFSRGGF GGPRGGFGGP RGGYGGYSRG GYGGYSRGGY GGSRGGYDSP
351 RGGYDSPRGG YSRGGYGGPR NDYGPPRGSY GGSRGGYDGP RGDYGPPRDA
401 YRTRDAPRER SPTR*
```

B.

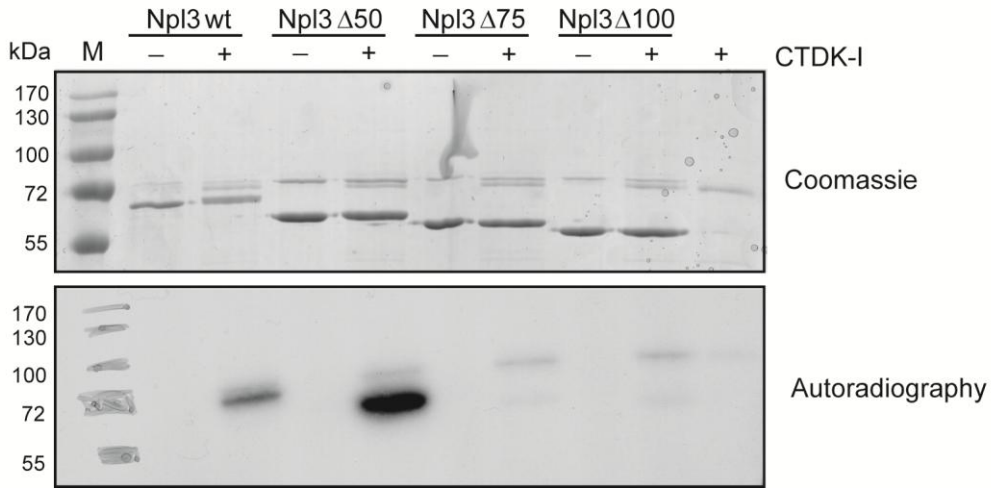

FIGURE 25: Npl3 is phosphorylated by Ctk1 *in vitro* within the C-terminal AA 50-75. *A*, Protein sequence of Npl3. Green: C-terminal 50 AA, blue: C-terimanl AA 50-75, orange: C-terminal AA 75-100, red: SP sites with a serine phosphorylated by Ctk1. *B*, *In vitro* kinase assay of C-terminal truncations of Npl3 by Ctk1.

Strikingly, a C-terminally TAP tagged Npl3 lacking the last 50 AA (Npl3Δ50-TAP), but not the last 75AA (Npl3Δ75-TAP) could still be phosphorylated by Ctk1 (FIGURE 25B). This indicates that the phosphorylation site of Ctk1 is localized between AA339 and AA364. In this stretch of AA (FIGURE 25A marked in blue), there are four serines, two of them (S349 and S356) being followed by a proline, thus matching the Ctk1 kinase motif (marked in red). These two serines were considered as probable phosphorylation sites and an S349A as well as an S356A mutant was analyzed for phosphorylation by Ctk1. Interestingly, the single mutated versions of Npl3 still served as substrates for Ctk1 in *in vitro* kinase assays (4.2.11), whereas the double mutations (S349A-S356A) did not (FIGURE 26A). This shows that Ctk1

phosphorylates Npl3 on S349 as well as on S356.

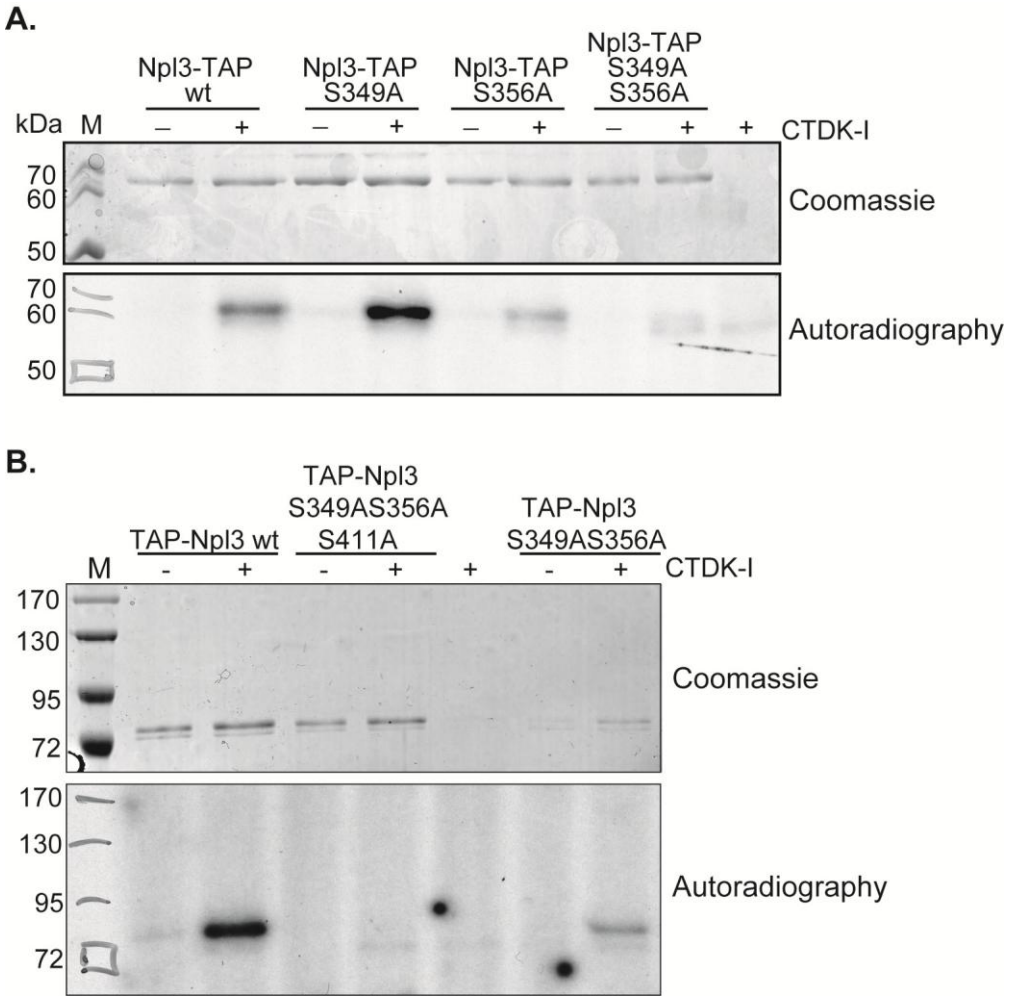

FIGURE 26: Npl3 is phosphorylated by Ctk1 on S349, S356 and S411. *A, In vitro* kinase assays of C-terminal tagged mutants of Npl3 by Ctk1 show that Npl3-S349A-S356A-TAP cannot be phosphorylated by Ctk1. *B,* Npl3 is additionally phosphorylated by Ctk1 on S411 in an N-terminally tagged mutant.

Surprisingly, however, an N-terminal TAP tagged Npl3-S349A-S356A mutant could still be phosphorylated by Ctk1 *in vitro* (FIGURE 26B). Thus, a third phosphorylation site must have been masked by the C-terminal TAP tag. Npl3 contains a third SP site in its very C-terminus (FIGURE 25A marked in red), which was likely to be this third phosphorylation site. Accordingly, an S349A-S356A-S411A mutant of Npl3 with an N-terminal TAP tag was created. As expected, this mutant could not be phosphorylated by Ctk1 *in vitro* anymore (FIGURE 26B).

2.6.4. *In vivo*, S411 is the main phosphorylation site of Npl3, and there is no major reduction of Npl3 phosphorylation upon Ctk1 depletion

As Ctk1 phosphorylates Npl3 *in vitro*, it needed to be assessed whether this is also the case *in vivo*. For this, C-terminally TAP tagged Npl3 was purified from either wt cells or cells depleted of Ctk1 and the phosphorylation status of Npl3 was analyzed by staining with the Pro-Q Diamond phosphostaining solution (4.2.12.2). This solution specifically stains phosphorylated proteins. When compared to the signal of a coomassie stain, the intensity of the signal obtained with Pro-Q Diamond phosphostain is dependent on the phosphorylation status of the protein. Depletion of Ctk1, however, did not lead to a reduction in the intensity of the Pro-Q Diamond phosphostain of Npl3, meaning that its phosphorylation status remains unchanged upon Ctk1 depletion. Since Npl3 is known to be phosphorylated on S411 by Sky1 and CK2 (Gilbert et al., 2001; Dermody et al., 2008), the phosphorylation status of an Npl3-S411A mutant was assessed *in vivo*. This way the phosphorylation by Sky1 and CK2 is abolished while only one phosphorylation site of Ctk1 is mutated. Thus, the phosphorylation by Ctk1 of the remaining two sites can be estimated without the background phosphorylation signal of Sky1 and CK2.

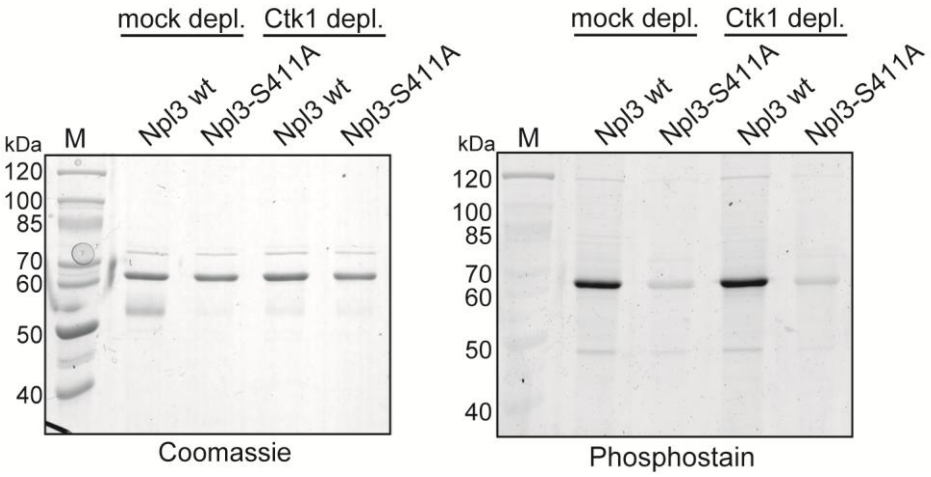

FIGURE 27: Npl3 is mainly phosphorylated on S411 *in vivo* and depletion of Ctk1 does not cause a major decrease in Npl3 phosphorylation *in vivo*. SDS-PAGE of purified Npl3 wt-TAP and Npl3-S411A-TAP followed by Coomassie and Pro-Q Diamond phosphostain in mock depleted and Ctk1 depleted cells.

As shown in FIGURE 27, almost all phosphorylation of Npl3 occurs on S411 *in vivo*, evident by the almost abolished phosphorylation signal of the Npl3-S411A mutant. Even though the phosphorylation signal of Npl3 did not change upon Ctk1 depletion, there could still be a low level of phosphorylation of Npl3 by Ctk1 *in vivo*, which is not enough to be detected in this

assay. In addition, the residual amount of Ctk1 still present after its depletion could be enough to phosphorylate Npl3 up to wt levels. Interestingly, a C-terminally TAP tagged version of Npl3 was used in this assay. Even though under these conditions, S411 could not be phosphorylated by Ctk1 *in vitro*, Sky and/or CK2 achieved to phosphorylate S411 in the context of a C-terminal TAP tag *in vivo*. Thus, the Npl3-S349A-S356A-TAP strain is a suitable mutant to test the functional importance of the possible *in vivo* phosphorylation of Npl3 by Ctk1, because it cannot be phosphorylated by Ctk1, but is likely to still be phosphorylated by Sky1 and CK2.

2.6.5. The Npl3-S349A-S356A-TAP, but not the Npl3-S349A-S356A-S411A mutant has a reduced rate of translation

To test whether the phosphorylation of Npl3 by Ctk1 is necessary for efficient translation, the Npl3 mutants that could not be phosphorylated by Ctk1 were analyzed for their efficiency to translate a luciferase reporter RNA. Translation active extracts of Npl3-TAP, Npl3-S349A-S356A-TAP, wt Npl3, Npl3-S349A-S356A and Npl3-S349A-S356A-S411A were prepared (4.2.4.1) and their activity tested by *in vitro* translation (4.2.4.2). Interestingly, the Npl3-S349A-S356A-TAP mutant showed reduced translation when compared to Npl3-TAP. The npl3-S349A-S356A-S411A and the Npl3-S349A-S356A mutant, however, did not have a defect in translation of the luciferase reporter (FIGURE 28).

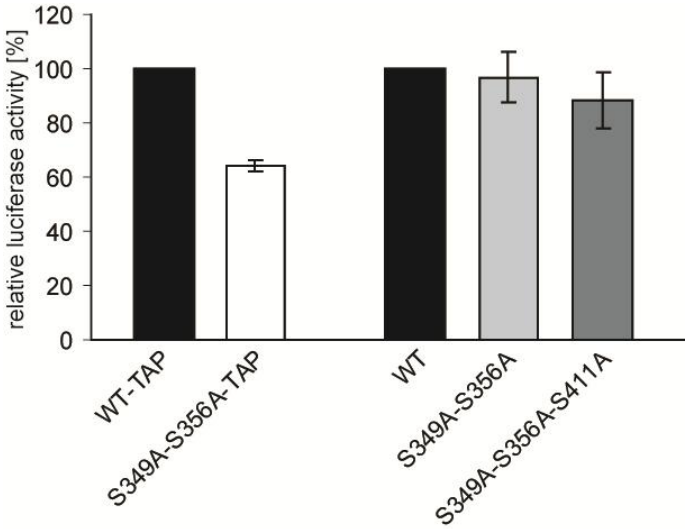

FIGURE 28: Translation active extracts of Npl3 mutants that cannot be phosphorylated by Ctk1 only have a reduced activity of translation, when they additionally contain a TAP tag. Luciferase assay with different Npl3 mutants. The activity of Npl3 wt-TAP and Npl3 wt is the same.

This result is surprising, since both the Npl3-S349A-S356A-TAP and the Npl3-S349A-S356A-S411A mutant cannot be phosphorylated by Ctk1 *in vitro*, but only the translation active extract of Npl3-S349A-S356A-TAP has a reduced translation rate. Consequently, only the combination of the C-terminal TAP tag on Npl3 together with the missing phosphorylation by Ctk1 caused the defect in the respective translation active extracts.

2.6.6. Loss of phosphorylation of Npl3 by Ctk1 does not lead to a translation initiation defect

In order to investigate whether Npl3 is a substrate of Ctk1, which is involved in translation initiation, translation initiation assays were carried out both with the Npl3-S349A-S356A-S411A (FIGURE 29A) and the Npl3-S349A-S356A-TAP (FIGURE 29B) mutant (4.2.5). Neither mutant showed a difference in incorporation of radioactively labeled mRNA compared to wt Npl3 (FIGURE 29). Taken together, these results indicate that phosphorylation of Npl3 is not the function of Ctk1, which is important for efficient translation initiation.

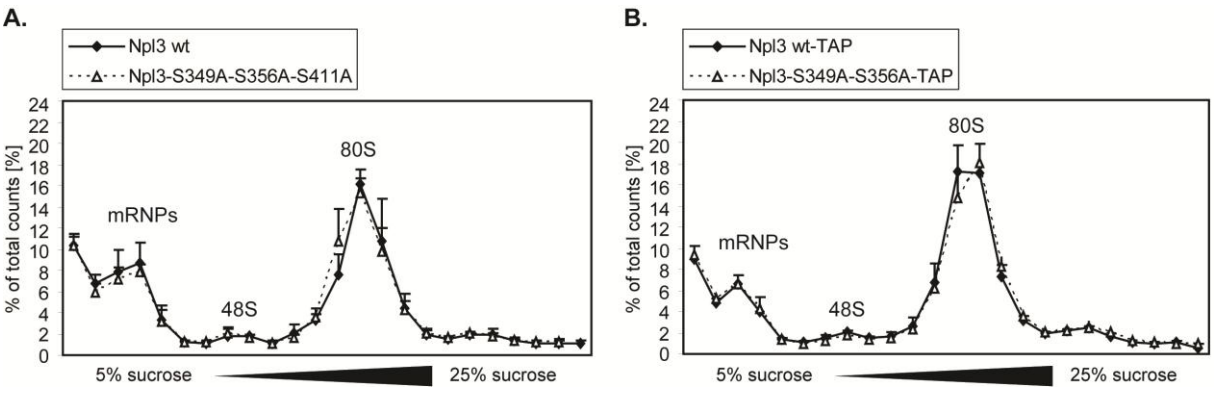

FIGURE 29: Npl3 mutants that cannot be phosphorylated by Ctk1 do not have a translation initiation defect. In a translation initiation assay, neither an Npl3-S349A-S356A-S411A mutant (*A*), nor an Npl3-S49A-S356A-TAP mutant (*B*) shows a defect.

2.6.7. The lethality of Npl3 overexpression in Δ*ctk1* cells is not due to the missing phosphorylation by Ctk1

If the phosphorylation of Npl3 by Ctk1 is not important for translation or at least not necessary for efficient translation initiation, it might have a role in nuclear events. The overexpression of Npl3 in a Δ*ctk1* background was toxic and reduced Npl3 levels in the nucleus rescued the *Δctk1* slow growth phenotype (2.6.1.; 2.6.2). This could be explained by

the two proteins having antagonistic functions in the nucleus, *e.g.* in mRNA 3'-end processing (1.5; 1.7). If the phosphorylation of Npl3 by Ctk1 is important for correct function of Npl3, overexpression of a non-phosphorylatable mutant of Npl3 might show the same growth defect as overexpression of wt Npl3 in a Δ*ctk1* background. In order to test this hypothesis, different serine to alanine mutants of Npl3 were overexpressed. However, overexpression of the Npl3 mutants did not cause a growth defect when compared to the overexpression of wt Npl3 (FIGURE 30). Thus, the phosphorylation of Npl3 by Ctk1 seems not to be important for the functional interaction of the two proteins in the nucleus.

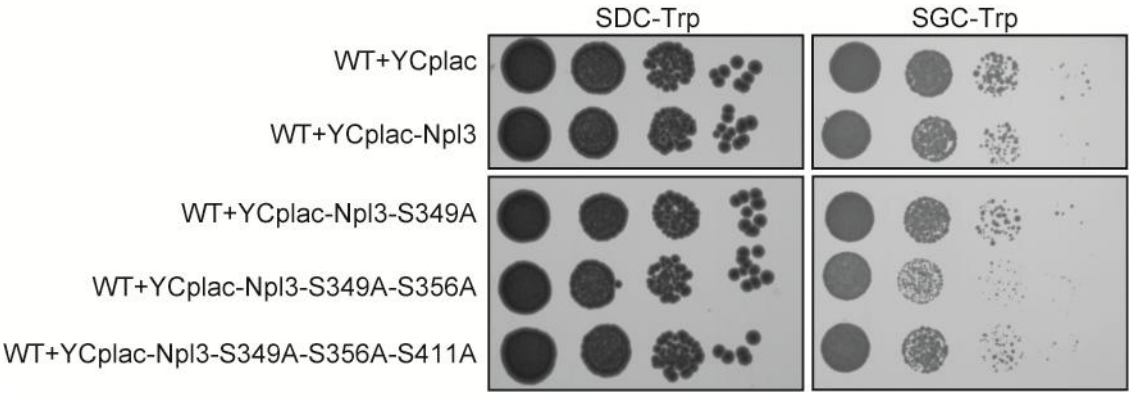

FIGURE 30: Overexpression of an Npl3 mutant that cannot be phosphorylated by Ctk1 does not lead to a major growth defect. Different Npl3 mutants are expressed under control of a *GAL1* promoter (YCplac plasmid) in glucose (SDC-Trp) and galactose (SGC-Trp) containing media.

3. DISCUSSION

3.1. Ctk1 function is crucial for subunit joining during translation initiation

Previously, it was shown that the transcription factor Ctk1 functions in translation elongation by enhancing translational accuracy through phosphorylation of the ribosomal protein Rps2 (Röther & Sträßer, 2007). In this study a second function of Ctk1 in translation is presented by showing that the kinase activity of Ctk1 is important for translation initiation. Specifically, Ctk1 function is needed for efficient subunit joining at the start codon and formation of 80S initiation complexes. Subunit joining itself is a multistep process. First, the start codon has to be recognized correctly, followed by eIF2-bound GTP hydrolysis, phosphate release, and dissociation of translation initiation factors. In a second step, the GTPase eIF5B facilitates joining of the 60S subunit, and GTP hydrolysis enables the release of the remaining initiation factors (reviewed in Acker & Lorsch, 2008; 1.1; FIGURE 31). It remains to be determined which of these steps Ctk1 functions in. However, initiation factors are likely to play a role because translation of the CrPV IRES containing reporter RNA, which does not depend on any translation initiation factors, was not significantly affected in cells depleted of Ctk1 (2.1.1.; FIGURE 6). Ctk1 could, for instance, phosphorylate an initiation factor and modulate its recruitment to or its dissociation from initiation complexes. Alternatively, Ctk1 could enhance subunit joining by phosphorylation of ribosomal proteins. This could in turn increase directly the binding of the small to the large subunit or the association of translation factors with the initiation complex or their dissociation from it. The phosphorylation event could either occur during translation initiation itself or before, with the modification having an impact later during the process. The different stages of subunit joining as well as the possible function of Ctk1 in this process are depicted in FIGURE 31.

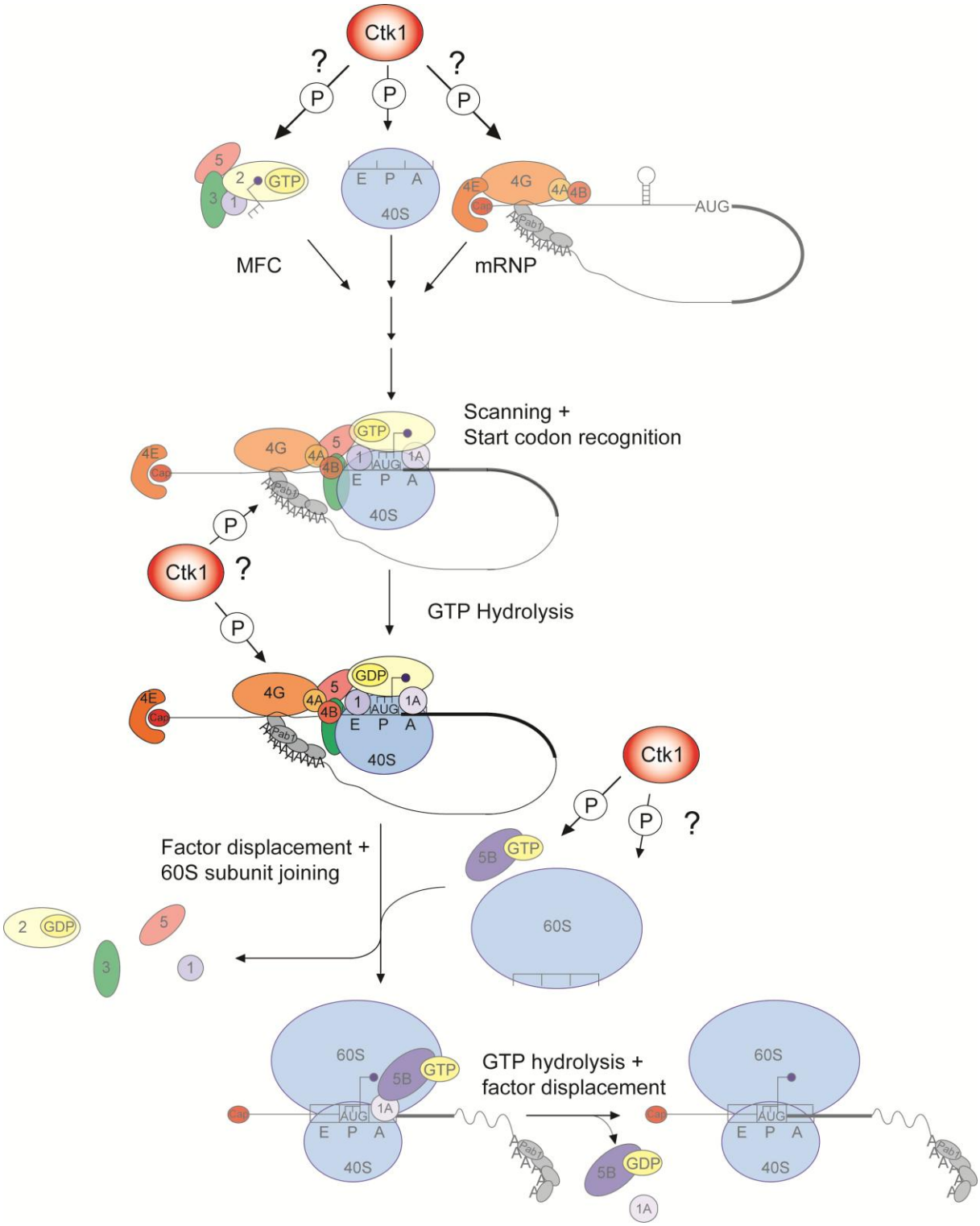

FIGURE 31: Ctk1 could phosphorylate a translation initiation factor or the ribosome itself and thus positively influence subunit joining during translation initiation. The process of translation initiation is depicted with a focus on subunit joining. Possible phosphorylations by Ctk1 are indicated with an arrow and a P.

3.2. No substrate involved in translation initiation that is phosphorylated by Ctk1 *in vitro* and *in vivo* could be identified

In the hypothesis-driven approach to identify a potential substrate of Ctk1 among translation initiation factors, candidate protein(s) (complexes) were purified and tested for *in vitro* phosphorylation by Ctk1 (2.2.1.). Here, Tif4631, Tif 4632 (both eIF4G), Nip, Rpg1 (both eIF3), Tif5 (eIF5) and the helicase Ded1, which fulfills a similar role as eIF4A by abolishing secondary structures in the 5'UTR during scanning (Iost et al., 1999), were at least weakly phosphorylated by Ctk1. *In vivo*, however, the proteins were either not phosphorylated at all, or there was no reduction seen in the phosphorylation signal upon Ctk1 depletion (2.2.2.). This could either mean that the *in vitro* phosphorylation is an artifact, solely happening under artificial *in vitro* conditions. This is rather likely, because it is known that *in vitro* phosphorylation events are often unspecific. On the other hand, it cannot be excluded that the *in vivo* phosphorylation assay did not give a positive result, even if the respective proteins are real substrates of Ctk1 in the cell. Ctk1 could phosphorylate the candidate protein only transiently, so that in the assay no phosphorylation signal could be detected. In addition, the potential substrate might be phosphorylated by more than one kinase so that depletion of Ctk1 does not lead to a substantial reduction of its phosphorylation state. As a possibility to nonetheless detect an *in vivo* phosphorylation by Ctk1, the phosphosites of the respective substrates could be determined and mutated to alanine. If a strain with the mutated substrate displayed the same defect as the Ctk1 depletion strain, an *in vivo* substrate could have been identified.

3.3. The phosphorylation of proteins involved in ribosome biogenesis and translation is decreased upon Ctk1 depletion, but no direct substrate of Ctk1 could be identified

Using an unbiased SILAC approach, numerous phosphosites on ribosomal proteins as well as on proteins involved in ribosome biogenesis and/or translation were identified which are less phosphorylated when Ctk1 is depleted (TABLE 2 and SUPPLEMENTAL TABLE 1). However, no direct substrate of Ctk1 with a function in translation initiation could be determined. There could be several reasons for this: First, the alleged substrate might not interact with the ribosome strongly enough to remain associated with the ribosome enriched fraction analyzed by mass spectrometry. Second, the peptide with the affected phosphorylation site might either not be efficiently purified by the Titansphere-chromatography used for phosphoenrichment or

might not be detectable by LC-MS/MS due to its charge or size. The latter is likely for quite some peptides because proteins were solely labeled with lysine and cut with LysC rendering relatively big peptides. This is also the reason why the phosphosite on Rps2 – a known substrate of Ctk1 (Röther & Sträßer, 2007) – was not identified. It is too big and too hydrophobic to be detectable. Third, Ctk1 could phosphorylate one of the candidate proteins only transiently, or the protein might be phosphorylated by more than one kinase so that depletion of Ctk1 would not lead to a substantial reduction of its phosphorylation state. Fourth, the protein that directly functions in translation initiation might be an indirect substrate of Ctk1.

The ribosomal proteins, which are less phosphorylated upon Ctk1 depletion, are located on all sites of the ribosome and do not cluster at any specific region (FIGURE 32). It is rather unlikely that one kinase is able to catalyze all these different phosphorylations and binds to such different sites of the ribosome. It could be that depletion of Ctk1 leads to decreased activity of other kinases, which affect the phosphorylation pattern of the ribosome (see also 3.6).

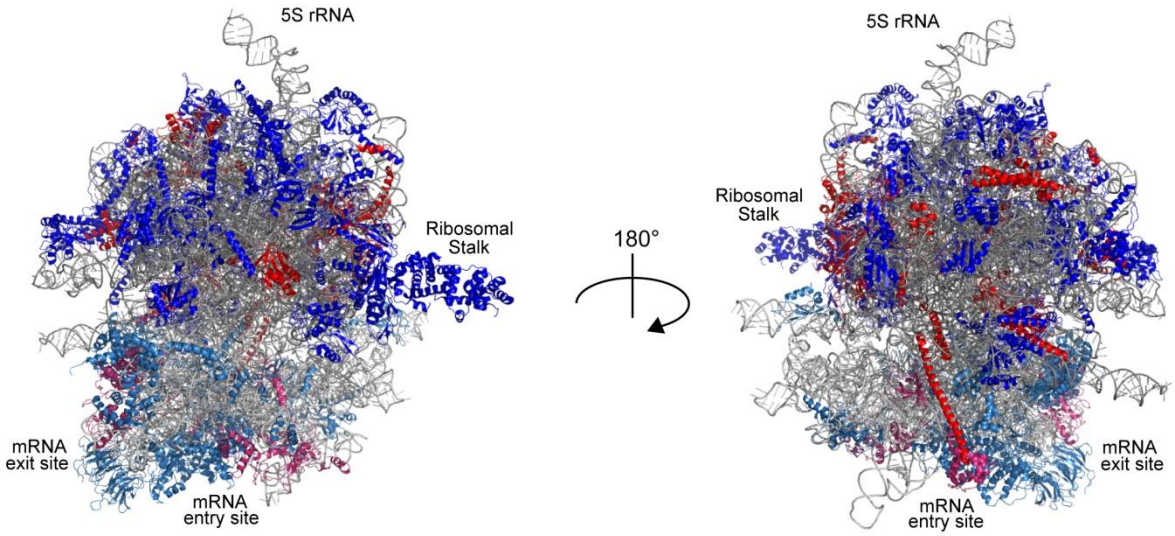

FIGURE 32: Proteins with phosphosites that are less phosphorylated upon Ctk1 depletion are distributed across the 80S ribosome and do not cluster. Proteins with phosphosites that are phosphorylated less upon Ctk1 depletion are shown in red (60S subunit) and pink (40S subunit). The *S.cerevisiae* ribosome structure is a model from Armache et al. (2010a+b). Dark blue: proteins of the big ribosomal subunit, light blue: proteins of the small ribosomal subunit, dark grey: rRNA of the 60S subunit, light grey: rRNA of the 40S subunit.

Even though numerous proteins involved in ribosome biogenesis are less phosphorylated upon Ctk1 depletion (2.3.1.; TABLE 2), a defect in ribosome biogenesis in Ctk1 depleted cells could not be detected on the level of rRNA processing (2.3.2). Here, however, only the

generation of stable rRNA intermediates was analyzed in Ctk1 depleted cells. It could still be, that there is a minor rRNA processing defect, which can only be detected by investigating the amount of short lived rRNA intermediates by Northern blots. Furthermore, ribosome biogenesis could be affected at a different part than rRNA processing, *e.g*. the assembly of ribosomal proteins or the modifications of the rRNA. A major export defect of the pre-ribosomal subunits, however, can be excluded, since in cells devoid of Ctk1, no export defect of ribosomal subunits could be detected (Susanne Röther, Sträßer lab, unpublished results).

3.4. The translation defect observed upon Ctk1 depletion is not due to stress

Ctk1 is known to fulfill an important function in transcription (1.4, 1.5). Consequently, when Ctk1 is depleted, the cell starts to have defects. In order to show that the translation initiation defect observed in Ctk1 depleted cells is specific to the loss of Ctk1 and not due to a general and thus unspecific stress response of the cell, the phosphorylation of eIF2α was assessed (2.1.3). eIF2α phosphorylation is the most investigated mechanism of translational control, which leads to reduced TC formation and thus inhibits translation (1.2; reviewed in Hinnebusch, 2005). Importantly, eIF2α phosphorylation was not increased in Ctk1 depleted cells in contrast to *Δctk1* cells (2.1.3). There are also other mechanisms of translational control that are induced upon stress, two of them functioning on the cap binding complex. The two 4E binding proteins (4EBPs) in yeast, Caf20 and Eap1, bind to eIF4E in a hypophosphorylated form thus inhibiting the interaction of eIF4E with eIF4G and therefore translation initiation. Phosphorylation of these two proteins is reduced upon certain stress conditions and leads to their dissociation from eIF4E (reviewed in Altmann & Linder, 2010). In yeast, the cleavage of eIF4G is also a mechanism to reduce translation initiation in certain unfavorable growth conditions (Berset et al., 1998; reviewed in Altmann & Linder, 2010). Both ways of translational control result in reduced 48S formation during initiation. Therefore, the amount of newly formed 48S complexes during translation initiation was analyzed in Ctk1 depleted and *Δctk1* translation active extracts (2.1.3). Importantly, 48S formation was rather increased in Ctk1 depleted and decreased in *Δctk1* cells, showing that a stress effect was solely visible in *Δctk1* cells.

The rate of translation is also modulated by the phosphorylation of ribosomal proteins. In mammals and also in yeast, Rps6 can be phosphorylated by a distinct kinase, which is induced through the TOR pathway and is activated when the translation rate is high. Upon

unfavorable growth conditions and stress, this phosphorylation is reduced (Urban et al., 2007; reviewed in Meyuhas, 2008). Importantly, Rps6 phosphorylation was not affected upon Ctk1 depletion as determined in the SILAC experiment. In addition, the phosphorylation pattern of ribosomal proteins upon Ctk1 depletion as determined by the SILAC experiment are distinct from those caused by glucose starvation or heat shock (Katharina Brünger, Sträßer lab, unpublished data). All these points strongly argue against an indirect stress related effect of Ctk1 depletion on translation initiation.

3.5. The translation initiation defect in Ctk1 depleted cells is small

Ctk1 depleted cells clearly show a significant defect in translation initiation as determined (i) by comparing the translation efficiency of capped mRNA and CrPV IRES containing mRNA in mock and Ctk1 depleted extracts (2.1.1.), (ii) by assessing the incorporation of different mRNAs into translation initiation complexes (2.1.2) and (iii) by toeprint assays (2.1.2), which show that the 40S subunit accumulates at the start codon in Ctk1 depleted extracts. Even though the defects are significant, the increase or decrease of the measured signals is only about 30% of the mock depleted sample.

In polysome gradients, no difference can be detected between mock depleted and Ctk1 depleted cells (2.1.3). If Ctk1 depleted cells had a bigger translation initiation defect, one would expect an increased 80S peak and a concomitant reduction in polysomes, which is a clear indication of a translation initiation defect. This kind of profile, however, can only be seen in the case of *Δctk1* cells, where translation is shut down unspecifically due to stress. A more pronounced subunit joining defect would lead to the appearance of halfmers, corresponding to complexes, where one or more 80S ribosomes and a 40S subunit are present on the mRNA simultaneously. However, halfmers could not be detected in polysome gradients of Ctk1 depleted cells (2.1.3). There is a discrepancy between the translation initiation defect of the Ctk1 depleted strain as detected by luciferase translation measurements, the incorporation of radiolabled mRNA into translation initiation complexes and the toeprint assay when compared with the normal looking polysome profile. This can be explained with the first three experiments being *in vitro* measurements and the latter being an *in vivo* assay. For recording the polysome profiles, the respective cultures were treated with cycloheximide *in vivo* thus freezing the ribosomal complexes to the RNA. *In vitro* experiments are usually more sensitive than *in vivo* experiments, so that the small translation initiation defect in Ctk1 depleted extracts detected *in vitro* might not be visible in *in vivo* polysome gradients.

3.6. The translation initiation defect upon Ctk1 depletion might be direct or indirect

Ctk1 has a well characterized function in transcription and was shown to be involved in translation elongation (1.5). Therefore, the question arises whether the translation initiation defect presented in this thesis is a direct effect of the depletion of Ctk1 or is an indirect result of the missing function of Ctk1 during transcription or translation elongation. Since a serine to alanine mutant of Rps2, which cannot be phosphorylated by Ctk1, does not have a translation initiation defect (2.1.5), a secondary defect as a result of the translation elongation defect can be excluded. However, it cannot be ruled out that the translation initiation defect is an indirect effect of the missing function of Ctk1 in transcription. This unlikely, because the translation initiation defect was measured in *in vitro* experiments, where *in vitro* transcribed mRNA was added to the translation active extracts. Defective mRNA therefore should not influence the results. The PolI transcription defect in cells lacking Ctk1 (Bouchoux et al., 2004; 1.5) could also lead to a translation initiation defect. However, this is also rather unlikely, because Bur2 depleted extracts most probably show the same translation initiation defect as Ctk1 depleted cells (2.5), but do not have a PolI transcription defect (2.3.2). To completely exclude that the translation initiation defect presented in this thesis is a secondary defect of another already known function of Ctk1, add back experiments would need to be performed. To do this, purified CTDK-I complex would have to be added to the translation active extracts prior to the respective experiment leading to a rescue of the translation defect. This experiment was repeatedly tried, but it never resulted in a rescue of the respective defect. The reason for this could be (i) that the translation initiation defect is either a direct or an indirect effect of a missing phosphorylation of a protein not present in the translation active extract, (ii) that the phosphorylation by Ctk1 has to occur during a different process than translation, so that it cannot be rescued during a translation reaction, (iii) that the experimental conditions are not suitable for Ctk1 function.

The fact that upon Ctk1 depletion phosphorylation of numerous ribosomal proteins and proteins involved in ribosome biogenesis and/or translation is decreased raises the interesting question whether (a) downstream kinase(s) activated by Ctk1 exist(s), which is/are responsible for these phosphorylations. Most of the phosphorylation motifs of the proteins listed in TABLE 2 can be assigned to casein kinase 2 (CK2; SUPPLEMENTAL TABLE 1). This is not surprising since CK2 has been reported to phosphorylate a multitude of substrates, many of them being involved in gene expression (Meggio & Pinna 2003; Poole et al., 2005). Whereas a role of CK2 in ribosome biogenesis has not been shown, CK2 functions in

translation initiation of the *ASH1* mRNA. Translation of the *ASH1* mRNA is repressed before its localization to the bud cortex during cell division by Puf6, and derepression occurs by phosphorylation of Puf6 by CK2 (Deng et al., 2008). Thus, in addition to translation of the *ASH1* mRNA CK2 might be important for translational control of many or even all transcripts and Ctk1 might have a function in its control.

Since many proteins involved in translation and ribosome biogenesis were identified whose phosphorylation decreases upon Ctk1 depletion, Ctk1 could be involved in the phosphorylation of more than one substrate, with all of them partly contributing to efficient translation initiation.

3.7. Is the ribosome integrity affected upon Ctk1 depletion?

If the phosphorylation of ribosomal proteins and proteins involved in ribosome biogenesis is affected by Ctk1 depletion, this could result in decreased ribosome integrity. Even a marginally altered ribosome could lead to the small translation initiation defect observed in Ctk1 depleted cells (*e.g.* by altering the binding capacity of the two ribosomal subunits or the association of the 40S subunit with translation initiation factors).

When translation active extracts were treated with micrococcal nuclease prior to the measurement in a luciferase reporter assay, there was an increased sensitivity to this treatment visible in Ctk1 depleted compared to mock depleted extracts (2.4.). This could hint to an altered ribosome integrity with the rRNA being more accessible so that it can be degraded more easily in Ctk1 depleted extracts. Since the micrococcal nuclease treatment was stopped prior to the addition of the luciferase mRNA, an increased degradation of the reporter mRNA in Ctk1 depleted extracts is unlikely. However, whether the ribosomes in Ctk1 depleted extracts are really more prone to degradation can only be analyzed by additional experiments, which directly enable the visualization of the rRNA integrity (like high resolution rRNA gels).

3.8. Ctk1 – a shuttling protein coupling multiple steps of gene expression?

The novel finding of this study that Ctk1 function is needed for efficient translation initiation in addition to transcription and translation elongation provides a new aspect of the emerging picture that different steps in gene expression are interconnected. Several studies unraveled dual or multiple functions of some proteins in gene expression: The DEAD-box RNA helicase and mRNA export factor Dbp5 shuttles between nucleus and cytoplasm and functions in mRNA export as well as in translation termination. It is important for efficient stop codon

recognition and is essential for recruitment of eRF3 into translation termination complexes (reviewed in Cole & Scarcelli, 2006; Gross et al., 2007). Gle1 is an essential, conserved mRNA export factor whose export function is dependent on the small molecule inositol hexakisphosphate (IP6) (Watkins et al., 1998; Alcazar-Roman et al., 2006; Weirich et al., 2006). In addition to mRNA export, Gle1 and IP6 are also required for efficient translation termination (Bolger et al., 2008). Furthermore, Gle1 alone has a function in translation initiation (Bolger et al., 2008). The PolII subunits Rpb4/7 interact with the translation initiation factor eIF3 to stimulate translation initiation apart from their essential function in transcription (Harel-Sharvit et al., 2010). Importantly, binding of Rpb4/7 to PolII in the nucleus is necessary for their function in translation. Npl3, Gbp2, and Hrb1, three yeast shuttling serine arginine rich (SR) proteins, are important for mRNP biogenesis in the nucleus and are also present on polysomes (Windgassen et al., 2004). Prolonged association of Npl3 with polysomes decreases translation activity (Windgassen et al., 2004). In addition, the shuttling La-motif containing protein Sro9 has multiple functions in gene expression ranging from transcription to translation (Sobel & Wolin, 1999; Tan et al., 2000; Röther et al., 2010).

Even though Ctk1 binds to ribosomes *in vivo* (Röther & Sträßer, 2007), it is not known whether the phosphorylation event(s) by Ctk1 necessary for efficient translation initiation take(s) place in the nucleus or in the cytoplasm, *i.e.* the site of translation (FIGURE 33).

It is tempting to speculate that Ctk1, as also proposed for the mRNP binding proteins mentioned above, binds to the mRNP cotranscriptionally and remains bound during nuclear export until it reaches the site of translation in the cytoplasm (FIGURE 33). This would explain how Ctk1 is able to fulfill its multiple functions in gene expression. Therefore, it would be interesting to elucidate whether Ctk1 indeed shuttles between the nucleus and the cytoplasm. Ctk1 is nuclear at steady state (Lee & Greenleaf, 1991) and physically and genetically interacts with the TREX complex, a complex coupling transcription to mRNA export (Sträßer et al., 2002; Hurt et al., 2004). Therefore, it can be hypothesized that Ctk1 is part of the exported mRNP and remains bound to the mRNP until its translation in the cytoplasm (Röther & Sträßer, 2007, FIGURE33). This would make sense biologically since only correctly processed and assembled transcripts would be “marked” by Ctk1 and then translated efficiently. It could also be, however, that Ctk1 binds to ribosomal precursers and is transported to the site of translation associated to them.

In any case, if Ctk1 does phosphorylate Rps2 and possibly (an) additional substrate(s) important for efficient translation initiation at the site of translation in the cytoplasm it also has to be transported back to the nucleus. It would be an interesting open question, how this

reimport is achieved and what import receptors are involved.

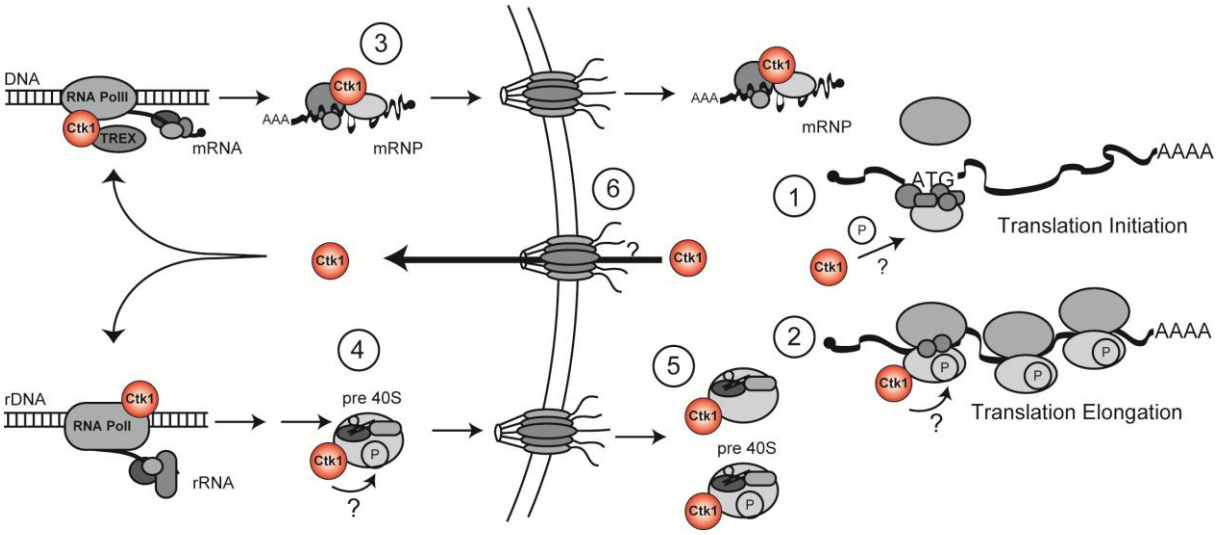

FIGURE 33: Different models for the function of Ctk1 in transcription and translation (adapted from Röther & Sträßer, 2007). (1) Ctk1 has an unknown function in translation initiation (this study). (2) Ctk1 functions in translation elongation by phosphorylating Rps2 (Röther & Sträßer, 2007). (3) Ctk1 could be exported together with the mRNP or (4) bound to the pre 40S particle. (5) The phosphorylation of Rps2 and (a) potential additional substrate(s) could take place in the nucleus or in the cytoplasm, so that Rps2 could be phosphorylated or unphosphorylated when exported to the cytoplasm. (6) If the function of Ctk1 in translation takes place in the cytoplasm, it needs to be reimported by a yet unknown mechanism.

3.9. Is Ctk1 involved in translational control of global mRNA or a specific subset of mRNAs?

Another aspect which remains to be analyzed is the question whether Ctk1 is important for global translation or for translation of a specific subset of mRNAs. The fact that the novel translation initiation defect presented here was observed with various different reporter mRNAs (luciferase, *RPL38*, *RPL41*, *PGK1*, two yeast IRESes) is in favor of a global translation control by Ctk1. However, all experiments were carried out *in vitro*, where the choice of mRNAs is limited. *In vivo*, Ctk1 might only be responsible for the translation of certain specific mRNAs. In order to determine this specifically it would be necessary to carry out ribosome profiling experiments to investigate which mRNAs are associated with polysomes in mock versus Ctk1 depleted cells.

3.10. The function of Bur1 and Ctk1 is similar regarding translation initiation, but different regarding rRNA processing

Translation active extracts of cells depleted of Bur2 showed a similar translation initiation defect as Ctk1 depleted cells. This was determined by measurement of luciferase mRNA translation as well as by the incorporation of radiolabeled mRNA into translation initiation complexes (2.5; FIGURE 22). Thus, it is likely that the two kinases have a similar function regarding translation initiation efficiency. During transcription, both proteins can phosphorylate the CTD of PolII on S2 although with different efficiencies. On the other hand, these two kinases also have distinct substrates, since only Bur1 was shown to phosphorylate Spt5 (Zhou et al., 2009) and only Ctk1 to phosphorylate Rps2 (Röther & Sträßer, 2007). Since no substrate of Ctk1 responsible for its role in translation initiation has been identified, it cannot be tested whether this substrate is also phosphorylated by Bur1. There are only indications that the roles of Bur1 and Ctk1 in this process are similar.

It is very interesting that Bur2 depletion, but not Ctk1 depletion leads to a defect in rRNA processing during ribosome biogenesis (2.3.2; FIGURE 20). To determine the function of Bur1 in rRNA processing more experiments are necessary. However, it can be speculated that the observed defect in rRNA processing is due to the missing phosphorylation of Spt5 in the Bur2 depleted strains. It was shown that the deletion of Spt4 – another part of the Spt4/Spt5 complex – leads to mild defects in PolI transcription and defects in rRNA processing (Schneider et al., 2006). In addition, it was shown that the PAF complex, which is recruited to the transcribing PolII by Bur1, also functions in PolI transcription (Zhang et al., 2009). However, a role for the PAF complex in rRNA processing has not been reported.

3.11. Ctk1 and Npl3 interact with each other and most likely have antagonistic functions in the nucleus

Overexpression of Npl3 is synthetic lethal with the deletion of *CTK1* and the mislocalization of Npl3 to the cytoplasm rescues the *Δctk1* growth phenotype (2.6.1., 2.6.2). In addition, Ctk1 phosphorylates Npl3 on three residues in its SR-domain (2.6.3.). However, overexpression of a non-phosphorylatable mutant of Npl3 did not lead to an increased growth defect when compared to the overexpression of wt Npl3 (2.6.7). This indicates that the accumulation of Npl3 regardless of its phosphorylation by Ctk1 causes the synthetic lethality phenotype in *Δctk1* cells. The model shown in FIGURE 34 explains how the imbalance of the amounts of

the two proteins could be lethal to the cell.

Ctk1 and Npl3 partially have antagonistic functions in the nucleus. Ctk1 by phosphorylation of S2 on the CTD of Rpb1 recruits polyadenylation and termination factors to the site of transcription (reviewed in Buratowski, 2005). Among them is the Pcf11 subunit of the yeast polyadenylation and cleavage factor IA (CF IA) (Licatalosi et al., 2002; Meinhart & Cramer, 2004). Npl3, on the other hand, prevents the premature association of polyadenylation and termination factors to the emerging mRNA. This has been shown for the CF IA subunit Rna15, but also for the Hrp1 subunit of the related CF IB (Bucheli & Buratowski, 2005; Bucheli et al., 2007; Kessler et al., 1997). Thus, Ctk1 is involved in the recruitment of CF I and Npl3 antagonizes association of CF I to the nascent mRNA. If *CTK1* is deleted (FIGURE 34B) or Npl3 is overexpressed (FIGURE 34C), the recruitment of CF I is reduced. If Npl3 is overexpressed in a *Δctk1* background, the recruitment of CF 1 is probably almost abolished thus causing the synthetic lethality phenotype (FIGURE 34D). The C-terminal TAP tag on Npl3 causes its mislocalization to the cytoplasm, which results in reduced Npl3 levels in the nucleus. In agreement with the model presented in FIGURE 34 this suppresses the *Δctk1* slow growth phenotype, because the recruitment of CF I should again resemble wt levels.

It could be observed that the Npl3-S349A-S356A-TAP mutant, which is not phosphorylated by Ctk1 *in vitro* and is mislocalized to the cytoplasm, has a translation defect in an *in vitro* luciferase translation assay, while the nuclear Npl3-S349A-S356A-S411A mutant was not reduced in *in vitro* translation activity of luciferase mRNA (2.6.5). This could mean that the phosphorylation of Npl3 by Ctk1 is important for proper function of Npl3 in translation, but that this defect is so small that it can only be detected when the TAP tag prevents association with the import factor Mtr10. However, this defect is not the same as observed in Ctk1 depleted cells when assessed in a translation initiation reaction (2.6.6). Therefore, even if the phosphorylation of Npl3 by Ctk1 is important for translation, this function of Ctk1 would not explain the translation initiation defect observed in Ctk1 depleted cells.

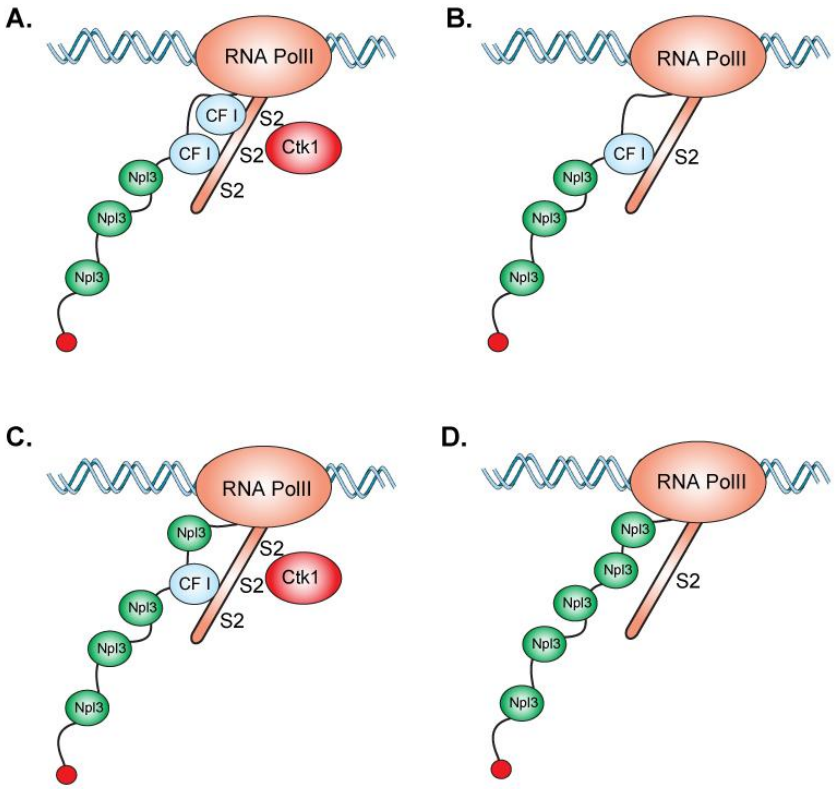

FIGURE 34: Model for the antagonistic functions of Npl3 and Ctk1 in the recruitment of polyadenylation and cleavage factor I (CF I). CF I is recruited to the CTD phosphorylated at S2 through its Pcf11 subunit. Npl3 competes with the CF I subunit Rna15 for binding of the nascent mRNA. *A*, Normal Npl3 and normal Ctk1 levels: The CTD is phosphorylated at S2 and normal levels of Npl3 prevent premature recruitment of the CF I complex. *B*, Ctk1 deletion results in reduced S2 phosphorylation and therefore reduced recruitment of CF I. *C*, overexpression of Npl3 causes reduced binding of CF I to the nascent mRNA. *D*, Ctk1 deletion and consequent reduction in S2 phosphorylation in combination with enhanced levels of Npl3 results in severely reduced CF I complex recruitment.

3.12. Might the function of Ctk1 in translation initiation be conserved?

Since Ctk1 is conserved from yeast to mammals it is of great interest whether its human homologue(s) also play(s) a role in translation initiation. Interestingly, one of the potential mammalian homologues – CDK9 – was reported to shuttle between the nucleus and the cytoplasm (Napolitano et al,. 2002) and associates with polysomes (Röther & Sträßer, 2007). Thus, CDK9, a transcription factor, might also function in translation in mammalian cells. It remains to be elucidated whether the newly identified homologues of Ctk1, CDK12 and CDK13 (Bartkowiak et al., 2010), also function in translation.

4. MATERIALS & METHODS

4.1. MATERIALS

4.1.1. Consumables and chemicals

Consumables and chemicals were purchased from the following companies:

Acros Organics (Geel, Belgium), Applichem (Darmstadt), Applied Biosciences (Darmstadt), Apollo Scientific Limited (Bredbury, UK), Becton Dickinson (Heidelberg), Beckman Coulter (Krefeld), Biaffin (Kassel), Biomol (Hamburg), Biorad (Munich), Biozym (Hess. Oldendorf), Chemicon (Temecula, Canada), Eppendorf (Hamburg), Fermentas (St. Leon-Rot), Formedium (Norwich, UK), GE Healthcare (Munich), Gilson (Bad Camberg), Invitrogen (Karlsruhe), Kedar (Warsaw, Poland), Macherey & Nagel (Düren), Medac (Hamburg), Medigenomix (Munich), MembraPure (Bodenheim), Merck Biosciences (Darmstadt), Millipore (Molsheim, France), Mobitec (Göttingen), MP Biomedical (Illkirch, France), NEB (Frankfurt), Neolab (Heidelberg), Nunc (Wiesbaden), Peske (Aindling-Arnhofen), Promega (Mannheim), Qiagen (Hilden), Roche (Mannheim), Roth (Karlsruhe), Santa Cruz (Santa Cruz, USA), Sarstedt (Nümbrecht), Semadeni (Düsseldorf), Serva (Heidelberg), Sigma (Taufkirchen), Stratagene (Amsterdam, The Netherlands), Thermo Scientific (Munich),VWR (Ismaning).

4.1.2. Commercially available kits

Name	Supplier
AmpliCap^{TM} SP6 High Yield Message Maker Kit	Biozym, Hess. Oldendorf
ECL kit	Applichem, Darmstadt
NucleoBond® PC100, NucleoSpin^{R} Extract II, NucleoSpin® Plasmid QuickPure	Macherey & Nagel, Düren
RNeasy® MinElute Cleanup Kit	Qiagen, Hilden
Sequenase^{TM} version 2.0 sequencing kit	USB/Affimetrix, Cleveland, USA
Pro-Q® Diamond Phosphoprotein Gel Stain	Molecular Probes^{TM}, Invitrogen, Karlsruhe

4.1.3. Equipment

Name	Supplier
Beckman DU650 spectrophotometer L80 ultracentrifuge Optima™ L-90 K ultracentrifuge Optima ™ MAX ultracentrifuge SW32, SW40 rotor, TLA 110 rotor	Beckman Coulter, Krefeld
T3 Thermocycler	Biometra, Göttingen
Gel dryer model 583 Mini-Protean II system Sequi-Gen™ Sequencing Gel and Cell (21x40) PowerPac™ HV Power Supply	Biorad, Munich
Sonifier 250	Branson
Lumat LB9607	EG&G Berthold
Bead Mill (Pulverisette)	Fritsch, Idar-Oberstein
Typhoon 9400	GE Healthcare, Munich
Research Pipettes P10, P20, P200, P1000	Gilson
Thermomixer compact Eppendorf centrifuge 5415D, 5415R BioPhotometer	Eppendorf, Hamburg
Rotanda 46R, 460R	Hettich, Tuttlingen
DMI 6000 B DFC 360 FX AF 6000 LX	Leica Microsystems GmbH, Wetzlar, Germany
Storm 860 imager	Molecular Dynamics (GE Healthcare, Munich)
Optimax TR developing machine	MS Laborgeräte, Dielheim
Akku Jet Electrophoresis Power Supply Consort E835 Heidolph shaker duomax 1030 Rotator Vortex Genie 2	Neolab, Heidelberg
Innova 44 shaking incubator	New Brunswick Scientific, Nürtingen

Semi-dry blotting device	Peqlab, Erlangen
Liquid scintillation analyzer TriCarb 2810 TR	PerkinElmer, Waltham, USA
Universal Analytical Balance	Sartorius, Göttingen
Dissection microscope manual MSM	Singer, Somerset, UK
Gradient machine Fractionator Foxy Jr. UA-6 UV/Vis Detector	Teledyne ISCO, Lincoln, USA
Sorvall Evolution RC Sorvall RC 5B Plus SLC6000, GS-3 rotor, SW34 rotor	Thermo Fisher Scientific, Munich
CO8000 Cell Density Meter	WPA, Cambridge, UK

4.1.4. Radioactivity

Radioactivity was purchased from Hartmann Analytik (Braunschweig):

γ-^{32}P-ATP

^{32}P phosphoric acid

α-^{32}P-UTP

α-^{32}P-dATP

4.1.5. Enzymes

Name	**Supplier**
Calf Intestine Alkaline Phosphatase (1U/µl) Restriction Endonucleases (*Bam*HI, *Bgl*II, *Bsr*BI, *Cla*I, *Dpn*I, *EcI*136II, *Eco*RV, *Eco*RI, *Hind*III, *Hpa*I, *Kpn*I, *Nsi*I, *Nco*I, *Nde*I, *Nhe*I, *Not*I, *Sph*I, *Pst*I, *Pvu*II, *Sac*I, *Sal*I, *Sma*I, *Spe*I, *Sph*I, *Xba*I, *Xho*I) T4-DNA Ligase Taq Polymerase for colony PCR and KNOP PCR (5U/µl) T7 Polymerase	Fermentas, St. Leon-Rot
SuperscriptII reverse transcriptase	Invitrogen, Karlsruhe
Micrococcal Nuclease T3 Polymerase	Roche, Mannheim

TEV protease Vent-Polymerase for KNOP-PCR	NEB, Frankfurt
Zymolyase 20.000T/100.000T	Medac, Hamburg
Phusion® High-Fidelity PCR Master Mix	Finnzymes, Vantaa, Finland

4.1.6. Antibodies

Primary Antibodies

Antibody	Source	Dilution	Company
α-Npl3	Rabbit	1:5000 for western blot 1:1000 for immunofluorescence	Guthrie lab
PAP	Rabbit	1:5000 for western blot	Sigma, Taufkirchen
α-ProtA	Rabbit	1:2000 for immunofluorescence	Sigma, Taufkirchen
α-eIF2α	Rabbit	1:2000 for western blot	Dever lab
α-eIF2α-P	Rabbit	1:1000 for western blot	Invitrogen, Karlsruhe

Secondary Antibodies

Antibody	Source	Dilution	Company
α-rabbit IgG-HRPO	Goat	1:3000 for western blot	BioRad, Munich
α-rabbit IgG-Alexa F488	Goat	1:500 for immunofluorescence	Invitrogen, Karlsruhe

4.1.7. Oligonucleotides

Oligonucleotides were purchased from Thermo Scientific, Ulm.

#	Name	Sequence
1	For_BamHI_3UTR_Rpl38	GGGGGATCCTTTTTGTTCCAGTCTCGTTATG
2	Rev_Sac_5UTR_Rpl38	GGGGAGCTCAGGTTGAATATAGTACGACAAAAT
3	For_Bam_3UTR_Rpl41a	GGGGGATCC ACTCTTGAAAGAATTTAAAACAAA
4	rev_Sac_5UTR_Rpl41a_22bp	GGGGAGCTC AGACCACATCGATTCAATCG
5	Rev_Sac_5UTR_Rpl41a_80bp	GGGGAGCTC GGACTTCTAAGCAACTCTCATT
6	For_BamHI_3UTR_Pgk1_earlyter	GGGGGATCCGGGAAAGAGAAAAGAAAAAAATTGATCTATCGATTTCAATTCAATTCAATTTAGGTCTACCCAAGTGAGAAGCCAA

#	Name	Sequence
7	Rev_Sac_5UTR_Pgk1	GGGGAGCTC AAGTTCTTAGATGCTTTCTTTTT
8	Rpl38_toeprint_50nt	GGCGGTCTTAACGTCAGCT
9	Ctk1_D324N_for	CAGGGGAATCTAAAAATAACAAATTTTGGACTAGCG AGGAAAATG
10	Ctk1_D324N_rev	CATTTTCCTCGCTAGTCCAAAATTTGTTATTTTTAGAT TCCCCTG
11	Tif5_oligo1	TTACGTGGTTAGAAACCGCTGAAAGTGACGATGATG AAGAAGACGACGAAtccatggaaaagagaag
12	Tif5_oligo2	AAACAACAGAACATAATCCTTATCTTACGCCATGTCA TATAATAATTTACtacgactcactataggg
13	Tif4632_oligo1	CAAGAGCTAATATGTTCGACGCATTAATGAATAACG ATGGGGACAGTGATtccatggaaaagagaag
14	Tif4632_oligo2	TTAATGCACAAAAAGGTTTAACACATGAATTAAAAA GGAAAAAGACTAGCtacgactcactataggg
15	Fun12_oligo1	AGATCCGATTGGCTGCTATTGAAGAAGCTGAAGGTC GTTTTCGGCATCGAAtccatggaaaagagaag
16	Fun12_oligo2	TTTATATACAATTACCTATTTAATTCATTAAATTTTGTA GAATGTGATTGctacgactcactataggg
17	Rpg1_oligo1	TGACTATGGCTGAAAAGTTGAGAGCCAAGAGATTG GCCAAGGGGGGCAGGtccatggaaaagagaag
18	Rpg1_oligo2	AAATTGTTATTATGTACACATACTCTTATACGTATAAA AAACGGTATAAAtacgactcactataggg
19	Tif35_oligo1	ATATGAATTTAATTTTACGTGTTGAATGGTCCAAACC TAAGGTTAAGGAAtccatggaaaagagaag
20	Tif35-oligo2	TTTCTTTCTTAATATCTACAATTTTTATATGAGAAGAG TAACATTAGAAAtacgactcactataggg
21	Tif3_oligo1	CTCAATTGACTGTTGAAGATGGTGACAATTGGGAAG TTGTTGGTAAGAAAtccatggaaaagagaag
22	Tif3_oligo2	AAGGAGAGTAGAAAAACAAGAAAGAAAAAAAGCA AACAGTAAATACAAATtacgactcactataggg
23	Sui1_oligo1	TGATCTCCCAACTGGGATTGCAAAAGAAGAACATTA AAATTCATGGGTTTtccatggaaaagagaag
24	Sui1_oligo2	GTTACGTTTTATATAGGATAACAACACTAAGAAAGA AAGCGAGCAGCGAG tacgactcactataggg
25	Gcd7_oligo1	CGTGGGATAATTACAAGCAAATTGATGTGCATTTGG ATAAAAATAAGGCGtccatggaaaagagaag
26	Gcd7_oligo2	ATTAATAATAAAAAAATTGTTTTGATCTACAAGATTT TTATTTATTTTCAtacgactcactataggg
27	Cbf5_oligo1	AGTCTGAAGACGGTGATTCTGAGGAAAAGAAATCT AAGAAATCTAAGAAAtccatggaaaagagaag
28	Cbf5_oligo2	TCTAATAATAGAAAAAGTTTTTTGAAAAAAAGAAAG CTGTTAAATATATAtacgactcactataggg

#	Name	Sequence
29	Pop1_oligo1_N	ACTTGAACATTTGGCAAGAAAGGTGAGAATTGACCT CATTATAATTACAAgaacaaaagctggagctcat
30	Pop1_oligo2_N	TTATTAAGAACTTTCTTTCCACCATTTCCTCTAGACA AACTCCCGCTCATcttatcgtcatcatcaagtg
31	Nop13_oligo1	GAGGTTCTGCAGCTATTGTCCCATCACAAGGTAAGA AAGTGAAGTTTGACtccatggaaaagagaag
32	Nop13_oligo2	ATGAATGATTGAATAATTTACAAGCGAAATAATCGCA TTATATACGTGGCtacgactcactataggg
33	Nop53_oligo1	GAAAGTATAAGCAGAAAATCACTGAAAAGTGGACA CATAAGGACTTCAAAtccatggaaaagagaag
34	Nop53_oligo2	ATATCTCACTTGATGAATCCACGTATCAAGGACAACC TTTTCATGGAAACtacgactcactataggg
35	Cic1_oligo1	AGCTTGAAAAAGAATCTAGCGAGTCAGAAGCTGTC AAGAAGGCTAAAAGTtccatggaaaagagaag
36	Cic1_oligo2	CACTCTATGAAATTCAAATTTTTTTCTTCACAAGAAA AAAATGAGAGAAAtacgactcactataggg
37	Sda1_oligo1	AGCAAAAAGTGTTACGTGCACACATCACCAAACAA AAGAAGAAGGGGTATtccatggaaaagagaag
38	Sda1_oligo2	GTCCTCATACAGTTGGAGAGATGAATGTATCTGTGTA TATGTATGTATATtacgactcactataggg
39	JJJ1_oligo1	CGGCAGTGAAAAACGTAGTGAAAAGAAAGAAAGT CAAGACCAAAAGAATAtccatggaaaagagaag
40	JJJ1_oligo2	GACTACAGTTAAATTAAACTCTACACAGCTCTACTAA TAATTTCTGTTTCtacgactcactataggg
41	Rei1_oligo1	GTGCCAAGTTCGTCAATAACCAACCACACTACAGAG ACCAACTTCTGCAGtccatggaaaagagaag
42	Rei1_oligo2	GAATTATCTAATGTACAAATGGTGAAGCAGTATATAT GCGACAAAATACTtacgactcactataggg
43	Mrs6_oligo1	ACGATGTCAATATGGAAGGTTCCGGTGAATTTGTAG GTGAAATGGAGATAtccatggaaaagagaag
44	Mrs6_oligo2	TCATTAACTTGTAAGAAGACATTAATCACCGTTTCCT GAAGGGAAAAAAAtacgactcactataggg
45	Ltv1_oligo1	AGAAAAAGAAACTTGAGAAGGTCACCAATACACTA AGCAGCTTAAAATTTtccatggaaaagagaag
46	Ltv1_oligo2	AATGCATTCTAGGCTAAGTATACATGTCTACACAGTA CTTGTAATGTAGGtacgactcactataggg
47	Rps16a_oligo1	AAATTCGGTGGTAAGGGTGCTCGTTCCAGATTCCAA AAATCTTACCGTtccatggaaaagagaag
48	Rps16a_oligo2	AGGCTGTTGTGTTTATTGATGGTATACAATTATAAGA AAATGAAAAGAGCtacgactcactataggg
49	Rps17b_oligo1	CTGTCATCAACGTTTCCGCTCAAAGAGACAGACGTT ACAGAAAGAGAAACtccatggaaaagagaag

#	Name	Sequence
50	Rps17b_oligo2	TACATAAGGAGAGTCCTCAATGAAATGGAGTAAAAC AGACGACATGATAAtacgactcactataggg
51	Rps18a_oligo1	GTTTGCGTGTTAGAGGTCAACACACCAAGACCACT GGTAGAAGAAGAGCTtccatggaaaagagaag
52	Rps18a_oligo2	AGTCAATTAGGAAGTGCTATGGAAATATATGTACTCG TACAAAAAAGATTtacgactcactataggg
53	Rps24a_oligo1	TCGGTACTGGTAAGAGATTGGCTAAGAAGGTTGCTC GTCGTAACGCCGATtccatggaaaagagaag
54	Rps24a_oligo2	AAGATACACATATTTATATATAGAAAACTAAACAATC CGTAAAAATGATTtacgactcactataggg
55	Rps5_oligo1	ACGCTATCAAGAAGAAGGATGAATTGGAACGTGTTG CCAAGTCTAACCGTtccatggaaaagagaag
56	Rps5_oligo2	GTACAAAGAAGATAAAAGTAATAATAAGAAAAACAT ATGTAATATTGAAAtacgactcactataggg
57	Sda1_5Prom_Bam	GGG GGATCC GGTGCATTAACTATTTAATATGTATG
58	Sda1_nostop_Xho	GGG CTCGAG ATACCCCTTCTTCTTTTGTTTG
59	Sda1_5_S591A	GATATGGAAGATGCTGACGATGAAAAAG
60	Sda1_3_S591A	CTTTTTCATCGTCAGCATCTTCCATATC
61	5_Mrs6_Pst_Prom	GGG CTGCAG CAAGCATGAATCTAGCCAAC
62	3_Mrs6_Xho_nostop	GGG CTCGAG TATCTCCATTTCACCTACAAATTC
63	5_Mrs6_S470A	CAGTTAAGTTAGGCCAAGCTTTTAAGGAGTATGTTC
64	3_Mrs6_S470A	GAACATACTCCTTAAAAGCTTGGCCTAACTTAACTG
65	5_Ltv1_Spe_Prom	GGGACTAGTCGTTAATATAGGATGATCCATC
66	3_Ltv1_Xho_nostop	CCCCTCGAGAAATTTTAAGCTGCTTAGTGTATTG
67	5_Ltv1_S281A	CGAAGATTTCAAAAAGATAACGCTATACTAGAAAAG CATAAC
68	3_Ltv1_S281A	GTTATGCTTTTCTAGTATAGCGTTATCTTTTTGAAATC TTCG
69	5_Nco_Nop16_Start	GGGCCATGGGCACATCCGTTAGAAAAAGAAAG
70	3_Xho_Nop16_nostop	GGGCTCGAGTTTTGATGCAATACCGTTTC
71	5_BamHI_Npl3ATG	GGGGGATCCATGTCTGAAGCTCAAGAAACTC
72	3_SalI_Npl3Ter	GGG GTCGAC GAAATTCCGTTGTAAAAAGG
73	Npl3-oligo1-N	TACTTTTGAAGGAATCAAAATTAAGCAATTACGCTA AAACCATAAGGATAGAACAAAAGCTGGAGCTCAT
74	Npl3-oligo2-N	ACAACAGATTCTGGTAGTTGCTCTACGTGAGTTTCT TGAGCTTCAGACATCTTATCGTCATCATCAAGTG
75	5_Bam_Prom_Npl3	GGG GGATCC CGTCTCTATCAATATGCAAATG
76	3_Xho_Ter_Npl3	GGG CTCGAG GATGTTAAATGTTATCATGG
77	5_npl3_S411A	GCTCCACGTGAAAGAGCTCCAACCAGGTAAGCC
78	3_npl3_S411A	GGCTTACCTGGTTGGAGCTCTTTCACGTGGAGC
79	5_npl3_S349A	AGAGGTGGTTACGATGCTCCTAGAGGTGGTTAC
80	3_npl3_S349A	GTAACCACCTCTAGGAGCATCGTAACCACCTCT
81	5_Npl3_S356A	AGAGGTGGTTACGATGCTCCAAGAGGTGGTTAT

#	Name	Sequence
82	3_npl3_S356A	ATAACCACCTCTTGGAGCATCGTAACCACCTCT
83	5_Npl3_S349AS356A	CGATGCTCCTAGAGGTGGTTACGATGCTCCA
84	3_Npl3_S349AS356A	TGGAGCATCGTAACCACCTCTAGGAGCATCG
85	3_Xho_nostop_Npl3	GGGCTCGAGCCTGGTTGGTGATCTTTCAC
86	Npl3_Xho_nostop_S411A	GGGCTCGAGCCTGGTTGGAGCTCTTTCAC
87	3_Npl3D50_Xho	GGGCTCGAGACCTCTGGAATAACCACCTC
88	3_Npl3D75_xho	GGGCTCGAGTCCGCCTCTGGAGTAGC
89	3_Npl3D100Xho	GGGCTCGA TCTGGGGCCACCGAAGCCG
90	3_Npl3_Ter_Not	GGGGGGCGGCCGCGATGTTAAATGTTATCATGGGAT
91	5_BamHI_CTK1_Prom	GGGGGATCCGTCTAGGATAATAATATTAGCGCT
92	Ctk1_nostop_Xho	GGGCTCGAGTTTATCATCATCGTCATTATTATTA
93	3_Not1_Adh1_Ter	GGGGGGCGGCCGCCGGTAGAGGTGTGGTCAATA
94	5_Nco_Nop16_Start	GGG CCATGG GC ACATCCGTTAGAAAAAGAAAG
95	3_Xho_Nop16_nostop	GGG CTCGAG TTTTGATGCAATACCGTTTC

4.1.8. Plasmids

The following plasmids were generated in this study.

Plasmid	How was it created?
BSEF-*RPL38*	The *Bam*HI/*Sac*I fragment of BSEF was exchanged with *RPL38* using primers 1+2
BSEF-*RPL41a* 22bp 5'UTR	The *Bam*HI/*Sac*I fragment of BSEF was exchanged with *RPL41* using primers 3+4
BSEF-*RPL41a* 80bp 5'UTR	The *Bam*HI/*Sac*I fragment of BSEF was exchanged with *RPL41*using primers 3+5
BSEF-*PGK1*	The *Bam*HI/*Sac*I fragment of BSEF was exchanged with *PGK1* using primers 6+7
pRS315-*ctk1*-D324N	Quickchange mutagenesis of pRS315-*CTK1*using primers 9+10
pRS315-*SDA1*-TAP-T_{ADH1}	The *Bam*HI/*Xho*I fragment of *SDA1* was inserted into pRS315-TAP-T_{ADH1} using primers 57+58
pRS315-*sda1*-S591A-TAP-T_{ADH1}	Quickchange mutagenesis of pRS315-*SDA1*-TAP-T_{ADH1} using primers 59+60
pRS316-*MRS6*-TAP-T_{ADH1}	The *PstI*/*Xho*I fragment of *MRS6* was inserted into pRS315-TAP-T_{ADH1} using primers 61+62
pRS315-*mrs6*-S470A-TAP-T_{ADH1}	Quickchange mutagenesis of pRS315-*MRS6*-TAP-T_{ADH1} using primers 63+64
pRS315-*LTV1*-TAP-T_{ADH1}	The *SpeI*/*Xho*I fragment of *LTV1* was inserted into pRS315-TAP-T_{ADH1} using primers 65+66
pRS315-*ltv1*-S281A-TAP-T_{ADH1}	Quickchange mutagenesis of pRS315-*LTV1*-TAP-T_{ADH1} using primers 67+68

Plasmid	How was it created?
pET28b-*NOP16*	The *Nco*I/*Xho*I fragment of *NOP16* was inserted into pET28b using primers 69+70
YCplac-*NPL3*	The *Bam*HI/*Sal*I fragment of pRS315-NPL3 was inserted into YCplac22G using primers 71+72
YCplac-*npl3*-S349A	The *Bam*HI/*Xho*I fragment of pRS315-*npl3*-S349A was inserted into *Bam*HI/*Sal*I cut YCplac22G using primers 71+76
YCplac-*npl3*-S349A-S356A	The *Bam*HI/*Xho*I fragment of pRS315-*npl3*-S349A-S356A was inserted into *Bam*HI/*Sal*I cut YCplac22G using primers 71+76
YCplac-*npl3*-S349A-S356A-S411A	The *Bam*HI/*Xho*I fragment of pRS315-*npl3*-S349A-S356A-S411A was inserted into *Bam*HI/*Sal*I cut YCplac22G using primers 71+76
pRS315-*NPL3*	The *Bam*HI/*Xho*I fragment of *NPL3* was inserted into pRS315 using primers 75+76
pRS316-*NPL3*	The *Bam*HI/*Xho*I fragment of *NPL3* was inserted into pRS316 using primers 75+76
pRS315-*npl3*-S411A	Quickchange mutagenesis using pRS315-*NPL3* and primers 77+78
pRS315-*npl3*-S349A	Quickchange mutagenesis using pRS315-*NPL3* and primers 79+80
pRS315-*npl3*-S356A	Quickchange mutagenesis using pRS315-*NPL3* and primers 81+82
pRS315-*npl3*-S349A-S356A	Quickchange mutagenesis using pRS315-*NPL3* and primers 83+84
pRS315-*npl3*-S349A-S356A-S411A	Quickchange mutagenesis using pRS315-*npl3*-S349A-S356A and primers 77+78
pRS315-*NPL3*-TAP-T_{ADH1}	The *Bam*HI/*Xho*I fragment of *NPL3* was inserted into pRS315-TAP-TADH1 using primers 75+85
pRS315-*npl3*-Δ50-TAP-T_{ADH1}	The *Bam*HI/*Xho*I fragment of *NPL3* was inserted into pRS315-TAP-TADH1 using primers 75+87
pRS315-*npl3*-Δ75-TAP-T_{ADH1}	The *Bam*HI/*Xho*I fragment of *NPL3* was inserted into pRS315-TAP-TADH1 using primers 75+88
pRS315-*npl3*-*Δ*100-TAP-T_{ADH1}	The *Bam*HI/*Xho*I fragment of *NPL3* was inserted into pRS315-TAP-TADH1 using primers 75+89
pRS315-*npl3*-S349A-TAP-T_{ADH1}	The *Bam*HI/*Xho*I fragment of *npl3* was inserted into pRS315-TAP-TADH1 using pRS315-*npl3*-S349A and primers 75+85
pRS315-*npl3*-S356A-TAP-T_{ADH1}	The *Bam*HI/*Xho*I fragment of *npl3* was inserted into pRS315-TAP-TADH1 using pRS315-*npl3*-S356A and primers 75+85

Plasmid	How was it created?
pRS315-*npl3*-S349A–S356A–TAP-T_{ADH1}	The *Bam*HI/*Xho*I fragment of Npl3 was inserted into pRS315-TAP-TADH1 using pRS315-*npl3*-S349A – S356A and primers 75+85
pNOP-TAP-*NPL3*	The *Bam*HI/*Not*I fragment of *NPL3* was inserted into pNOP-TAP using primers 71+90
pNOP-TAP-*npl3*-S349A-S356A	The *Bam*HI/*Not*I fragment of *npl3* was inserted into pNOP-TAP using pRS315-*npl3*-S349A-S356A and primers 71+90
pNOP-TAP-*npl3*-S349A-S356A-S411A	The *Bam*HI/*Not*I fragment of *npl3* was inserted into pNOP-TAP using pRS315-*npl3*-S349A-S356A and primers 71+90
pRS315-*CTK1*-TAP-T_{ADH1}	The *Bam*HI/*Xho*I fragment of *CTK1* was inserted into pRS315-TAP-TADH1 using primers 91+92
pRS426-*CTK1*-TAP-T_{ADH1}	The *Bam*HI/*Not*I fragment of pRS315-*CTK1*-TAP-T_{ADH1} was inserted into pRS426 using primers 91+93
pET28b-*NOP16*	The *Nco*I/*Xho*I fragment of NOP16 was inserted into pET28b using primers 94+95

Additionally, the following plasmids were used in this study:

Plasmid	Source
pWG273	Gilbert et al., 2007
pWG290	Gilbert et al., 2007
pWG299	Gilbert et al., 2007
pWG324	Gilbert et al., 2007
pWG186	Gilbert et al., 2007
pSP6P	Verge et al., 2004
BSEF	Beckmann et al., 2005
pRS315-*CTK1*	Röther & Sträßer, 2007
pRS316-*CTK1*	Röther & Sträßer, 2007
YCplac22GAL	Gift from Markus Künzler
pRS315	Sikorski & Hieter, 1989
pRS316	Sikorski & Hieter, 1989
pBSKS(+)	Alting-Mees et al., 1992
pRS315-*RPS2*	Röther & Sträßer, 2007
pRS315-*rps2-S238A*	Röther & Sträßer, 2007
pGEX4T-2-*SRP40*	Gift from Adolfo Saiardi (Bhandari et al., 2007)
pRS315-TAP-T_{ADH1}	Röther & Sträßer, 2007
pNOP-TAP	Sittinan Chanarat (Sträßer lab)
pRS425-*CTK2-CTK3*	Gift from Arno Greenleaf (Lee & Greenleaf, 1997)
pBS1539	Puig et al., 2001
pBS1479	Puig et al., 2001

Plasmid	Source
pBS1761	Puig et al., 2001
pBS1776	Puig et al., 2001
pET28b	Novagen (Merck Chemicals Ltd.), Nottingham, UK

4.1.9. Strains

Escherichia coli

DH5a; Invitrogen, Karlsruhe	F^-, endA1, hsdr17, (r_k^-, m_k^-), supE44, thi-1, recA1, gyrA96, RelA1, 80dlacZ, DM15
Rosetta (DE3); Novagen, Merck Chemicals Ltd., Nottingham, UK	F– ompT hsdSB(rB– mB-) gal dcm (DE3) pRARE2 (CamR)

Saccharomyces cerevisiae

Strain	Genotype	Origin
W303	*Mata/α; ura3-1; trp1-1; his3-11,15; leu2-3,112; ade2-1; can1-100; GAL+*	
RS453	*Mata/α; ura3-52; trp1-1; his3-11,15; leu2-3,112; ade2-1; can1-100; GAL+*	
GAL1::CTK1-TAP	*MAT*a; as W303; *CTK1-TAP::TRP1-KL HIS3-PGAL1::CTK1*	Susanne Röther, Sträßer lab
CTK1 shuffle	*MATa/α*; as W303; *CTK1::HIS3* (pRS316-*CTK1*)	Susanne Röther, Sträßer lab
RPS2 shuffle	*MATa/α*; as W303; *CTK1::HIS3* (pRS316-*CTK1*)	Katharina Brünger, Sträßer lab
NIP1-TAP	*MAT*a; as W303; *NIP1-TAP::TRP1-KL*	Jansen Lab
TIF5-TAP	*MATa/α*; as W303; *TIF5-TAP::TRP1-KL*	*TIF5-TAP::TRP1* PCR product was integrated C-terminal of *TIF5* into W303
TIF4632-TAP	*MATα*; as W303; *TIF4632-TAP::TRP1-KL*	*TIF4632-TAP::TRP1* PCR product was integrated C-terminal of *TIF4632* into W303
Fun12-TAP	*MATα*; as W303; *FUN12-TAP::TRP1-KL*	*FUN12-TAP::TRP1* PCR product was integrated C-terminal of *FUN12* into W303
RPG1-TAP	*MAT*a; as W303; *RPG1-TAP::TRP1-KL*	*RPG1-TAP::TRP1* PCR product was integrated C-terminal of *RPG1* into W303

Strain	**Genotype**	**Origin**
TIF35-TAP	*MAT*a; as W303; *TIF35-TAP::TRP1-KL*	*TIF35-TAP::TRP1* PCR product was integrated C-terminal of *TIF35* into W303
TIF4631-TAP	*MAT*a; as RS453; *TIF4631-TAP::TRP1-KL*	Susanne Röther, Sträßer lab
TIF3-TAP	*MAT*α; as W303; *TIF3-TAP::TRP1-KL*	*TIF3-TAP::TRP1* PCR product was integrated C-terminal of *TIF3* into W303
SUI1-TAP	*MAT*α; as W303; *SUI1--TAP::TRP1-KL*	*SUI1-TAP::TRP1* PCR product was integrated C-terminal of *SUI1* into W303
GCD7-TAP	*MAT*a; as W303; *GCD7-TAP::TRP1-KL*	*GCD7-TAP::TRP1* PCR product was integrated C-terminal of *GCD7* into W303
TIF6-TAP	*MAT*a; as W303; *TIF6-TAP::TRP1-KL*	*TIF6-TAP::TRP1* PCR product was integrated C-terminal of *TIF6* into W303
PRT1-TAP	*MAT*a; as RS453; *PRT1-TAP::TRP1-KL*	Susanne Röther, Sträßer lab
DED1-TAP	*MAT*a; as RS453; *DED1-TAP::TRP1-KL*	Susanne Röther, Sträßer lab
GAL1::CTK1-TAP *RPG1-TAP*	*MAT*a; as W303; *RPG1-TAP::TRP1-KL;* *CTK1-TAP::TRP1-KL* *HIS3-PGAL1::CTK1*	*RPG1-TAP::URA3* PCR product was integrated C-terminal of *RPG1* into *GAL1::CTK1-TAP*
GAL1::CTK1-TAP *TIF5-TAP*	*MAT*a; as W303; *NIP1-TAP::TRP1-KL;* *CTK1-TAP::TRP1-KL;* *HIS3-PGAL1::CTK1*	*TIF5-TAP::URA3* PCR product was integrated C-terminal of *TIF5* into *GAL1::CTK1-TAP*
GAL1::CTK1-TAP *DED1-TAP*	*MAT*a; as W303; *DED1-TAP::TRP1-KL;* *CTK1-TAP::TRP-KL* *HIS3-PGAL1::CTK1*	*DED1-TAP::URA3* PCR product was integrated C-terminal of *DED1* into *GAL1::CTK1-TAP*
GAL1::CTK1-TAP *TIF4632-TAP*	*MAT*a; as W303; *TIF4632-TAP::TRP1-KL* *CTK1-TAP::TRP-KL* *HIS3-PGAL1::CTK1*	*TIF4632-TAP::URA3* PCR product was integrated C-terminal of *TIF4*632 into *GAL1::CTK1-TAP*
CBF5-TAP	*MAT*α; as W303; *CBF5-TAP::TRP1-KL*	*CBF5-TAP::TRP1* PCR product was integrated C-terminal of *CBF5* into W303
NOP13-TAP	*MAT*α; as W303; *NOP13-TAP::TRP1-KL*	*NOP13-TAP::TRP1* PCR product was integrated C-terminal of *NOP13* into W303

Strain	Genotype	Origin
REI1-TAP	*MAT*α; as W303; *REI1-TAP::TRP1-KL*	*REI1-TAP::TRP1* PCR product was integrated C-terminal of *REI1* into W303
CIC1-TAP	*MAT*α; as W303; *CIC1-TAP::TRP1-KL*	*CIC1-TAP::TRP1* PCR product was integrated C-terminal of *CIC1* into W303
SDA1-TAP	*MAT*α; as W303; *SDA1-TAP::TRP1-KL*	*SDA1-TAP::TRP1* PCR product was integrated C-terminal of *SDA1* into W303
NOP53-TAP	*MAT*α; as W303; *NOP53-TAP::TRP1-KL*	*NOP53-TAP::TRP1* PCR product was integrated C-terminal of *NOP53* into W303
MRS6-TAP	*MAT*α; as W303; *MRS6-TAP::TRP1-KL*	*MRS6-TAP::TRP1* PCR product was integrated C-terminal of *MRS6* into W303
JJJ1-TAP	*MAT*α; as W303; *JJJ1-TAP::TRP1-KL*	*JJJ1-TAP::TRP1* PCR product was integrated C-terminal of *JJJ1* into W303
STM1-TAP	*MAT*a; as W303; *STM1-TAP::TRP1-KL*	Heidrun Schreck, Jansen lab
GAL1::TAP-POP1	*MAT*α; as W303; *TRP1-KL-PGAL1::TAP-POP1*	*TRP1-KL-PGAL1::TAP-POP1* PCR product was integrated N-terminal of *POP1*
LTV1-TAP	*MAT*α; as W303; *LTV1-TAP::TRP1-KL*	*LTV1-TAP::TRP1* PCR product was integrated C-terminal of *LTV1* into W303
RPS16A-TAP	*MAT*α; as W303; *RPS16A-TAP::TRP1-KL*	*RPS16a-TAP::TRP1* PCR product was integrated C-terminal of *RPS16A* into W303
RPS17B-TAP	*MAT*α; as W303; *RPS17B-TAP::TRP1-KL*	*RPS17B-TAP::TRP1* PCR product was integrated C-terminal of *RPS17B* into W303
RPS18A-TAP	*MAT*α; as W303; *RPS18A-TAP::TRP1-KL*	*TIF5-TAP::TRP1* PCR product was integrated C-terminal of *TIF5* into W303
RPS24A-TAP	*MAT*α; as W303; *RPS24A-TAP::TRP1-KL*	*RPS24A-TAP::TRP1* PCR product was integrated C-terminal of *RPS24A* into W303
RPS1A-TAP	*MAT*a; as RS453; *RPS1A-TAP::TRP1-KL*	Susanne Röther, Sträßer lab
RPS1B-TAP	*MAT*a; as RS453; *RPS1B-TAP::TRP1-KL*	Susanne Röther, Sträßer lab

Strain	Genotype	Origin
RPS5-TAP	*MAT*α; as W303; *RPS5-TAP::TRP1-KL*	*Rps5-TAP::TRP1* PCR product was integrated C-terminal of *RPS5* into W303
RPS6A-TAP	*MAT*a; as RS453; *RPS6A-TAP::TRP1-KL*	Susanne Röther, Sträßer lab
RPS8A-TAP	*MAT*a; as RS453; *RPS8A-TAP::TRP1-KL*	Susanne Röther, Sträßer lab
RPS8B-TAP	*MAT*a; as RS453; *RPS8B-TAP::TRP1-KL*	Susanne Röther, Sträßer lab
RPS9B-TAP	*MAT*a; as RS453; *RPS9B-TAP::TRP1-KL*	Susanne Röther, Sträßer lab
RPS11A-TAP	*MAT*α; as W303; *RPS11A-TAP::TRP1-KL*	*Rps11A-TAP::TRP1* PCR product was integrated C-terminal of *RPS11A* into W303
GAL1::CTK1-TAP *Δlys*	*MAT*a/α; as W303; *CTK1-TAP::TRP1-KL* *HIS3-PGAL1::CTK1* *Δlys::KANMX6*	*GAL1::CTK1-TAP* was crossed to *Δlys* (Katharina Brünger, Sträßer lab)
RS453: *GAL1::CTK1--TAP*	*MAT*α; as RS453; *CTK1-TAP::TRP1-KL* *HIS3-PGAL1::CTK1*	Susanne Röther, Sträßer lab
RS453: *GAL1::BUR2-TAP*	*MAT*a; as RS453; *BUR2-TAP::TRP1-KL* *HIS3-PGAL1::BUR2*	Lina Karakasili, Sträßer lab
NPL3-TAP	*MAT*α; as W303; *NPL3-TAP::TRP1-KL*	Susanne Röther, Sträßer lab
TAP-NPL3	*MAT*a; as W303; *TAP-NPL3*	*TRP1-KL-PGAL1::TAP-NPL3* PCR product was integrated N-terminal of NPL3 in W303; *TRP1-KL-PGAL1* was removed with Cre recombinase
NPL3 shuffle	*MATa/α*; as W303; *NPL3::HIS3* (pRS316-*NPL3*)	Susanne Röther, Sträßer lab
NPL3 shuffle *GAL1::CTK1-TAP*	*MATa/α*; as W303; *NPL3::HIS3* (pRS316-*NPL3*) *CTK1-TAP::TRP1-KL* *HIS3-PGAL1::CTK1*	*GAL1::CTK1-TAP* was mated to *NPL3* shuffle; spore Vb+Vd
RS453: *CTK1-TAP*	*MATa/α*; as W303; *CTK1-TAP::TRP1-KL*	Susanne Röther, Sträßer lab

4.2. METHODS

4.2.1. Standard methods

Cloning procedures were done according to Sambrook and Russell (2001) and cover restriction digests, ligations, transformation of vectors in *Escherichia coli*, and separation of DNA in agarose gels. Commercially available kits were used according to maufacturer's instructions.

Point mutations were generated by site directed mutagenesis using the Invitrogen protocol (Invitrogen, Karlsruhe). The PCR sample was digested with 10 U *Dpn*I for 2h at 37°C and transformed into *E. coli*. All plasmids were sequenced by MWG, Eurofins (Munich).

4.2.1.1. PCR reactions

If not indicated differently, all PCR reactions were done in a 20µl Phusion PCR reaction:

10µl Phusion® High-Fidelity PCR Master Mix
0.5 µl 10pmol/µl primer1
0.5µl 10pmol/µl primer1
1 µl template DNA (100-300ng/µl)
ad 20 µl ddH_2O

Typical amplification cycle:

98°C 1min
98°C 15 sec
55°C 20 sec } 35x
68°C 20 sec/1000bp
68°C 5 min

For TAP tag integration, a 100µl KNOP PCR with the following concentrations was done:

0.5 µM primer1
0.5 µM primer2
0.2 mM of each dNTP
1x KNOP buffer (50 mM Tris-HCl, pH 9,2; 16mM $(NH_4)_2SO_4$; 2,25 mM MgCl2)
100-300ng DNA
1µl KNOP polymerase (2 U Taq, 0.56 U Vent)
ad 100µl ddH_2O

amplification cycle:

94°C	2 min	
94°C	1 min	⎫
55°C	30 sec	⎬ 35x
68°C	1 min/1000bp	⎭
68°C	10 min	

4.2.2. Yeast specific techniques

4.2.2.1. Culture of S. cerevisiae

Yeast strains were cultured in either full medium or synthetic complete (SC) medium.

Full medium
1% yeast extract (Becton Dickinson, Heidelberg)
2% Bacto-Peptone (Becton Dickinson, Heidelberg)
2% of either Glucose (YPD) or Galactose (YPG)

SC medium
0,67% yeast nitrogen base (Formedium, Norwich, UK)
0,06% complete synthetic mix (including all essential AA except the auxotrophy markers leucine, tryptophane, histidine, uracil and adenine
2% of either Glucose (SCD-X) or Galactose (SGC-X)

4.2.2.2. Transformation of yeast cells

50 ml of a yeast culture was grown to an optical density of 0.5 to 0.8 and harvested by centrifugation at 3600 rpm (Rotanda 46R centrifuge) and room temperature (RT) for 3 min. After washing with 10 ml of H_2O, the pellet was washed once with 500 µl of solution I (10 mM Tris-HCl, pH 7.5, 1 mM EDTA, 100 mM Li-acetate) and resuspended in 250 µl solution I. 1-3 µg DNA and 5 µl of single stranded carrier DNA (DNA of salmon of herring testis, 2 mg/ml) were mixed with 50µl of cells in solution I and incubated with 300 µl solution II (10 mM Tris-HCl, pH7,5; 1mM EDTA; 100 mM Li-acetate; 40% PEG-4000) on a turning wheel at RT for 30 min. The samples were heat shocked at 42°C for 10 min, followed by a 3 min incubation on ice. 1 ml of H_2O was added, the sample centrifuged, the pellet resuspended in 50 µl H_2O and plated on a selective plate. For genomic integrations, the pellets were resuspended in 1 ml YPD or YPG and incubated on a turning wheel for 1 h prior to plating. To transform yeast cells grown on plate, 1 loop of logarithmically grown cells was resuspended in 30 µl of 100 mM Li-acetate and vortexed. The rest of the transformation was done according to the protocol described above.

4.2.2.3. Preparation of genomic DNA

10 ml of an overnight W303 culture with an OD_{600} >1 were harvested by centrifugation at 3600 rpm (Rotanda 46R centrifuge) and RT for 3 min and washed with 10 ml H_2O. The cells were resuspended in 500µl H_2O and 200 µl lysis buffer (2% Triton X-100, 1% SDS, 100mM NaCl, 10 mM Tris-HCl, pH 8.0, 1 mM EDTA). For lysis, 300 µl glass beads and 300 µl phenol:chloroform:isomamylalcohol (25:24:1) were added and the sample vortexed for 3 min. After centrifugation at 16000g for 10 min, the upper phase was removed and incubated with an equal volume of chloroform. After another centrifugation step, 1.2 ml of 100% ethanol was added to the upper phase for precipitation of genomic DNA. The solution was incubated at -20°C for at least 10 min. After centrifugation at 16000g and 4°C for 30 min, the pellet was dried and resuspended in 400µl TE buffer (10 mM Tris-HCl, pH 8.0, 1 mM EDTA). To remove the RNA, the DNA was incubated with 20 µl RNaseA (10mg/ml) at 37°C for 40 min. The genomic DNA was precipitated by addition of 40 µl 3 M Na-acetate, pH 5.2 and 800 µl 100% ethanol at -20°C for at least 10 min. After centrifugation at 16000g and 4°C for 30 min, the pellet was washed with 80% ethanol, dried and resuspended in 30 µl TE buffer.

4.2.2.4. Genomic integration of a TAP (tandem affinity purification) tag

TAP tagging was done according to Puig et al. 2001. The genomic integration of a TAP tag is accomplished by homologous recombination of the C-terminal or N-terminal region of the respective gene with a PCR product containing the tag and an auxotrophy marker. For C-terminal tagging, the 5'primer consists of the C-terminal 50 nucleotides (nt) of the ORF of the respective gene without the stop codon and the sequence 5'-tccatggaaaagagaag-3'(XYZ-oligo1), which anneals at the 5'end of the CBP coding sequence. The 3' primer is made of the 50 nucleotides in the 3'UTR, 30 nt downstream of the stop codon plus 5'-tacgactcactataggg-3', a sequence that anneals downstream of the auxotrophy marker (XYZ-oligo2). These primers were used to amplify the TAP tag and the selection marker with pBS1539 (URA3) or pBS1479 (TRP1) as template with a KNOP PCR (4.2.2). The PCR product was purified via phenol chloroform extraction. For this, 100 µl PCR product was mixed with 60 µl phenol:chloroform:isoamylalcohol (25:24:1). After centrifugation at 16000g for 10 min, the upper phase was removed, mixed with an equal volume of chloroform, centrifuged again and once more, the upper phase was taken. It was then incubated with 1/10 volume of 3 M Na-acetate and two volumes of 100% ethanol at -20°C for at least 1h. The DNA was pelleted by centrifugation at 16000g and 4°C for 30 min and once washed with 70% ethanol. The pellet was dried, resuspended in 10 µl TE buffer and transformed completely into yeast cells

(4.2.2.2) for homologous recombination. Transformants are then tested for correct integration by western blotting against the TAP tag (4.2.17, 4.2.18).

For N-terminal TAP tagging, the primers were constructed analogous to the primer for the C-terminal TAP tag. The 5' primer consists of the last 50 nt of the promoter of the respective gene followed by the sequence 5'-gaacaaaagctggagctcat-3' which anneals to the auxotrophy tag. The 3' primer contains the first 50 nt of the respective gene and the sequence 5'-cttatcgtcatcatcaagtg-3' which is complementary to the end of the CBP tag. As a template, pBS1761 is used. After correct integration of the PCR product, the auxotrophy marker is under the control of the promoter of the respective gene and the tagged gene itself is controlled by a *GAL1* promoter. In order to put the tagged gene under control of its own promoter again, the auxotrophy marker and the *GAL1* promoter are flanked by Cre recombinase cutting sites and the tagged strains are transformed with a plasmid containing the Cre recombinase (pBS1776). Correctly processed transformants are selected by loss of the auxotrophy marker and the plasmid.

4.2.2.5. Depletion of Ctk1 and Bur2 by glucose repression

Depletion of Ctk1 and Bur2 was achieved by using a strain carrying a C-terminal TAP tagged version of the respective protein (allowing determination of protein levels using anti-ProtA antibody) driven by the *GAL1* promoter (*GAL1::CTK1-TAP* and *GAL1::BUR2-TAP*). As a preculture, cells were grown in galactose containing media until stationary phase. The respective amount of glucose containing media was inoculated with the preculture in such a way, that 18 h later the cells could be harvested at an OD_{600} between 0,5 – 1,0.

4.2.3. *In vitro* transcription

The IRES plasmids and the corresponding m^7GpppG capped positive control were linearized with *EcI*136II before being transcribed with T7 polymerase (New England Biolabs). The GpppA cap for the IRES constructs and the m^7GpppG cap for the positive control (both from KEDAR, Poland) were added to the reaction together with ATP, CTP, and UTP. After a 5 min incubation at 37°C, GTP was added and the DNA transcribed for 1 h at 37°C. The template DNA was digested with DNAse for 15 min at 37°C. The capped luciferase mRNA was *in vitro* transcribed from pSP6P (Verge et al., 2004) after its linearization with BsrBI (Fermentas). The *in vitro* transcription was carried out with the AmpliCap high-yield message

maker kit (Biozym) according to the manufacturer's directions. For generating radiolabeled mRNA the BSEF-*RPL38*, BSEF-*RPL41a*-22bp5'UTR, BSEF-*RPL41a*-80bp5'UTR, and BSEF-*PGK1* plasmids were linearized with *Hind*III before being *in vitro* transcribed with T3 polymerase (Roche). m^7GpppG (KEDAR, Poland) together with ATP, CTP, and ^{32}P-αUTP were added to the reaction. After a 5 min incubation at 37°C, GTP was added and the DNA transcribed at 37°C for 1 h. The template DNA was then digested with DNAse for 15 min at 37°C. Template mRNA for the toeprint assay was generated accordingly, except for the use of non-radioactive UTP. All mRNAs were purified by using the RNA MinElute Kit according to the manufacturer's directions (Qiagen, Hilden).

4.2.4. *In vitro* translation

4.2.4.1. Preparation of yeast translation active extracts

In vitro translation active extracts were prepared as described in Altmann and Trachsel 1997. For (mock) depletion, 4 l YPD cultures were inoculated with an overnight culture of cells grown in YPG. Cells were harvested after 18 hours at OD_{600} 1.0 – 1.2. Cells were harvested by centrifugation at 3000g and 4°C for 5 min and washed with 50 ml H_2O. The cells were weighed and incubated with 40 ml buffer 1 (1 M sorbitol, 2 mM EDTA, 4 mM β-ME) on a shaking device at RT for 30 min. After centrifugation, the pellet was resuspended in 40 ml 1 M sorbitol containing 1 mg zymolyase 20000T per g cells for spheroblasting. The reaction was monitored by taking 5 µl of the cell suspension and measuring the OD_{600} when put into 1 ml of H_2O. If after 1 min the OD_{600} of this cell suspension dropped to 50% of the original value, the cells were pelleted by centrifugation at 3000g and 4°C for 5 min. The pellet was carefully resuspended in YPD additionally containing 1 M sorbitol and incubated with gentle shaking for regeneration for 1 h. After another centrifugation, the cells were resuspended in 0.63 translation buffer (30 mM Hepes-KOH, pH 7.4, 100 mM K-acetate, 2 mM DTT) per g cells pellet and homogenized with 30 strokes of a Dounce homogenizer with a tight fitting pistil. The cell lysate was then centrifuged at 15000 rpm (SW40 rotor) and 4°C for 19 min. The supernatant was put into a fresh tube and centrifuged at 25000 rpm (SW40 rotor) and 4°C for 21 min. The lipid layer was removed by aspiration and 2.5 ml of the supernatant applied onto a PD10 column, which had been pre-equilibrated with 25 ml translation buffer. The first 1 ml was discarded and the next 2.5 ml collected, aliquoted and stored in liquid nitrogen.

4.2.4.2. Determination of translation activity of in vitro transcribed luciferase mRNA

In vitro translation assays were performed as described in Altmann & Trachsel, 1997. 1.25 A_{260} of the respective extract were incubated with 1.6 µg of creatin kinase (5 mg/ml (Roche) in 30 mM Hepes-KOH pH 7.4, 50% glycerol) in a total volume of 20 µl for 5 min in ice, followed by an incubation with 2 mM Mg-Acetate, 76 mM KCl, 0.4 mM GTP, 1 mM ATP, 50 µM of each amino acid, 12.5 mM creatin phosphate and 4 U RNase inhibitor (RNasin, Promega) in a total volume of 30 µl for 7.5 min, leading to ribosome run-off. 300 ng of *in vitro* transcribed luciferase mRNA were added and *in vitro* translated at RT for 30 min. For measurement of luciferase activity, 25 µl of the *in vitro* translation reaction were mixed with 100 µl of 25 mM glycyl-glycine, pH 7.8, 10 mM K-phosphate, pH 7.8, 12 mM $MgSO_4$, 3.2 mM EGTA, 2 mM ATP, 1 mM DTT, and 200 µM luciferin using a Lumat LB9507 Luminometer (EG&G Berthold). The emitted luminescence was detected for 10 sec. WT activity was set to 100% and the activity of the mutant strain calculated accordingly. The results are the mean of two independent experiments for each three independently prepared extracts.

When the influence of micrococcal nuclease (MN) treatment on the translation activity was tested, the experiment was performed as above, only that 0, 0.1, 0.2 and 1 U MN were added to the translation active extract together with the creatin kinase and 1 mM $CaCl_2$. The samples were incubated at RT for 15 min and the reaction stopped by transferring the samples on ice and by adding 2.2 mM EDTA. After this treatment, the experiment was continued as above.

4.2.5. Translation initiation assay

Three A_{260} of translation active extract were incubated with 6.25 µg creatin kinase (Roche) for 5 min on ice, followed by 30 min incubation with 1.25 mM EGTA, 2 mM MgAc, 76 mM KCl, 0.4 mM GTP, 1 mM ATP, 50 µM of each amino acid, 12.5 mM creatin phosphate, 1 mM cycloheximide, 8 U RNAse inhibitor, 35 ng of *in vitro* transcribed radioactive mRNA, and, where indicated, 1.25 mM GMP-PNP in a total volume of 120 µl at room temperature. The entire reaction was loaded on a 5-25% sucrose gradient and centrifuged at 39,000 rpm (SW40 rotor) for 2 h. 450 µl fractions were taken off and 300 µl of each fraction were counted with 3 ml of scintillation cocktail (Roth) using a scintillation counter (Tri-Carb 2810TR, PerkinElmer, Waltham, USA).

4.2.6. Toeprint assay

Gradients with translation initiation reactions were set up as described above, only that 1.3 mM cycloheximide and, where indicated, 0.3 mM GMP-PNP were used and that the extracts were incubated with 200-250 ng of *in vitro* transcribed non-radioactively labeled *RPL38* mRNA. 400 µl fractions were taken off with a Teledyne ISCO gradient machine, 25 µl of each fraction diluted 1:4 with dilution buffer (50 mM Tris-HCl pH7.5, 60 mM KCl, 6 mM $MgCl_2$, 5 mM DTT, 0.5 mM cycloheximide, 0.5 mM dTTP, dCTP, dGTP each, 5 nM dATP, and RNAse inhibitor), and the reaction mixture was incubated for 105 s at 52°C, placed on ice, and incubated with 25 pmol primer (5'-GGCGGTCTTAACGTCAGCT-3') at 37°C for 5 min. For reverse transcription, 0.5 µl ^{32}P-α-dATP and 1 µl SuperscriptII (Invitrogen, Karlsruhe) were added and the reaction was incubated at 37°C for 15 min. Then, 60µl of a 0.6% SDS and 30mM EDTA mix was added followed by a phenol/chloroform extraction of the reverse transcripts. The DNA was precipitated with rRNA as co-precipitator, ammonium acetate, glycogen and ethanol, centrifuged at 14000 rpm (table top centrifuge) and 4°C for 20 min, resuspended in denaturing formamide loading buffer, and loaded on a pre-run 13% polyacrylamide denaturing sequencing gel. In case of the 48S fraction of Ctk1 depleted cells, only half of the resuspended pellet was loaded on the gel. The gel was run at 45 W for 1 h 50 min, dried and exposed to a phosphoimager for at least 3 days. The plate was scanned with a storm 860 imager (Molecular Dynamics) and the bands quantified using multi gauge (Fujifilm). The sequencing reaction was done according to manufacturer's directions (USB sequenase 2.0).

4.2.7. Polysome gradients

Polysome gradients were performed as described in Altmann & Trachsel, 1997. 50 ml of yeast cells were grown in YPD to an OD_{600} of 0,5. 0.1mg/ml cycloheximide was then added and the cells incubated at 30°C for 10 min before harvesting by centrifugation for 3600 rpm for 3 min. The cells were resuspended in polysome buffer (20 mM HEPES-KOH, pH 7,6; 75 mM KCl; 2,5 mM MgCl2; 1 mM EGTA; 1 mM DTT) plus 0,1 mg/ml cycloheximide. Lysis was done by adding 250 µl glass beads and vortexing at 4°C for 5 min. After removal of the cell debris by centrifugation at 16000g for 5 min, extract corresponding to 250 µg RNA was loaded onto a 10-12 ml 10-50% linear sucrose gradient in polysome buffer plus 0,1 mg/ml cycloheximide and centrifuged at 40000 rpm for 2 h using an SW40 Ti rotor. The absorption

profile at 254 nm was recorded with a Teledyne ISCO gradient machine.

4.2.8. TAP purification

Essentially, the purification was done according to Puig et al. (2001).

4.2.8.1. Cell harvest and lysis

A 2 L culture of yeast cells was harvested at an OD_{600} of 3,0 – 3,5 by centrifugation at 4000 rpm (SLC6000 rotor) for 4 min, washed once with 500 ml H_2O and once with TAP buffer (50 mM Tris-HCl, pH 7.5, 100 mM NaCl, 1.5 mM $MgCl_2$, 0,15% NP40). Cells were then flash frozen in liquid nitrogen and stored at -80°C.

For lysis, cells were resuspended in an equal volume of TAP buffer (containing 1mM DTT and protease inhibitors – 1.3 µg/ml pepstatin A, 0.28µg/ml leupeptin, 170 µg/ml PMSF, 330 µg/ml benzamidine) and mixed with a double volume of glass beads. Lysis occurred while shaking in a bead mill (Fritsch, Idar-Oberstein) by following this protocol: 3 x (500rpm for 4 min, 2 min breaks in between). The glass beads were removed and washed once with buffer, so that the lysate comprised 25 ml. After centrifugation at 4000 rpm (Rotanda 46R centrifuge) at 4°C for 10 min, the supernatant was subjected to ultracentrifugation (27000 rpm – SW32 rotor, 4°C, 1 h). The fatty phase was removed by aspiration and the clear lysate collected. It was either used directly or glycerol (final concentration of 5%) was added for flash freezing in liquid nitrogen and storage at -80°C.

4.2.8.2. Purification

0,4 ml IgG sepharose (GE Healthcare, Munich) were washed 3 x in TAP buffer (1800 rpm (Rotanda 46R centrifuge), 4°C, 2 min) and added to the lysate. After incubation for at least 1 h and up to overnight incubation on a turning wheel at 4°C, the beads were centrifuged down and transferred to a mobicol column containing a 35 µm filter. The beads were washed with 10 ml TAP buffer containing 0.5 mM DTT by gravity flow.

To elute the protein (complex), 4µl of TEV protease (0.2 – 10 µg/µl) and 150 µl TAP buffer (+ 0.5 mM DTT) were added to the beads and incubated on a turning wheel at 16°C for 1 h 20 min. For elution, the mobicol was centrifuged in a table top centrifuge at 2000 rpm for 1 min. The eluate was mixed with glycerol to a final concentration of 5-10%, flash frozen and stored at -80°C.

4.2.8.3. Specific modifications for purification

A: Purification of the CTDK-I complex

12 L culture of SDC-URA-Leu media were inoculated with 72 OD_{600} (approx. 15 ml saturated culture) of the strain *CTK1-TAP* (RS453) containing the plasmids pRS425-*CTK2-CTK3* and pRS426-*CTK1*-TAP. The cells were harvested and lysed according to the normal TAP purification protocol (4.2.8.1). The lysate was directly incubated with the IgG beads overnight. The beads were washed with 8 ml TAP buffer containing 1M NaCl and 0.5 mM DTT, followed by 5 ml of normal TAP buffer (+ 1 mM DTT). The TEV cleavage and IgG elution was done according to standard methods (4.2.8.2). During TEV cleavage, 0.5 ml calmodulin beads (GE Healthcare, Munich) were washed 3 x in TAP buffer plus 1 mM DTT and 2 mM $CaCl_2$. After removal of surplus buffer, the beads were mixed with 150µl TAP buffer containing 1 mM DTT and 4 mM $CaCl_2$ and incubated with 150µl TEV eluate at 4°C on a turning wheel for at least 1 h. The beads were washed with 5 ml TAP buffer plus 1 mM DTT and 2 mM $CaCl_2$.

To elute the proteins, the beads were incubated in a thermomixer at 10°C, 650 rpm for 2 h with elution buffer (50 mM Tris-HCl, pH 7.5, 150 mM NaCl 10 mM EGTA, 1mM DTT, Protease inhibitors) and then eluted by centrifugation in a tabletop centrifuge at 2000 rpm for 1 min. The eluate was concentrated using a 100 kDa MembraSpin Mini (membraPure, Bodenheim) filter until a volume of approximately 100 µl. Glycerol was added to a final concentration of 5-10 % and the eluate flash frozen in liquid nitrogen and stored at -80°C.

B: Purification of candidate substrates for *in vitro* kinase assays

For purification of candidate substrates of Ctk1, the corresponding TAP tagged strains were cultured, harvested and lysed according to the standard protocol (4.2.8.1). When protein complexes were purified, the standard purification protocol was used (4.2.8.2). When single proteins were purified, a high salt washing step with 10 ml TAP buffer containing 1 M NaCl was included during the washing of the IgG beads, followed by a 2 ml wash with normal TAP buffer. After elution from the IgG beads, the eluate was concentrated to approximately 10-20 µl using a MembraSpin Mini concentrator (10 kDa; 30 kDa or 100 kDa cutoff; membraPure, Bodenheim). Glycerol was added to a final concentration of 5-10 % and the eluate flash frozen in liquid nitrogen and stored at -80°C.

C: Small scale TAP purification

A 100 ml culture of the respective yeast strain was grown to an OD_{600} of 1,0 – 1,2 and the

cells harvested by centrifugation (3600 rpm – Rotanda 46R centrifuge, 3 min, 4°C). The pellet was washed with 1 ml of cold H_2O and finally resuspended in 1 ml cold TAP buffer containing 1 M NaCl, protease inhibitors (1.3 µg/ml pepstatin A, 0.28µg/ml leupeptin, 170 µg/ml PMSF, 330 µg/ml benzamidine), phosphatase inhibitors (10 mM NaF, 1 mM $NaVO_4$, 5 mM β-glycerophosphate) and 1 mM DTT. For lysis, 1 ml of glass beads were added and the samples vortexed 5 x at RT for 3 min with 3 min breaks on ice. The lysate was collected by piercing of the reaction tube with a syringe and subsequent centrifugation (1800 rpm – Rotanda 46R centrifuge, 2 min, 4°C). The lysate was cleared by centrifugation at 13000 rpm in a table top centrifuge and 4°C for 30 min. 900µl of the supernatant were mixed with 50 µl pre-washed IgG beads and incubated on a turning wheel at 4°C for 1 h. The beads were then washed 10 x with TAP buffer containing 1 M NaCl, protease inhibitors and phosphatase inhibitors and 1 mM DTT by centrifugation at 2000 rpm (table top centrifuge) and 4°C for 2 min each. After the final washing step, 150 µl of TAP buffer (plus phosphatase inhibitors and 1 mM DTT) and 0.5 µl TEV protease (0.2 – 10 µg/µl) were added to the beads and the sample incubated at 16°C for 1 h 30 min. The TEV eluate was collected by centrifugation (1800 rpm – Rotanda 46R centrifuge, RT, 2 min) and precipitated as well as desalted according to the sample preparation and electrophoresis section of the Pro-Q® Diamond Phosphostain Gel Stain manual (Molecular Probes, Invitrogen, Karlsruhe).

4.2.9. Purification of ribosomes by sucrose cushion

Cells were cultured and harvested as described in 4.2.8.1. For lysis, the cell pellet was resuspended in the same amount of buffer 1 than cell pellet (buffer 1: 20 mM Hepes pH7.5, 100 mM K-acetate, 5 mM Mg-acetate, 2 mM DTT, protease inhibitors – 1.3 µg/ml pepstatin A, 0.28µg/ml leupeptin, 170 µg/ml PMSF, 330 µg/ml benzamidine). Double the volume of beads were added and the suspension vortexed twice at 4°C for 3 min with a 3 min break on ice. The lysate was centrifuged at 4000 rpm (Rotanda 46R centrifuge) and 4°C for 4 min, transferred to an SW40 tube and centrifuged at 15000 rpm (SW40 rotor) and 4°C for 20 min. Subsequently, the fatty phase was removed and clear lysate loaded on two sucrose cushions each made of 250 µl 1.5 M sucrose in 500 mM K-acetate and 250 µl 1 M sucrose in 500 mM K-acetate. The cushions were centrifuged at 100000 rpm (TLA 110 rotor) and 4°C for 3 h and the pellet resuspended in 500 µl buffer 1 while shaking at 4°C for 1 h. A second cushion with 250 µl 1 M sucrose and 0.5 M KCl was prepared and the combined pellets of the previous cushion loaded. The tubes of the previous cushion were washed with 500 µl buffer 1, and the tubes with the second cushion filled up to 2 ml. The cushion was centrifuged at 100000 rpm

(TLA 110 rotor) and 4°C for 45 min and the pellet resuspended in 100 µl buffer 1 while shaking at 4°C for 1 h. The A_{260} was measured, the sample flash frozen in liquid nitrogen and stored at -80°C

4.2.10. Purification of recombinant proteins in *Escherichia coli*

4.2.10.1. Purification of His tagged proteins

Nop16 was purified by Nickel affinity purification. For this, pET28b-Nop16 was transformed into Rosetta cells. 2 L culture of LB media with the respective antibiotic were inoculated with an overnight culture of the Rosetta cells carrying the corresponding plasmid and grown at 37°C. At an OD_{600} of 0.3 the cultures were transferred to an 18°C incubator and shaken until the cells reached an OD_{600} of 0.5-0.6. The expression of the Histidin (His) tagged protein was induced with the addition of 200µl of 1M IPTG (Isopropyl-β-D-thiogalactopyranosid) and incubated overnight. The cells were harvested at an OD_{600} of 4.5 – 5.0 by centrifugation at 4000 rpm (SLC600 rotor) and 4°C for 15 min. The pellet was washed with 25 ml of buffer 1 (200 mM KCl, 50 mM Tris-HCl, pH 7.5, 2 mM EDTA, 2mM β-ME) and resuspended in 7 ml lysis buffer (200 mM KCl, 50 mM Tris-HCl pH 7.5, 2 mM β-ME, 10 mM imidazole). After sonication for 10 min on ice (output: 7, duty cycle: 50) the lysate was centrifuged at 16000g (SS34 rotor) and 4°C for 40 min. The supernatant was then incubated with 1 ml of Ni-NTA beads (Sigma, Taufkirchen), which had been pre-washed with lysis buffer, on a turning wheel at 4°C for at least 1 h. The suspension was transferred to a column (Poly-Prep® Chromatography columns, BioRad, Munich) and the lysate removed by gravity flow. After the beads were washed with 30 ml lysis buffer, the column was closed and 1 ml of elution buffer (200 mM KCl, 50 mM Tris-HCl pH 7.5, 300 mM Imidazole, 2 mM β-ME) was added. The beads were incubated with elution buffer at RT on a turning wheel for 10 min, before the eluate was collected by centrifugation at 1800 rpm (table top centrifuge) for 1 min. The eluate was furthermore dialysed against buffer 1 for 1 h and concentrated in a 10 kDa membraPure concentrator to a volume of approximately 200 µl.

4.2.10.2. Purification of GST tagged proteins

Srp40 was purified with GST affinity purification. For this, pGEX4-T2-Srp40 was transformed into Rosetta cells. 200 ml culture of LB media with Ampicillin were inoculated

with an overnight culture of the Rosetta cells carrying the pGEX4-T2-Srp40 and grown at 37°C to an OD_{600} of 0.5. The expression of the GST tagged protein was then induced with the addition of 20 µl of 1M IPTG and incubated for 5 h. The cells were harvested by centrifugation at 4000 rpm (GS-3 rotor) and 4°C for 15 min. The pellet was washed with 25 ml of buffer 2 (100 mM NaCl, 50 mM Tris-HCl pH 7.5, 2 mM EDTA, 2mM DTT) and resuspended in 10 ml buffer 2. After sonication for 5 x 15 pulses (output: 2, duty cycle: 50), the lysate was centrifuged at 16000g (SS34 rotor) and 4°C for 30 min. The supernatant was then incubated with 260 µl Glutathione Sepharose 4B (GE Healthcare, Munich), which had been pre-washed with buffer 2, on a turning wheel at 4°C for at least 1 h. The beads were centrifuged down (1800 rpm – Rotanda 46R centrifuge, 4°C, 1 min) and the supernatant discarded. The beads were washed 5 x with 250 µl buffer 2 and the protein was then eluted by incubation with 150 µl buffer 2 additionally containing 20 mM reduced glutathione. The beads were centrifuged down (1800 rpm – Rotanda 46R centrifuge, 4°C, 1 min), the eluate collected and concentrated in a 30 kDa membraPure concentrator to a volume of approximately 200 µl. For removal of the GST tag, the eluate was incubated with 40 µl PreScission protease (1mg/ml) at 4°C on a turning for 18 h.

4.2.11. *In vitro* kinase assay

For *in vitro* kinase assays approximately 100 ng - 1µg of the substrate and 50 ng – 200 ng of the CTDK-I complex were mixed with kinase buffer (0.5 mM ATP, 1 mM DTT, 100 mM Tris-HCl, pH 7.5, 1 mM MgCl2, 1 mM EGTA) in a 20 µl reaction. 1 µCi (γ-^{32}P)-ATP was added and the reaction incubated at 30°C for 30 min. To stop the reaction, 6 µl 4 x sample buffer (4x SB, 0.2 M Tris pH 6.8 at 25°C; 40% glycerol; 8% SDS; few grains Bromophenol Blue; 0.1M DTT) were added to the reaction, the sample was vortexed for 1 min and incubated at 95 °C for 5 min. After centrifugation at 16000g in a table top centrifuge at RT for 3 min, the entire sample was loaded on a 10-15% SDS-PAGE (4.2.18) according to the molecular weight of the substrates and stained with Coomassie. The gel was scanned, dried and incubated with a light sensitive film (GE Healthcare, Munich) at least overnight and up to 5 days.

4.2.12. *In vivo* kinase assay

For detection of phosphorylated proteins *in vivo*, the candidate substrates were purified and their phosphorylation status either assessed by radioactive labeling or by staining with a

phosphor-sensitive stain.

4.2.12.1. Radioactive in vivo kinase assay

A yeast culture with the corresponding strain was grown in phosphate depleted YPD (YPD-P) to an OD_{600} of 1.2. The cells were harvested by centrifugation at 3600 rpm (Rotanda 46R centrifuge) for 5min and resuspended in 5 ml of YPD-P. To label the phosphorylated proteins, $^{32}P_i$ was added to a final concentration of 0.05 mCi/ml and the sample incubated in a shaking waterbath at 30°C for 3 h. The cells were then collected by centrifugation (3600 rpm - Rotanda 46R centrifuge, 5min) and resuspended in the same volume of TAP buffer (see 4.2.8) plus 1 mM DTT; phosphatase inhibitors and protease inhibitors. For lysis, double of the volume of glass beads were added and the samples vortexed 4 x 2 min at RT with 2 min breaks on ice. The lysate was centrifuged at 13000 rpm (table top centrifuge) for 10 min and the supernatant incubated with 10 µl of IgG beads (GE Healthcare, Munich), which had been pre-washed with TAP buffer, on a turning wheel at RT for 1h. The beads were then pelleted by centrifugation at 1800 rpm (table top centrifuge) for 1 min, the supernatant removed and the beads washed 10 x with 1 ml of TAP buffer plus 1 mM DTT, protease inhibitors and phosphatase inhibitors. For elution, 30µl of SB was added, the samples incubated at 95°C for 4 min, centrifuged at 1300 rpm (table top centrifuge) and RT for 5 min, and 20 µl loaded onto a 10 – 15% SDS-PAGE (4.2.18). The gel stained with Coomassie, scanned, dried and exposed to a light sensitive film (GE Healthcare, Munich).

4.2.12.2. In vivo kinase assay using Pro-Q® Diamond phosphostain

In order to detect the phosphorylation of candidate substrates, the respective proteins were purified using the small scale TAP purification protocol (4.2.8.3). They were separated on a 12% SDS-PAGE (4.2.18) and stained with the Pro-Q® Diamond-phosphostain according to the maufacturer's instructions (Invitrogen, Karlsruhe). The long protocol was chosen and the fluorescence detected with a Typhoon 9400 scanner (GE Healthcare, Munich) using an excitation of 532 nm and an emission filter of 560 nm longpass.
Afterwards, the proteins were stained with Coomassie (4.2.18) or Sypro Orange (Invitrogen, Karlsruhe) according to the manufacturer's instructions.

4.2.13. SILAC experiments

The labeling of yeast cells with stable isotopes was adapted from (Gruhler & Kratchmarova,

2008). Two cultures of 500 ml of liquid YNB medium containing 30 mg/ml lysine or [13C6] lysine were inoculated with *Δlys::KANMX6* or *GAL1::CTK1-TAP Δlys::KANMX6* cells from a stationary YPG culture. Yeasts were grown at 30°C for 18h until they reached an OD_{600} of 0.5-0.7. Cell pellets were resuspended in 5 ml lysis buffer (20 mM HEPES-KOH pH 7.5, 75 mM KCl, 2.5 mM $MgCl_2$, 1 mM EGTA, 1 mM DTT, 0.5 mM PMSF, 10 mM NaF, 1 mM $NaVO_4$, 5 mM β-glycerophosphate) and vortexed with glass beads at 4°C for 5 min. The samples were centrifuged at 27,000 rpm (SW40 rotor) at 4°C for 15 min. Equal amounts of A_{280} of the supernatant of *Δlys::KANMX6* and *GAL1::CTK1-TAP Δlys::KANMX6* extracts were diluted 1:1 with lysis buffer containing 1 M KCl, loaded on a 15% sucrose cushion containing 500 mM KCl and centrifuged at 42,000 rpm (Ti45 rotor) for 4 h. The pellet was resuspended in lysis buffer (as above, but $NaVO_4$ concentration reduced to 200 µM), loaded on a 5-15% sucrose gradient and centrifuged at 32,000 rpm (SW32 rotor) for 2 h. The pooled ribosomal gradient fractions were pelleted by ultracentrifugation (100,000 rpm, TLA110 rotor, 50 min, 4°C) and washed once with lysis buffer. Purified ribosomes were resuspended in 6 M urea, 2 M thiourea, and 10 mM Tris-HCl pH 8 and protein concentrations were determined using Bradford Assay (BioRad, Munich).

Protein samples were digested in-solution with Lys-C, and phosphopeptides were enriched by TiO_2 chromatography (Olsen et al., 2006). The resulting phosphopeptide fractions were analyzed by online nanoLC-MS/MS on a high-resolution LTQ-Orbitrap Velos instrument using Higher-energy collisional dissociation (HCD) for high-mass accuracy tandem mass spectrometry (Olsen et al., 2007). Peptides and phosphopeptides were identified by Mascot (www.matrixscience.com) and SILAC pairs were quantified and normalized using the MaxQuant software suite (Cox & Mann, 2008).

4.2.14. Analysis of rRNA intermediates

50 ml phosphate depleted YPD (YPD-P) was inoculated with wt or *GAL1::CTK1-TAP* cells growing at stationary phase in YPG. After 12 h, cells were diluted to OD_{600} of 0.3 in YPD-P and grown exponentially for 6 h. Cells were labeled at OD_{600} 0.8 with 15 µCi/ml $^{32}P_i$ for 5 min. 2 ml of cells were harvested, washed, and resuspended in buffer containing 1 M sorbitol. The suspension was incubated with 100 U zymolyase 20T and 0.2% β-ME at 37°C for 5 min, centrifuged (300 rpm/1 min), and the pellet washed before lysis according to the RNAeasy standard protocol (Qiagen, Hilden). The RNA was isolated using the RNAeasy kit (Qiagen, Hilden). 1 or 3 µg RNA were mixed with formamide and EtBr (Ethidium Bromide)

containing loading dye and run on a 1% denaturing formaldehyde agarose gel at 110 V for 5 h. The 25S RNA was detected with UV-light and the rRNA intermediates analyzed with a phosphoimager (10 min exposure) and quantified with AIDA software. For a better comparison of the amounts of processed rRNA intermediates, wt signals of the lane with 1 µg total RNA and Ctk1 depleted signals of the lane with 3 µg total RNA were quantified.

4.2.15. Dot Spots

One loop of freshly growing cells on plate was resuspended in 1 ml H_2O. Four 10 fold dilutions were prepared and 10 µl of each dilution spotted onto the corresponding plate (YPD, YPG, SDC-Trp, SGC-Trp).

4.2.16. Indirect immunofluorescence

For fixation of the cells, 10 ml of an exponentially grown yeast culture (OD_{600} of 0.5 – 1.0) were incubated with 1 ml of 37% HCOH on a turning wheel at 30°C for 90 min. The cells were pelleted by centrifugation at 3000 rpm and RT for 5 min (Rotanda 46R centrifuge), washed twice with spheroblasting premix (1.2 M sorbitol, 0.1 M K-phosphate buffer, pH 7.4, 0.5 mM $MgCl_2$), resuspended in 1 ml spheroblasting premix and stored at 4°C up to 18h. Afterwards, the cells were pelleted and resuspended in 200µl sheroblasting premix additionally containing 100 µg of 100T zymolyase and incubated in a 30°C waterbath for 30 min. Following spheroblasting, the cells were pelleted by centrifugation at 2000 rpm and RT (table top centrifuge) for 4 min and resuspended in at least 10 x the volume of the cells in spheroblasting premix. 1 drop of the suspension was placed on a slide used for fluorescence microscopy, which had been precoated with polylysine. After a 5 min incubation the drops were pipetted off and the bound cells washed with 1 drop of blocking buffer (1% BSA powder in PBS (phosphate buffered saline, 2.7 mM KCl, 7.9 mM Na_2HPO_4, 1.5 mM KH_2PO_4, 137 mM NaCl). To fix the cells, the slide was incubated with methanol in a staining jar at -80°C for 6 min followed by a 30 sec incubation in -80°C cold acetone. The slides were dried at RT and incubated with 100 µl blocking buffer for 10 min. The solution was aspirated off and the cells incubated with 20 µl of the first antibody solution (antibody diluted in 1% BSA in PBS) at RT for 2 h. The antibody was washed off by 3 x 1 min incubations with 10 µl blocking buffer additionally containing 0,1 % Triton-X at RT. The cells were incubated in the dark with 20 µl of the second antibody diluted in blocking buffer for 1 h. Finally, the cells

were washed 3 x with blocking buffer plus 0,1 % Triton-X. For DAPI staining the slides were put in a jar containing SSC buffer (300 mM NaCl; 30 mM Na-citrate, pH 7.0) and 5µl of DAPI (10mg/ml) in the dark for 10 min. After washing the slide for 5 min with a 1:4 dilution of SSC buffer at RT for 5 min in the dark, the slide was dried, the cells covered with 80% glycerin and the cover slide mounted.

The fluorescence was analyzed with a DMI 6000 B fluorescence microscope (Leica Microsystems, Wetzlar). The signal of the alexa F488 coupled antibody was detected at an emission wavelength of 529 nm whereas the DAPI signal was detected at an emission of 461 nm. The excitation occurred at 495 nm and 358 nm, respectively. The intensity was 3 in the case of the alexa F488, and 2 in the case of the DAPI signal. In both cases, a gain of 3.5 was used. The fluorescence signal was analyzed with the LAS AF Lite software (Leica Microsystems, Wetzlar) and the pictures arranged using ImageJ (NIH, Bethesda, USA).

4.2.17. Whole cell extracts

For testing the correct integration of the TAP tag, a fast protocol for whole cell extracts was used. A 2 ml overnight culture with the corresponding strain was harvested by centrifugation at 3600 rpm for 3 min (Rotanda 46R centrifuge), the pellet resuspended in 100 µl of pre-heated SB (95°C) and vortexed with 100 µl glass beads with the following protocol: 3 x (1 min vortexing at full speed, 3 min incubation at 95°C). After centrifugation at 16000g for 5 min, 5 µl of this extract were subjected to SDS-PAGE and western blotting (4.2.18). Using the PAP antibody, the cultures were tested for the presence of the Tap tag.

In order to assess the phosphorylation status of eIF2α, denaturing protein extraction was used. It was carried out essentially as described in Knop et al. (1996). Five OD_{600} of exponentially grown cells were resuspended in 500 µl of H_2O before 150 µl of pre-treatment solution (7.5% β-ME; 1,85 M NaOH) were added and the mixture was incubated on ice for 20 min. After addition of 150 µl of 55% Trichloroacetic acid (TCA) and a further 20 min incubation on ice, the tubes were centrifuged at 16000g and 4°C for 20 min. The supernatant was removed and the pellets resuspended in 100 µl SB and 20µl 1 M Tris base. The samples were then incubated at 95°C for 2 min. After centrifugation at full speed for 5 min the supernatant was loaded on an SDS-PAGE (4.2.18).

For treatment with 3AT, the cells were grown in SDC-His media until an OD_{600} of 0,5. 3AT was added to a final concentration of 40 mM and the cells were further grown to an OD_{600} of 1.2 before being harvested as described above.

4.2.18. SDS-PAGE and western blotting

Sodium dodecylsulfate polyacrylamide gel electrophoresis (SDS-PAGE) was done according to Laemmli (Laemmli, 1970) using the Mini-Protean II system (Biorad, Munich).

For blotting, the proteins were transferred onto a nitrocellulose membrane using a semi-dry blotting machine (Peqlab, Erlangen). For this, 3 layers of Whatman paper followed by the nitrocellulose membrane, the SDS-PAGE gel and another 3 layers of Whatman paper, all presoaked in blotting buffer (50 mM Tris, 40 mM Glycin, 1.3 mM SDS, 10% Methanol), were assembled in the blotting machine. The transfer occurred at 7 V for 40 min. In order to assess the transfer and to mark the protein ladder, the membrane was stained with PonceauS.

After transfer, the membrane was blocked with blocking buffer (2% milk powder in PBS) and incubated with the first antibody at 4°C overnight. The antibody was removed by washing the membrane with blocking buffer at RT for 45 min. Then, the membrane was incubated with the corresponding second antibody at RT for at least 2 h. The immunostained proteins were detected with the ECL kit (Applichem, Darmstadt) and exposure of the membrane to light-sensitive films (GE Healthcare; Munich). The films were developed with a Kodak X omat M35 developing machine (Kodak GmbH, Stuttgart).

5. REFERENCES

Acker, M. G. and J. R. Lorsch (2008). "Mechanism of ribosomal subunit joining during eukaryotic translation initiation." Biochem Soc Trans **36**(Pt 4): 653-7.

Ahn, S. H., M. Kim and S. Buratowski (2004). "Phosphorylation of serine 2 within the RNA polymerase II C-terminal domain couples transcription and 3' end processing." Mol Cell **13**(1): 67-76.

Ahn, S. H., M. C. Keogh and S. Buratowski (2009). "Ctk1 promotes dissociation of basal transcription factors from elongating RNA polymerase II." Embo J **28**(3): 205-12.

Alcazar-Roman, A. R., E. J. Tran, S. Guo and S. R. Wente (2006). "Inositol hexakisphosphate and Gle1 activate the DEAD-box protein Dbp5 for nuclear mRNA export." Nat Cell Biol **8**(7): 711-6.

Alting-Mees, M. A., J. A. Sorge and J. M. Short (1992). "pBluescriptII: multifunctional cloning and mapping vectors." Methods Enzymol **216**: 483-95.

Altmann, M., N. Schmitz, C. Berset and H. Trachsel (1997). "A novel inhibitor of cap-dependent translation initiation in yeast: p20 competes with eIF4G for binding to eIF4E." Embo J **16**(5): 1114-21.

Altmann, M. and P. Linder Power of yeast for analysis of eukaryotic translation initiation (2010). J Biol Chem. **285:** 31907-12.

Ansel, K. M., W. A. Pastor, N. Rath, A. D. Lapan, E. Glasmacher, C. Wolf, L. C. Smith, N. Papadopoulou, E. D. Lamperti, M. Tahiliani, J. W. Ellwart, Y. Shi, E. Kremmer, A. Rao and V. Heissmeyer (2008). "Mouse Eri1 interacts with the ribosome and catalyzes 5.8S rRNA processing." Nat Struct Mol Biol **15**(5): 523-30.

Armache, J. P., A. Jarasch, A. M. Anger, E. Villa, T. Becker, S. Bhushan, F. Jossinet, M. Habeck, G. Dindar, S. Franckenberg, V. Marquez, T. Mielke, M. Thomm, O. Berninghausen, B. Beatrix, J. Soding, E. Westhof, D. N. Wilson and R. Beckmann (1020). "Cryo-EM structure and rRNA model of a translating eukaryotic 80S ribosome at 5.5-A resolution." Proc Natl Acad Sci U S A **107**(46): 19748-53.

Armache, J. P., A. Jarasch, A. M. Anger, E. Villa, T. Becker, S. Bhushan, F. Jossinet, M. Habeck, G. Dindar, S. Franckenberg, V. Marquez, T. Mielke, M. Thomm, O. Berninghausen, B. Beatrix, J. Soding, E. Westhof, D. N. Wilson and R. Beckmann (2010). "Localization of eukaryote-specific ribosomal proteins in a 5.5-A cryo-EM map of the 80S eukaryotic ribosome." Proc Natl Acad Sci U S A **107**(46): 19754-9.

Asano, K., J. Clayton, A. Shalev and A. G. Hinnebusch (2000). "A multifactor complex of eukaryotic initiation factors, eIF1, eIF2, eIF3, eIF5, and initiator tRNA(Met) is an important translation initiation intermediate in vivo." Genes Dev **14**(19): 2534-46.

Barilla, D., B. A. Lee and N. J. Proudfoot (2001). "Cleavage/polyadenylation factor IA associates with the carboxyl-terminal domain of RNA polymerase II in Saccharomyces cerevisiae." Proc Natl Acad Sci U S A **98**(2): 445-50.

Bartkowiak, B., P. Liu, H. P. Phatnani, N. J. Fuda, J. J. Cooper, D. H. Price, K. Adelman, J. T. Lis and A. L. Greenleaf (2010). "CDK12 is a transcription elongation-associated CTD kinase, the metazoan ortholog of yeast Ctk1." Genes Dev **24**(20): 2303-16.

Beckmann, K., M. Grskovic, F. Gebauer and M. W. Hentze (2005). "A dual inhibitory mechanism restricts msl-2 mRNA translation for dosage compensation in Drosophila." Cell **122**(4): 529-40.

Berset, C., H. Trachsel and M. Altmann (1998). "The TOR (target of rapamycin) signal transduction pathway regulates the stability of translation initiation factor eIF4G in the yeast Saccharomyces cerevisiae." Proc Natl Acad Sci U S A **95**(8): 4264-9.

Bhandari, R., A. Saiardi, Y. Ahmadibeni, A. M. Snowman, A. C. Resnick, T. Z. Kristiansen, H. Molina, A. Pandey, J. K. Werner, Jr., K. R. Juluri, Y. Xu, G. D. Prestwich, K. Parang and S. H. Snyder (2007). "Protein pyrophosphorylation by inositol pyrophosphates is a posttranslational event." Proc Natl Acad Sci U S A **104**(39): 15305-10.

Bolger, T. A., A. W. Folkmann, E. J. Tran and S. R. Wente (2008). "The mRNA export factor Gle1 and inositol hexakisphosphate regulate distinct stages of translation." Cell **134**(4): 624-33.

Bouchoux, C., G. Hautbergue, S. Grenetier, C. Carles, M. Riva and V. Goguel (2004). "CTD kinase I is involved in RNA polymerase I transcription." Nucleic Acids Res **32**(19): 5851-60.

Bucheli, M. E. and S. Buratowski (2005). "Npl3 is an antagonist of mRNA 3' end formation by RNA polymerase II." Embo J **24**(12): 2150-60.

Bucheli, M. E., X. He, C. D. Kaplan, C. L. Moore and S. Buratowski (2007). "Polyadenylation site choice in yeast is affected by competition between Npl3 and polyadenylation factor CFI." RNA **13**(10): 1756-64.

Buratowski, S. (2005). "Connections between mRNA 3' end processing and transcription termination." Curr Opin Cell Biol **17**(3): 257-61.

Buratowski, S. (2009). "Progression through the RNA polymerase II CTD cycle." Mol Cell **36**(4): 541-6.

Chapman, R. D., M. Heidemann, T. K. Albert, R. Mailhammer, A. Flatley, M. Meisterernst, E. Kremmer and D. Eick (2007). "Transcribing RNA polymerase II is phosphorylated at CTD residue serine-7." Science **318**(5857): 1780-2.

Cho, E. J., M. S. Kobor, M. Kim, J. Greenblatt and S. Buratowski (2001). "Opposing effects of Ctk1 kinase and Fcp1 phosphatase at Ser 2 of the RNA polymerase II C-terminal domain." Genes Dev **15**(24): 3319-29.

Cho, E. J., T. Takagi, C. R. Moore and S. Buratowski (1997). "mRNA capping enzyme is recruited to the transcription complex by phosphorylation of the RNA polymerase II carboxy-terminal domain." Genes Dev **11**(24): 3319-26.

Cho, H., T. K. Kim, H. Mancebo, W. S. Lane, O. Flores and D. Reinberg (1999). "A protein phosphatase functions to recycle RNA polymerase II." Genes Dev **13**(12): 1540-52.

Cole, C. N. and J. J. Scarcelli (2006). "Transport of messenger RNA from the nucleus to the cytoplasm." Curr Opin Cell Biol **18**(3): 299-306.

Cosentino, G. P., T. Schmelzle, A. Haghighat, S. B. Helliwell, M. N. Hall and N. Sonenberg (2000). "Eap1p, a novel eukaryotic translation initiation factor 4E-associated protein in Saccharomyces cerevisiae." Mol Cell Biol **20**(13): 4604-13.

Cox, J. and M. Mann (2008). "MaxQuant enables high peptide identification rates, individualized p.p.b.-range mass accuracies and proteome-wide protein quantification." Nat Biotechnol **26**(12): 1367-72.

Cridge, A. G., L. M. Castelli, J. B. Smirnova, J. N. Selley, W. Rowe, S. J. Hubbard, J. E. McCarthy, M. P. Ashe, C. M. Grant and G. D. Pavitt (2010)."Identifying eIF4E-binding protein translationally-controlled transcripts reveals links to mRNAs bound by specific PUF proteins." Nucleic Acids Res **38**(22): 8039-50.

de Breyne, S., Y. Yu, A. Unbehaun, T. V. Pestova and C. U. Hellen (2009). "Direct functional interaction of initiation factor eIF4G with type 1 internal ribosomal entry sites." Proc Natl Acad Sci U S A **106**(23): 9197-202.

Deka, P., M. E. Bucheli, C. Moore, S. Buratowski and G. Varani (2008). "Structure of the yeast SR protein Npl3 and Interaction with mRNA 3'-end processing signals." J Mol Biol **375**(1): 136-50.

Deloche, O., J. de la Cruz, D. Kressler, M. Doere and P. Linder (2004). "A membrane transport defect leads to a rapid attenuation of translation initiation in Saccharomyces cerevisiae." Mol Cell **13**(3): 357-66.

Deng, Y., R. H. Singer and W. Gu (2008). "Translation of ASH1 mRNA is repressed by Puf6p-Fun12p/eIF5B interaction and released by CK2 phosphorylation." Genes Dev **22**(8): 1037-50.

Dermody, J. L., J. M. Dreyfuss, J. Villen, B. Ogundipe, S. P. Gygi, P. J. Park, A. S. Ponticelli, C. L. Moore, S. Buratowski and M. E. Bucheli (2008). "Unphosphorylated SR-like protein Npl3 stimulates RNA polymerase II elongation." PLoS One **3**(9): e3273.

Doudna J. A., P. Sarnow (2007). "Translation initiation by viral internal ribosome entry sites." Cold Spring Harbor Laboratory Press 129-153.

Du, L. and S. L. Warren (1997). "A functional interaction between the carboxy-terminal domain of RNA polymerase II and pre-mRNA splicing." J Cell Biol **136**(1): 5-18.

Egloff, S., D. O'Reilly, R. D. Chapman, A. Taylor, K. Tanzhaus, L. Pitts, D. Eick and S. Murphy (2007). "Serine-7 of the RNA polymerase II CTD is specifically required for snRNA gene expression." Science **318**(5857): 1777-9.

Estrella, L. A., M. F. Wilkinson and C. I. Gonzalez (2009). "The shuttling protein Npl3 promotes translation termination accuracy in Saccharomyces cerevisiae." J Mol Biol **394**(3): 410-22.

Fraser, C. S. and J. A. Doudna (2007). "Structural and mechanistic insights into hepatitis C viral translation initiation." Nat Rev Microbiol **5**(1): 29-38.

Gabel, H. W. and G. Ruvkun (2008). "The exonuclease ERI-1 has a conserved dual role in 5.8S rRNA processing and RNAi." Nat Struct Mol Biol **15**(5): 531-3.

Gilbert, W., C. W. Siebel and C. Guthrie (2001). "Phosphorylation by Sky1p promotes Npl3p shuttling and mRNA dissociation." RNA **7**(2): 302-13.

Gilbert, W. and C. Guthrie (2004). "The Glc7p nuclear phosphatase promotes mRNA export by facilitating association of Mex67p with mRNA." Mol Cell **13**(2): 201-12.

Gilbert, W. V., K. Zhou, T. K. Butler and J. A. Doudna (2007). "Cap-independent translation is required for starvation-induced differentiation in yeast." Science **317**(5842): 1224-7.

Gilbert, W. V. (2010). "Alternative ways to think about cellular internal ribosome entry." J Biol Chem **285**(38): 29033-8.

Granneman, S. and S. J. Baserga (2004). "Ribosome biogenesis: of knobs and RNA processing." Exp Cell Res **296**(1): 43-50.

Grenetier, S., C. Bouchoux and V. Goguel (2006). "CTD kinase I is required for the integrity of the rDNA tandem array." Nucleic Acids Res **34**(17): 4996-5006.

Gross, T., A. Siepmann, D. Sturm, M. Windgassen, J. J. Scarcelli, M. Seedorf, C. N. Cole and H. Krebber (2007). "The DEAD-box RNA helicase Dbp5 functions in translation termination." Science **315**(5812): 646-9.

Gruhler, S. and I. Kratchmarova (2008). "Stable isotope labeling by amino acids in cell culture (SILAC)." Methods Mol Biol **424**: 101-11.

Gross, T. (2009). "Charakterisierung neuer Funktionen der mRNA-Exportfaktoren Npl3p und Dbp5p in der Translation." PhD Thesis.

Hampsey, M. and D. Reinberg (2003). "Tails of intrigue: phosphorylation of RNA polymerase II mediates histone methylation." Cell **113**(4): 429-32.

Harel-Sharvit, L., N. Eldad, G. Haimovich, O. Barkai, L. Duek and M. Choder (2010)."RNA polymerase II subunits link transcription and mRNA decay to translation." Cell **143**(4): 552-63.

Hellen, C. U. (2009). "IRES-induced conformational changes in the ribosome and the mechanism of translation initiation by internal ribosomal entry." Biochim Biophys Acta **1789**(9-10): 558-70.

Henras, A. K., J. Soudet, M. Gerus, S. Lebaron, M. Caizergues-Ferrer, A. Mougin and Y. Henry (2008). "The post-transcriptional steps of eukaryotic ribosome biogenesis." Cell Mol Life Sci **65**(15): 2334-59.

Hinnebusch, A. G. (2005). "Translational regulation of GCN4 and the general amino acid control of yeast." Annu Rev Microbiol **59**: 407-50.

Hinnebusch, A. G., T. E. Dever, K. Asano (2007). "Mechanism of translation initiation in the yeast Saccharomyces cerevisiae." Cold Spring Harbor Laboratory Press 225-268.

Hirose, Y., R. Tacke and J. L. Manley (1999). "Phosphorylated RNA polymerase II stimulates pre-mRNA splicing." Genes Dev **13**(10): 1234-9.

Hurt, E., M. J. Luo, S. Rother, R. Reed and K. Strasser (2004). "Cotranscriptional recruitment of the serine-arginine-rich (SR)-like proteins Gbp2 and Hrb1 to nascent mRNA via the TREX complex." Proc Natl Acad Sci U S A **101**(7): 1858-62.

Iost, I., M. Dreyfus and P. Linder (1999). "Ded1p, a DEAD-box protein required for translation initiation in Saccharomyces cerevisiae, is an RNA helicase." J Biol Chem **274**(25): 17677-83.

Jackson, R. J., C. U. Hellen and T. V. Pestova (2010). "The mechanism of eukaryotic translation initiation and principles of its regulation." Nat Rev Mol Cell Biol **11**(2): 113-27.

Jan, E. and P. Sarnow (2002). "Factorless ribosome assembly on the internal ribosome entry site of cricket paralysis virus." J Mol Biol **324**(5): 889-902.

Jan, E., T. G. Kinzy and P. Sarnow (2003). "Divergent tRNA-like element supports initiation, elongation, and termination of protein biosynthesis." Proc Natl Acad Sci U S A **100**(26): 15410-5.

Jang, C. J., M. C. Lo and E. Jan (2009). "Conserved element of the dicistrovirus IGR IRES that mimics an E-site tRNA/ribosome interaction mediates multiple functions." J Mol Biol **387**(1): 42-58.

Jang, S. K., H. G. Krausslich, M. J. Nicklin, G. M. Duke, A. C. Palmenberg and E. Wimmer (1988). "A segment of the 5' nontranslated region of encephalomyocarditis virus RNA directs internal entry of ribosomes during in vitro translation." J Virol **62**(8): 2636-43.

Kadowaki, T., S. Chen, M. Hitomi, E. Jacobs, C. Kumagai, S. Liang, R. Schneiter, D. Singleton, J. Wisniewska and A. M. Tartakoff (1994). "Isolation and characterization of Saccharomyces cerevisiae mRNA transport-defective (mtr) mutants." J Cell Biol **126**(3): 649-59.

Keogh, M. C., V. Podolny and S. Buratowski (2003). "Bur1 kinase is required for efficient transcription elongation by RNA polymerase II." Mol Cell Biol **23**(19): 7005-18.

Kessler, M. M., M. F. Henry, E. Shen, J. Zhao, S. Gross, P. A. Silver and C. L. Moore (1997). "Hrp1, a sequence-specific RNA-binding protein that shuttles between the nucleus and the cytoplasm, is required for mRNA 3'-end formation in yeast." Genes Dev **11**(19): 2545-56.

Kieft, J. S. (2008). "Viral IRES RNA structures and ribosome interactions." Trends Biochem Sci **33**(6): 274-83.

Kieft, J. S. (2009). "Comparing the three-dimensional structures of Dicistroviridae IGR IRES RNAs with other viral RNA structures." Virus Res **139**(2): 148-56.

Kim, E., L. Du, D. B. Bregman and S. L. Warren (1997). "Splicing factors associate with hyperphosphorylated RNA polymerase II in the absence of pre-mRNA." J Cell Biol **136**(1): 19-28.

Kim, M., S. H. Ahn, N. J. Krogan, J. F. Greenblatt and S. Buratowski (2004). "Transitions in RNA polymerase II elongation complexes at the 3' ends of genes." Embo J **23**(2): 354-64.

Kim, M., N. J. Krogan, L. Vasiljeva, O. J. Rando, E. Nedea, J. F. Greenblatt and S. Buratowski (2004). "The yeast Rat1 exonuclease promotes transcription termination by RNA polymerase II." Nature **432**(7016): 517-22.

Kizer, K. O., H. P. Phatnani, Y. Shibata, H. Hall, A. L. Greenleaf and B. D. Strahl (2005). "A novel domain in Set2 mediates RNA polymerase II interaction and couples histone H3 K36 methylation with transcript elongation." Mol Cell Biol **25**(8): 3305-16.

Knop, M., A. Finger, T. Braun, K. Hellmuth and D. H. Wolf (1996). "Der1, a novel protein specifically required for endoplasmic reticulum degradation in yeast." Embo J **15**(4): 753-63.

Komar, A. A. and M. Hatzoglou (2005). "Internal ribosome entry sites in cellular mRNAs: mystery of their existence." J Biol Chem **280**(25): 23425-8.

Komarnitsky, P., E. J. Cho and S. Buratowski (2000). "Different phosphorylated forms of RNA polymerase II and associated mRNA processing factors during transcription." Genes Dev **14**(19): 2452-60.

Kress, T. L., N. J. Krogan and C. Guthrie (2008). "A single SR-like protein, Npl3, promotes pre-mRNA splicing in budding yeast." Mol Cell **32**(5): 727-34.

Kressler, D., D. Roser, B. Pertschy and E. Hurt (2008). "The AAA ATPase Rix7 powers progression of ribosome biogenesis by stripping Nsa1 from pre-60S particles." J Cell Biol **181**(6): 935-44.

Kressler, D., E. Hurt and J. Bassler (2010). "Driving ribosome assembly." Biochim Biophys Acta **1803**(6): 673-83.

Krishnamurthy, S., X. He, M. Reyes-Reyes, C. Moore and M. Hampsey (2004). "Ssu72 Is an RNA polymerase II CTD phosphatase." Mol Cell **14**(3): 387-94.

Laemmli, U. K. (1970). "Cleavage of structural proteins during the assembly of the head of bacteriophage T4." Nature **227**(5259): 680-5.

Laribee, R. N., N. J. Krogan, T. Xiao, Y. Shibata, T. R. Hughes, J. F. Greenblatt and B. D. Strahl (2005). "BUR kinase selectively regulates H3 K4 trimethylation and H2B ubiquitylation through recruitment of the PAF elongation complex." Curr Biol **15**(16): 1487-93.

Lee, J. M. and A. L. Greenleaf (1991). "CTD kinase large subunit is encoded by CTK1, a gene required for normal growth of Saccharomyces cerevisiae." Gene Expr **1**(2): 149-67.

Lee, J. M. and A. L. Greenleaf (1997). "Modulation of RNA polymerase II elongation efficiency by C-terminal heptapeptide repeat domain kinase I." J Biol Chem **272**(17): 10990-3.

Lee, J. S., A. Shukla, J. Schneider, S. K. Swanson, M. P. Washburn, L. Florens, S. R. Bhaumik and A. Shilatifard (2007). "Histone crosstalk between H2B monoubiquitination and H3 methylation mediated by COMPASS." Cell **131**(6): 1084-96.

Lee, M. S., M. Henry and P. A. Silver (1996). "A protein that shuttles between the nucleus and the cytoplasm is an important mediator of RNA export." Genes Dev **10**(10): 1233-46.

Lempiainen, H. and D. Shore (2009). "Growth control and ribosome biogenesis." Curr Opin Cell Biol **21**(6): 855-63.

Licatalosi, D. D., G. Geiger, M. Minet, S. Schroeder, K. Cilli, J. B. McNeil and D. L. Bentley (2002). "Functional interaction of yeast pre-mRNA 3' end processing factors with RNA polymerase II." Mol Cell **9**(5): 1101-11.

Liu, Y., L. Warfield, C. Zhang, J. Luo, J. Allen, W. H. Lang, J. Ranish, K. M. Shokat and S. Hahn (2009). "Phosphorylation of the transcription elongation factor Spt5 by yeast Bur1 kinase stimulates recruitment of the PAF complex." Mol Cell Biol **29**(17): 4852-63.

Lo, K. Y., Z. Li, C. Bussiere, S. Bresson, E. M. Marcotte and A. W. Johnson (2010). "Defining the pathway of cytoplasmic maturation of the 60S ribosomal subunit." Mol Cell **39**(2): 196-208.

Lorsch, J. R. and T. E. Dever (2010). "Molecular view of 43 S complex formation and start site selection in eukaryotic translation initiation." J Biol Chem **285**(28): 21203-7.

Marr, M. T., 2nd, J. A. D'Alessio, O. Puig and R. Tjian (2007). "IRES-mediated functional coupling of transcription and translation amplifies insulin receptor feedback." Genes Dev **21**(2): 175-83.

Mascarenhas, C., L. C. Edwards-Ingram, L. Zeef, D. Shenton, M. P. Ashe and C. M. Grant (2008). "Gcn4 is required for the response to peroxide stress in the yeast Saccharomyces cerevisiae." Mol Biol Cell **19**(7): 2995-3007.

Max, T., M. Sogaard and J. Q. Svejstrup (2007). "Hyperphosphorylation of the C-terminal repeat domain of RNA polymerase II facilitates dissociation of its complex with mediator." J Biol Chem **282**(19): 14113-20.

McBride, A. E., J. T. Cook, E. A. Stemmler, K. L. Rutledge, K. A. McGrath and J. A. Rubens (2005). "Arginine methylation of yeast mRNA-binding protein Npl3 directly affects its function, nuclear export, and intranuclear protein interactions." J Biol Chem **280**(35): 30888-98.

Meggio, F. and L. A. Pinna (2003). "One-thousand-and-one substrates of protein kinase CK2?" Faseb J **17**(3): 349-68.

Meier, K. D., O. Deloche, K. Kajiwara, K. Funato and H. Riezman (2006). "Sphingoid base is required for translation initiation during heat stress in Saccharomyces cerevisiae." Mol Biol Cell **17**(3): 1164-75.

Meinhart, A. and P. Cramer (2004). "Recognition of RNA polymerase II carboxy-terminal domain by 3'-RNA-processing factors." Nature **430**(6996): 223-6.

Meyuhas, O. (2008). "Physiological roles of ribosomal protein S6: one of its kind." Int Rev Cell Mol Biol **268**: 1-37.

Milkereit, P., O. Gadal, A. Podtelejnikov, S. Trumtel, N. Gas, E. Petfalski, D. Tollervey, M. Mann, E. Hurt and H. Tschochner (2001). "Maturation and intranuclear transport of pre-ribosomes requires Noc proteins." Cell **105**(4): 499-509.

Mosley, A. L., S. G. Pattenden, M. Carey, S. Venkatesh, J. M. Gilmore, L. Florens, J. L. Workman and M. P. Washburn (2009). "Rtr1 is a CTD phosphatase that regulates RNA polymerase II during the transition from serine 5 to serine 2 phosphorylation." Mol Cell **34**(2): 168-78.

Murray, S., R. Udupa, S. Yao, G. Hartzog and G. Prelich (2001). "Phosphorylation of the RNA polymerase II carboxy-terminal domain by the Bur1 cyclin-dependent kinase." Mol Cell Biol **21**(13): 4089-96.

Napolitano, G., P. Licciardo, R. Carbone, B. Majello and L. Lania (2002). "CDK9 has the intrinsic property to shuttle between nucleus and cytoplasm, and enhanced expression of cyclin T1 promotes its nuclear localization." J Cell Physiol **192**(2): 209-15.

Ng, H. H., F. Robert, R. A. Young and K. Struhl (2003). "Targeted recruitment of Set1 histone methylase by elongating Pol II provides a localized mark and memory of recent transcriptional activity." Mol Cell **11**(3): 709-19.

Ni, Z., B. E. Schwartz, J. Werner, J. R. Suarez and J. T. Lis (2004). "Coordination of transcription, RNA processing, and surveillance by P-TEFb kinase on heat shock genes." Mol Cell **13**(1): 55-65.

Nissan, T. A., J. Bassler, E. Petfalski, D. Tollervey and E. Hurt (2002). "60S pre-ribosome formation viewed from assembly in the nucleolus until export to the cytoplasm." Embo J **21**(20): 5539-47.

Olsen, J. V., B. Blagoev, F. Gnad, B. Macek, C. Kumar, P. Mortensen and M. Mann (2006). "Global, in vivo, and site-specific phosphorylation dynamics in signaling networks." Cell **127**(3): 635-48.

Olsen, J. V., B. Macek, O. Lange, A. Makarov, S. Horning and M. Mann (2007). "Higher-energy C-trap dissociation for peptide modification analysis." Nat Methods **4**(9): 709-12.

Ostapenko, D. and M. J. Solomon (2003). "Budding yeast CTDK-I is required for DNA damage-induced transcription." Eukaryot Cell **2**(2): 274-83.

Palmer, L. K., J. L. Shoemaker, B. A. Baptiste, D. Wolfe and R. L. Keil (2005). "Inhibition of translation initiation by volatile anesthetics involves nutrient-sensitive GCN-independent and -dependent processes in yeast." Mol Biol Cell **16**(8): 3727-39.

Pelletier, J. and N. Sonenberg (1988). "Internal initiation of translation of eukaryotic mRNA directed by a sequence derived from poliovirus RNA." Nature **334**(6180): 320-5.

Pestova, T. V., C. U. Hellen and I. N. Shatsky (1996). "Canonical eukaryotic initiation factors determine initiation of translation by internal ribosomal entry." Mol Cell Biol **16**(12): 6859-69.

Pestova, T. V., I. N. Shatsky and C. U. Hellen (1996). "Functional dissection of eukaryotic initiation factor 4F: the 4A subunit and the central domain of the 4G subunit are sufficient to mediate internal entry of 43S preinitiation complexes." Mol Cell Biol **16**(12): 6870-8.

Pestova, T. V., I. N. Shatsky, S. P. Fletcher, R. J. Jackson and C. U. Hellen (1998). "A prokaryotic-like mode of cytoplasmic eukaryotic ribosome binding to the initiation codon during internal translation initiation of hepatitis C and classical swine fever virus RNAs." Genes Dev **12**(1): 67-83.

Pestova, T. V. and C. U. Hellen (2003). "Translation elongation after assembly of ribosomes on the Cricket paralysis virus internal ribosomal entry site without initiation factors or initiator tRNA." Genes Dev **17**(2): 181-6.

Phatnani, H. P. and A. L. Greenleaf (2006). "Phosphorylation and functions of the RNA polymerase II CTD." Genes Dev **20**(21): 2922-36.

Poole, A., T. Poore, S. Bandhakavi, R. O. McCann, D. E. Hanna and C. V. Glover (2005). "A global view of CK2 function and regulation." Mol Cell Biochem **274**(1-2): 163-70.

Preiss, T. and W. H. M (2003). "Starting the protein synthesis machine: eukaryotic translation initiation." Bioessays **25**(12): 1201-11.

Prelich, G. (2002). "RNA polymerase II carboxy-terminal domain kinases: emerging clues to their function." Eukaryot Cell **1**(2): 153-62.

Puig, O., F. Caspary, G. Rigaut, B. Rutz, E. Bouveret, E. Bragado-Nilsson, M. Wilm and B. Seraphin (2001). "The tandem affinity purification (TAP) method: a general procedure of protein complex purification." Methods **24**(3): 218-29.

Qiu, H., C. Hu and A. G. Hinnebusch (2009). "Phosphorylation of the Pol II CTD by KIN28 enhances BUR1/BUR2 recruitment and Ser2 CTD phosphorylation near promoters." Mol Cell **33**(6): 752-62.

Richter, J. D. and N. Sonenberg (2005). "Regulation of cap-dependent translation by eIF4E inhibitory proteins." Nature **433**(7025): 477-80.

Raught, B. and A.-C. Gingras (2007). "Signaling to translation initiation." Cold Spring Harbor Laboratory Press 369-400.

Rother, S., C. Burkert, K. M. Brunger, A. Mayer, A. Kieser and K. Strasser (2010). "Nucleocytoplasmic shuttling of the La motif-containing protein Sro9 might link its nuclear and cytoplasmic functions." RNA **16**(7): 1393-401.

Rother, S. and K. Strasser (2007). "The RNA polymerase II CTD kinase Ctk1 functions in translation elongation." Genes Dev **21**(11): 1409-21.

Sambrook, J. and D. W. Russell (2001). "Molecular Cloning: A Laboratory Manual." New York, Cold Spring Harbor Laboratory Press.

Schafer, T., D. Strauss, E. Petfalski, D. Tollervey and E. Hurt (2003). "The path from nucleolar 90S to cytoplasmic 40S pre-ribosomes." Embo J **22**(6): 1370-80.

Schneider, D. A., S. L. French, Y. N. Osheim, A. O. Bailey, L. Vu, J. Dodd, J. R. Yates, A. L. Beyer and M. Nomura (2006). "RNA polymerase II elongation factors Spt4p and Spt5p play roles in transcription elongation by RNA polymerase I and rRNA

processing." Proc Natl Acad Sci U S A **103**(34): 12707-12.
Senger, B., G. Simos, F. R. Bischoff, A. Podtelejnikov, M. Mann and E. Hurt (1998). "Mtr10p functions as a nuclear import receptor for the mRNA-binding protein Npl3p." Embo J **17**(8): 2196-207.
Senger, B., D. L. Lafontaine, J. S. Graindorge, O. Gadal, A. Camasses, A. Sanni, J. M. Garnier, M. Breitenbach, E. Hurt and F. Fasiolo (2001). "The nucle(ol)ar Tif6p and Efl1p are required for a late cytoplasmic step of ribosome synthesis." Mol Cell **8**(6): 1363-73.
Sikorski, R. S. and P. Hieter (1989). "A system of shuttle vectors and yeast host strains designed for efficient manipulation of DNA in Saccharomyces cerevisiae." Genetics **122**(1): 19-27.
Sobel, S. G. and S. L. Wolin (1999). "Two yeast La motif-containing proteins are RNA-binding proteins that associate with polyribosomes." Mol Biol Cell **10**(11): 3849-62.
Sonenberg, N. and A. G. Hinnebusch (2009). "Regulation of translation initiation in eukaryotes: mechanisms and biological targets." Cell **136**(4): 731-45.
Sterner, D. E., J. M. Lee, S. E. Hardin and A. L. Greenleaf (1995). "The yeast carboxyl-terminal repeat domain kinase CTDK-I is a divergent cyclin-cyclin-dependent kinase complex." Mol Cell Biol **15**(10): 5716-24.
Strasser, K., S. Masuda, P. Mason, J. Pfannstiel, M. Oppizzi, S. Rodriguez-Navarro, A. G. Rondon, A. Aguilera, K. Struhl, R. Reed and E. Hurt (2002). "TREX is a conserved complex coupling transcription with messenger RNA export." Nature **417**(6886): 304-8.
Tan, Q., X. Li, P. P. Sadhale, T. Miyao and N. A. Woychik (2000). "Multiple mechanisms of suppression circumvent transcription defects in an RNA polymerase mutant." Mol Cell Biol **20**(21): 8124-33.
Tardiff, D. F., K. C. Abruzzi and M. Rosbash (2007). "Protein characterization of Saccharomyces cerevisiae RNA polymerase II after in vivo cross-linking." Proc Natl Acad Sci U S A **104**(50): 19948-53.
Tietjen, J. R., D. W. Zhang, J. B. Rodriguez-Molina, B. E. White, M. S. Akhtar, M. Heidemann, X. Li, R. D. Chapman, K. Shokat, S. Keles, D. Eick and A. Z. Ansari (2010). "Chemical-genomic dissection of the CTD code." Nat Struct Mol Biol **17**(9): 1154-61.
Thompson, S. R., K. D. Gulyas and P. Sarnow (2001). "Internal initiation in Saccharomyces cerevisiae mediated by an initiator tRNA/eIF2-independent internal ribosome entry site element." Proc Natl Acad Sci U S A **98**(23): 12972-7.
Urban, J., A. Soulard, A. Huber, S. Lippman, D. Mukhopadhyay, O. Deloche, V. Wanke, D. Anrather, G. Ammerer, H. Riezman, J. R. Broach, C. De Virgilio, M. N. Hall and R. Loewith (2007). "Sch9 is a major target of TORC1 in Saccharomyces cerevisiae." Mol Cell **26**(5): 663-74.
Verge, V., M. Vonlanthen, J. M. Masson, H. Trachsel and M. Altmann (2004). "Localization of a promoter in the putative internal ribosome entry site of the Saccharomyces cerevisiae TIF4631 gene." Rna **10**(2): 277-86.
Watkins, J. L., R. Murphy, J. L. Emtage and S. R. Wente (1998). "The human homologue of Saccharomyces cerevisiae Gle1p is required for poly(A)+ RNA export." Proc Natl Acad Sci U S A **95**(12): 6779-84.
Weirich, C. S., J. P. Erzberger, J. S. Flick, J. M. Berger, J. Thorner and K. Weis (2006). "Activation of the DExD/H-box protein Dbp5 by the nuclear-pore protein Gle1 and its coactivator InsP6 is required for mRNA export." Nat Cell Biol **8**(7): 668-76.
West, S., N. Gromak and N. J. Proudfoot (2004). "Human 5' --> 3' exonuclease Xrn2 promotes transcription termination at co-transcriptional cleavage sites." Nature **432**(7016): 522-5.

Wilker, E. W., M. A. van Vugt, S. A. Artim, P. H. Huang, C. P. Petersen, H. C. Reinhardt, Y. Feng, P. A. Sharp, N. Sonenberg, F. M. White and M. B. Yaffe (2007). "14-3-3sigma controls mitotic translation to facilitate cytokinesis." Nature **446**(7133): 329-32.

Wilson, J. E., M. J. Powell, S. E. Hoover and P. Sarnow (2000). "Naturally occurring dicistronic cricket paralysis virus RNA is regulated by two internal ribosome entry sites." Mol Cell Biol **20**(14): 4990-9.

Wilson, S. M., K. V. Datar, M. R. Paddy, J. R. Swedlow and M. S. Swanson (1994). "Characterization of nuclear polyadenylated RNA-binding proteins in Saccharomyces cerevisiae." J Cell Biol **127**(5): 1173-84.

Windgassen, M., D. Sturm, I. J. Cajigas, C. I. Gonzalez, M. Seedorf, H. Bastians and H. Krebber (2004). "Yeast shuttling SR proteins Npl3p, Gbp2p, and Hrb1p are part of the translating mRNPs, and Npl3p can function as a translational repressor." Mol Cell Biol **24**(23): 10479-91.

Wong, C. M., H. Qiu, C. Hu, J. Dong and A. G. Hinnebusch (2007). "Yeast cap binding complex impedes recruitment of cleavage factor IA to weak termination sites." Mol Cell Biol **27**(18): 6520-31.

Wong, C. M., H. M. Tang, K. Y. Kong, G. W. Wong, H. Qiu, D. Y. Jin and A. G. Hinnebusch (2010). "Yeast arginine methyltransferase Hmt1p regulates transcription elongation and termination by methylating Npl3p." Nucleic Acids Res **38**(7): 2217-28.

Wood, A., J. Schneider, J. Dover, M. Johnston and A. Shilatifard (2003). "The Paf1 complex is essential for histone monoubiquitination by the Rad6-Bre1 complex, which signals for histone methylation by COMPASS and Dot1p." J Biol Chem **278**(37): 34739-42.

Wood, A., J. Schneider, J. Dover, M. Johnston and A. Shilatifard (2005). "The Bur1/Bur2 complex is required for histone H2B monoubiquitination by Rad6/Bre1 and histone methylation by COMPASS." Mol Cell **20**(4): 589-99.

Wood, A. and A. Shilatifard (2006). "Bur1/Bur2 and the Ctk complex in yeast: the split personality of mammalian P-TEFb." Cell Cycle **5**(10): 1066-8.

Xiao, T., Y. Shibata, B. Rao, R. N. Laribee, R. O'Rourke, M. J. Buck, J. F. Greenblatt, N. J. Krogan, J. D. Lieb and B. D. Strahl (2007). "The RNA polymerase II kinase Ctk1 regulates positioning of a 5' histone methylation boundary along genes." Mol Cell Biol **27**(2): 721-31.

Xu, C. and M. F. Henry (2004). "Nuclear export of hnRNP Hrp1p and nuclear export of hnRNP Npl3p are linked and influenced by the methylation state of Npl3p." Mol Cell Biol **24**(24): 10742-56.

Yang, R., S. A. Wek and R. C. Wek (2000). "Glucose limitation induces GCN4 translation by activation of Gcn2 protein kinase." Mol Cell Biol **20**(8): 2706-17.

Yun, C. Y. and X. D. Fu (2000). "Conserved SR protein kinase functions in nuclear import and its action is counteracted by arginine methylation in Saccharomyces cerevisiae." J Cell Biol **150**(4): 707-18.

Zemp, I. and U. Kutay (2007). "Nuclear export and cytoplasmic maturation of ribosomal subunits." FEBS Lett **581**(15): 2783-93.

Zhang, J., P. Harnpicharnchai, J. Jakovljevic, L. Tang, Y. Guo, M. Oeffinger, M. P. Rout, S. L. Hiley, T. Hughes and J. L. Woolford, Jr. (2007). "Assembly factors Rpf2 and Rrs1 recruit 5S rRNA and ribosomal proteins rpL5 and rpL11 into nascent ribosomes." Genes Dev **21**(20): 2580-92.

Zhang, Y., M. L. Sikes, A. L. Beyer and D. A. Schneider (2009). "The Paf1 complex is required for efficient transcription elongation by RNA polymerase I." Proc Natl Acad Sci U S A **106**(7): 2153-8.

Zhou, K., W. H. Kuo, J. Fillingham and J. F. Greenblatt (2009). "Control of transcriptional elongation and cotranscriptional histone modification by the yeast BUR kinase substrate Spt5." Proc Natl Acad Sci U S A **106**(17): 6956-61.

6. ABBREVIATIONS

aa-tRNA	aminoacyl tRNA
A-site	acceptor site of the ribosome
3AT	3-amino-1,2,4-triazole
ATP	adenosine triphosphate
β-ME	β-mercapto ethanole
bp	basepair
°C	degree celsius
CBP	calmodulin binding protein
CDK	cyclin dependent kinase
CTD	C-Terminal Domain of the largest RNAPII subunit
CTDK-I	C-terminal domain kinase I
d	day
Da	dalton
DAPI	4‘,6-diamino-2-phenylindole
DNA	deoxyribonucleic acid
dNTP	deoxyribonucleosid triphosphate
E. coli	*Escherichia coli*
ECL	enhanced chemoluminiscence
eIF	eukaryotic initiation factor
E-site	exit site of the ribosome
et al.	et alia (Latin and others)
5’-FOA	5-Fluoorotic Acid
g	gram
GAP	GTPase activating protein
h	hours
hnRNP	Heterogeneous nuclear ribonucleoprotein
IPTG	Isopropyl-β-D-thiogalactopyranosid
kDa	kilo Dalton
L	litre
LB	Luria-Bertani
M	molar
MFC	multi factor complex
min	minute
mRNA	messenger ribonuleic acid
mRNP	messenger ribonucleoprotein
NLS	nuclear localisation sequence
nt	nucleotide
OD	optical density
ORF	open reading frame
PAGE	polyacrylamide gelelectrophoresis
PBS	phosphate-buffered saline
PCR	polymerase chain reaction
pH	potential of hydrogen
PIC	pre-initiation complex
PolI	RNA Polymerase I
PolII	RNA Polymerase II

Rpl	ribosomal protein of the large ribosomal subunit
Rps	ribosomal protein of the small ribosomal subunit
P-site	peptidyl-site oft he ribosome
P-TEFb	positive transcription elongation factor b
RNA	ribonucleic acid
rpm	rotation per minute
rRNA	ribosomal RNA
RT	room temperature
S	svedberg, serine
sb	sample buffer
SDS	sodium dodecyl-sulphate
sec	second
SL	synthetic lethal
SR proteins	serine-arginine rich proteins
TAP	tandem affinity purification
TBS	tris-buffered saline
TCA	trichloroacetic acid
TEV	Tobacco Etch Virus
TF	transcription factor
TREX	transcription/Export complex
tRNA	transfer RNA
UTR	untranslated region
YPD	yeast extract, peptone, glucose; glucose containing medium
YPG	yeast extract, peptone, galactose; galactose containing medium
Wt	wild-type
µ	micro

7. CURRICULUM VITAE

B R I T T A C O O R D E S

PERSONAL DATA

Date of Birth:	July 7, 1981
Place of Birth:	Bremen
Citizenship:	German

EDUCATION

Since November 2006	Ph.D. student in the laboratory of Dr. Katja Sträßer, Gene Center Munich
July 2006	"Diplom" at the University of Göttingen, Germany
September 2005 - July 2006	"Diplomarbeit" in the laboratory of Prof. Dr. Ralf Ficner, Institute for molecular structural Biology in Göttingen, Germany
April 2003 - July 2006	Study of Biology at the University of Göttingen, Germany
September 2002 – February 2003	Study of English Literature at the University of Hull, UK
July and August 2002	"Zwischenprüfung" in English and Biology at the University of Kiel, Germany
Ocotber 2000 – August 2002	Study of English and Biology at the University of Kiel, Germany
June 2000	"Abitur" at the „Ökumenisches Gymnasium zu Bremen", Germany

8. ACKNOWLEDGEMENT

I would like to thank all people who were involved in the completion of this thesis.

First of all I want to thank Katja Sträßer for giving me the opportunity to work in her lab on this challenging project and for her help over the years.
I would also like to thank Ralf-Perter Jansen for being my first "Doktorvater" and Roland Beckmann for adopting me half way through the thesis. Both of them and the other members of my PhD thesis committee – Daniel Wilson and Klaus Förstemann – I am very grateful for fruitful discussions about the PhD project. Furthermore, I thank Klaus Förstemann for being the second examiner of this thesis.

Due to my wonderful colleagues, past and present, I managed to get through the good and the frustrating times of this PhD. I am especially grateful to Juliane, who did many experiments of this thesis. Thanks for the great technical assistance, for being willing to learn a lot of techniques and never getting tired of spending long days purifying Ctk1. Special thanks go to Katharina for being my translation partner and always being there for helpful scientific and non-scientific discussions. Thanks to my longest PhD-mate Lina for being such a cheerful and talkative person. Anja, I don't know the lab without you – thanks for being always kind and helpful and trying to keep the lab clean! Thank you, Sittinan, for having many good scientific ideas and for bringing the buddist attitude to the lab. I would also like to thank Connie and Dominik for being such good labmates and always being willing to help. To Viter I am grateful for helpful scientific advice during the last months. Thanks also to Petra for great help during the first part of the thesis and to Emanuel for support and his daily portion of jokes as well as Susi for originating this PhD project. Thanks to Chiara, Shivendra, Dmitry, Patricia and Ninda for creating such a nice working atmosphere in the lab. I am grateful to our collaborators of the lab of Matthias Mann and Dirk Eick for experiments and discussions.
My three students Mika, Irina and Florian I would like to thank for their help with the project and for giving me the opportunity to teach.
I would like to thank the AG Hopfner members for discussions, collaborations, and for being always there to talk and cheering me up in less encouraging times.

I deeply thank the Boehringer Ingelheim Fonds for personal and scientific support. Thanks for

inspiring Hirschegg meetings and for enabling me to attend the Cold Spring Harbour as well as the EMBO conference on Translational Control.

I especially thank my parents for their constant support, for being so loving and understanding and handling my complaints during hard times. Thanks to my sister Anne for making my life easier during the last two years and showing me that there is another life besides the lab.

Thank you, Christian, for fruitful scientific discussions and help with my project as well as for enabling me to collaborate with you. I thank you for always being there for me, for enduring my frustrations and always cheering me up, simply for sharing the good and bad times with me.

SUPPLEMENTAL TABLE 1: List of phosphosites, which are less phosphorylated upon Ctk1 depletion as determined by SILAC.

Uniprot Name	Phosphosite	Protein ID	Ratio Ctk1/wt MV*	Ratio Ctk1/wt 1	Ratio Ctk1/wt 2	Ratio Ctk1/wt 3	Ratio Ctk1/wt 4	Ratio Ctk1/wt 5	Ratio Ctk1/wt 6	Sequence Window	Kinase Motifs Matching
ZRG8_YEAST	S365	YER033C	1,56			1,31	1,59		1,80	HGDLQSSPSKVNK	CDK1;CDK2;NEK6;Polo box;Proline-directed
ZRG8_YEAST	S676	YER033C	1,53	1,24	1,87	1,50	1,55	1,52	2,15	SLKRNNSDDETEH	CAMK2;CHK1;CHK1/2;CK2;PKA;PKD
ZEO1_YEAST	S40	YOL109W	1,71				1,71			KEQAEASIDNLKN	PLK1
ZEO1_YEAST	T49	YOL109W	4,08			4,30	3,85			NLKNEATPEAEQV	FHA KAPP;Proline-directed
vZAP1_YEAST	S858	YJL056C	5,02			6,58	3,46			CSDCSKSFDDLGK	CK2
YRA1_YEAST	S8	YDR381W	1,83					1,83		SANLDKSLDEIIG	CK2;NEK6;PLK;PLK1
YRA1_YEAST	S211	YDR381W	1,39		1,39	1,13	1,09	1,42	1,52	EKPAKKSLEDLDK	AURORA;CK2
YP146_YEAST	S31	YPL146C	0,64	0,52	0,72	0,55	0,75	0,54	0,98	RKNIDLSDVEQYM	CK2
YP146_YEAST	S363	YPL146C	0,80		0,80					EETEILSAIESDS	CK1;CK2;GSK3
YP146_YEAST	S367	YPL146C	0,73	0,59		0,55	0,88		1,17	ILSAIESDSNKVK	CK1
YP105_YEAST	S394	YPL105C	2,92			3,32	2,52			DRKDVISTADEPK	CK2
YP009_YEAST	S780	YPL009C	2,13	1,49	1,96	2,39	2,30	1,79	2,69	DSTKNNSFEHDNL	CK1
YP009_YEAST	S802	YPL009C	2,25						2,25	ISSDTDSDSGNAK	CK1
YOX1_YEAST	S344	YML027W	0,56	0,56						INSIDHSPSKAKR	CDK1;CDK2;CK1;Proline-directed
YO287_YEAST	S14	YOR287C	1,03	1,09	1,00	0,79	1,06	0,99	1,22	LKPDLNSDVEEDD	CK2
YO287_YEAST	S41	YOR287C	1,02		1,02	0,76	1,06	1,01	1,31	EIDEQESSDDELK	CK2
YO287_YEAST	S42	YOR287C	1,05	1,64	1,02	0,68	1,07	0,94	1,22	IDEQESSDDELKT	CK2
YO093_YEAST	S751	YOR093C	1,69				1,69			KAIDISSLSGETS	
YO006_YEAST	S286	YOR006C	0,73			0,94	0,53			KSREAQSEESEDE	
YO006_YEAST	S289	YOR006C	0,89			0,89	0,87		0,98	EAQSEESEDEESG	CK1;CK2
YNL0_YEAST	S56	YNL110C	0,89	0,77	0,92	0,98	0,87	0,71	1,36	IEGLAASDDEQSG	CK2;NEK6
YNG2_YEAST	S188	YHR090C	0,98			1,22	0,73		0,98	KSVTPVSPSIEKK	ERK/MAPK;Proline-directed;WW GroupIV
YMR1_YEAST	S654	YJR110W	1,44			1,44				LRHKRDSVPISVD	AURORA;AURORA-A;GSK3;PKA
YM8V_YEAST	S11	YMR295C	1,51			1,58	1,45			RKKSSISNTSDHD	CK1
YM8V_YEAST	S14	YMR295C	1,51			1,58	1,45			SSISNTSDHDGAN	CK1;CK2
YJ11B_YEAST	S36	YJR027W	4,97			4,97				QDPLDVSASKTEE	NEK6
YJ11B_YEAST	S960	YJR027W	2,68	1,90	2,14	2,68	2,85		3,95	VLSKAVSPTDSTP	CHK1;CK1;CK2;GSK3;PKD;Proline-directed
YJ11B_YEAST	S1081	YJR027W	1,24	1,18		1,24	1,59			KTVPQISDQETEK	CK2
YHU6_YEAST	S271	YHR146W	0,86	0,77	0,83	0,99	0,89	0,72	2,49	SSVTEKSPALPQA	Proline-directed
YHU6_YEAST	S319	YHR146W	1,12			1,12				TPEAQISIPESSK	CK2;GSK3
YHU6_YEAST	S332	YHR146W	1,52		1,46	1,41	1,58		4,78	VEPVEGSLQSKLV	PLK1
YHU6_YEAST	S343	YHR146W	0,90	0,68	0,92	0,88	0,99	0,68	2,51	LVEKRESTEGVLD	CHK1;PKA;PKD
YHU6_YEAST	S390	YHR146W	2,06	1,43		2,42	2,32	1,81		TAEGRKSPAVSEE	GSK3;PKA;Proline-directed
YHU6_YEAST	S394	YHR146W	2,03	1,43		2,42	2,25	1,81		RKSPAVSEEKEKK	CK1
YG169_YEAST	S6	YGR169C-A	0,88	0,66	0,93	0,37	0,88		1,02	_MGKRFSESAAKK	CHK1;PKA
YD333_YEAST	S119	YDR333C	1,69	1,25	1,59	1,95	1,79	1,36	3,49	AAKDKGSDDDDDD	CK2

Uniprot Name	Phosphosite	Protein ID	Ratio Ctk1/wt MV	Ratio Ctk1/wt 1	Ratio Ctk1/wt 2	Ratio Ctk1/wt 3	Ratio Ctk1/wt 4	Ratio Ctk1/wt 5	Ratio Ctk1/wt 6	Sequence Window	Kinase Motifs Matching
YD266_YEAST	S557	YDR266C	1,04	1,12			0,91		1,04	ESKKGSSSTSLNN	
YCQ6_YEAST	S21	YCR016W	0,83		0,98	0,68	1,00	0,62		KRQTISSGDESKE	CK2;GSK3
YCQ6_YEAST	S223	YCR016W	1,69			1,69				IAEDKASEPINGE	
YCFI_YEAST	S251	YDR135C	3,52				3,52			KLPRNFSSEELSQ	CAMK2;CHK1;CHK1/2;CK2;PKD
YC21B_YEAST	S367	YCL019W	18,05			18,05				SEYKNVSRTSPNT	
YC21B_YEAST	S370	YCL019W	10,95			18,05	3,84			KNVSRTSPNTTNT	CK1;PKA;Proline-directed
YAP1_YEAST	S14	YML007W	2,34			2,56	2,13			RSLDVVSPGSLAE	ERK/MAPK;Proline-directed
YAP1_YEAST	S528	YML007W	1,69			1,35	2,03			KKAANMSDDESSL	CK2;GSK3
YAB9_YEAST	S451	YAL019W	2,61			2,61				EGFDETSAEPTPA	
XRN1_YEAST	S1329	YGL173C	1,89			1,89				KRPAQKSSENVQV	
XRN1_YEAST	S1510	YGL173C	4,44			4,44				NSTECQSPKSQSN	CDK1;CK1;Proline-directed
VTC3_YEAST	S198	YPL019C	4,38				6,02		2,74	SKLSHFSNLEDAS	CK1;CK2
VTC3_YEAST	S592	YPL019C	2,78	5,02		1,98	3,11	2,46		RRLSKISVPDGKT	AURORA;CK1;CK2
VTC2_YEAST	T324	YFL004W	0,03		0,03		0,04			IFLEKKTLIEDEA	AURORA;CK2
VTC2_YEAST	S657	YFL004W	1,87			1,87				KLMGVDSEEEEIE	CK2
VPS68_YEAST	S8	YOL129W	1,94			1,94	2,01		1,52	EADDHVSLFRFPF	
VPS5_YEAST	S184	YOR069W	0,93				0,93			AKRTTASDDTIKT	
VPS41_YEAST	S44	YDR080W	1,20			1,27	1,13			EDVNVTSPTKSVS	CDK1;CDK2;ERK/MAPK;GSK3;Proline-directed
VPS35_YEAST	S868	YJL154C	2,29			2,28	2,29			SNADDGSVITDKE	PLK1
VPS1_YEAST	S599	YKR001C	2,30			2,70	1,91			KLAALESPPPVLK	Proline-directed
VIP1_YEAST	T1106	YLR410W	0,63				0,63			FTPVNITSPNLSF	
VIP1_YEAST	S1107	YLR410W	0,56				0,56			TPVNITSPNLSFQ	GSK3;Proline-directed
VID27_YEAST	S207	YNL212W	1,42	1,23		1,61	0,95		2,16	QDAKDTSFEHEKE	PLK1
VID27_YEAST	S222	YNL212W	1,73			2,25	1,22			ILERTPSPLKKVP	CAMK2;CDK1;CDK2;CHK1;CHK1/2;PKD;Proline-directed
VBA4_YEAST	S106	YDR119W	0,66				0,50	0,67	0,66	PQDEVNSIKGKPA	
VAN1_YEAST	S25	YML115C	2,88			2,88				GLSLPISRNGSSN	CK1;GSK3;NEK6
VAN1_YEAST	S29	YML115C	2,88			2,88				PISRNGSSNNIKD	CAMK2;CHK1;CK1;PKD
VAL1_YEAST	S4	YBR069C	0,98			0,98				___MDDSVSFIAK	PLK1
UTP8_YEAST	S148	YGR128C	1,09					1,09		TSNDHLSESDIDN	CK2
UTP23_YEAST	S215	YOR004W	1,80			1,80				KKKKVNSPSDEVK	CK2;ERK/MAPK;Proline-directed
UTP22_YEAST	S10	YGR090W	1,33	1,10	1,20	1,10	1,45	1,71	1,84	SVKRKASETSDQN	CAMK2;CHK1;PKA;PKD
UTP14_YEAST	S423	YML093W	1,37	1,12		1,38	1,36		2,60	RELAAVSSDEDNE	CK2
UTP14_YEAST	S424	YML093W	1,33	1,12		1,35	1,31		2,60	ELAAVSSDEDNED	CK2
UTP14_YEAST	S488	YML093W	1,44		1,58		1,30			KMLDRNSDDEEDG	CK2;PKA
UTP14_YEAST	S500	YML093W	1,44		1,58		1,30			GRVQTLSDVENEE	CK2
UTP14_YEAST	S562	YML093W	1,41	1,00	1,59	1,41	1,42	1,10	2,88	DIKLFESDEEETN	CK2;NEK6

Uniprot Name	Phosphosite	Protein ID	Ratio Ctk1/wt MV	Ratio Ctk1/wt 1	Ratio Ctk1/wt 2	Ratio Ctk1/wt 3	Ratio Ctk1/wt 4	Ratio Ctk1/wt 5	Ratio Ctk1/wt 6	Sequence Window	Kinase Motifs Matching
UTP14_YEAST	S668	YML093W	1,42	1,18	1,47	1,57	1,36	1,12	2,83	PWLANESDEEHTV	CK2
UTP14_YEAST	T673	YML093W	1,20	1,10	1,31					ESDEEHTVKKQSS	PLK1
UTP14_YEAST	Y735	YML093W	1,04	1,09				0,99		LKIVDPYGGSDDE	
UTP14_YEAST	S738	YML093W	1,47			1,87		1,07		VDPYGGSDDEQGD	CK2
UTP12_YEAST	S736	YLR129W	1,55			1,55				GVEDEASGVHKQT	
ULS1_YEAST	S335	YOR191W	3,16			3,16				KIKRKHSGDFADN	CAMK2;CHK1;PKA;PKD
UBP3_YEAST	S335	YER151C	2,71			3,20	2,21			SVEENTSKTSSPS	GSK3
UBP10_YEAST	S258	YNL186W	0,72			0,72				EEEENDSSSKISE	
UBP1_YEAST	S618	YDL122W	1,39	1,29		1,11	1,49		1,61	KRIIEHSDVENEN	CK2
UAF30_YEAST	S218	YOR295W	1,19			1,28	1,11			KEKPIVSDSEQSD	CK2
TRF5_YEAST	S613	YNL299W	0,52				0,52			KGRDTPSGQDEKS	CK2
TRA1_YEAST	S542	YHR099W	1,36			1,66	1,07			KEDINDSPDVEMT	Proline-directed
TOP2_YEAST	T1314	YNL088W	1,34			4,53	1,34	1,34		ATSKENTPEQDDV	Proline-directed
TNA1_YEAST	S9	YGR260W	0,22						0,22	NKFTMESPKHLVD	CDK1;Proline-directed
THO1_YEAST	S22	YER063W	0,76	0,81			0,70			LTKRNLSVGGLKN	CAMK2;PKA
THO1_YEAST	S78	YER063W	2,02				2,02			TEKKEVSSEPKET	
TGS1_YEAST	S286	YPL157W	0,96			0,96				EKEELSSENEELS	CK2
TGL1_YEAST	S538	YKL140W	1,36				1,36			QLDANSSTTALDA	
TAN1_YEAST	S72	YGL232W	2,47			2,47				KEGEDESENDEKK	CK2
TAF2_YEAST	S261	YCR042C	1,51			1,51	1,32		3,05	GQNGEESEKEKED	CK2
TAF2_YEAST	T268	YCR042C	1,73	1,66		3,83	1,73			EKEKEDTPEHDEE	Proline-directed
TAF12_YEAST	S287	YDR145W	1,05				1,05			NQRKISSSNSTEI	
TAF10_YEAST	S58	YDR167W	2,25			2,25				AVVDDGSENAFGI	
T2FA_YEAST	T200	YGR186W	1,29			1,29	1,29			VKDGSQTPTVDSV	Proline-directed
T2FA_YEAST	S515	YGR186W	1,87			1,87				RDEEAPSENEEDE	CK2
SWI5_YEAST	S505	YDR146C	0,91				0,91			SKYEGRSPQFGTH	Proline-directed
SWI5_YEAST	S522	YDR146C	0,93				0,93			NTYTTNSPSKITR	CDK1;CDK2;Proline-directed
SUR1_YEAST	S349	YPL057C	1,76			1,76	1,82	1,28		KRLRKDSNTNIVL	CAMK2;PKA;PKA/AKT
SUB1_YEAST	S119	YMR039C	2,01	1,22	1,78	2,64	2,01		7,20	KMVRLLSDDEYED	CAMK2;CHK1;CK2
SUB1_YEAST	S263	YMR039C	2,26			2,26				VSNINESKDANSS	
STP3_YEAST	S215	YLR375W	1,90		0,77	1,90			2,68	GKGGSVSPNDDDT	CK2;Proline-directed
STM1_YEAST	S2	YLR150W	1,34		1,34	1,41	1,35		1,33	_____MSNPFDLL	
STM1_YEAST	S55	YLR150W	0,55	0,44	0,58	0,47	0,61	0,52	0,58	KNRPRPSGNEGAI	CK2;PKA
STM1_YEAST	T181	YLR150W	1,11	1,11	1,08	1,31	1,23		1,02	DAERIETAEKEAY	CAMK2
STM1_YEAST	T248	YLR150W	0,78						0,78	ARKGNNTANATNS	FHA KAPP
STM1_YEAST	T252	YLR150W	1,04						1,04	NNTANATNSANTV	FHA KAPP

Uniprot Name	Phosphosite	Protein ID	Ratio Ctk1/wt MV	Ratio Ctk1/wt 1	Ratio Ctk1/wt 2	Ratio Ctk1/wt 3	Ratio Ctk1/wt 4	Ratio Ctk1/wt 5	Ratio Ctk1/wt 6	Sequence Window	Kinase Motifs Matching
STM1_YEAST	S254	YLR150W	1,07			1,14	1,02		1,07	TANATNSANTVQK	
STH1_YEAST	S1232	YIL126W	2,23			3,33	1,13			EKPESKSPAKKTA	CDK1;CDK2;Proline-directed
STE6_YEAST	T617	YKL209C	1,31				1,34		1,28	AKTIVDTETEEKS	CK2
STE6_YEAST	T619	YKL209C	1,66			1,66				TIVDTETEEKSIH	
STE20_YEAST	T573	YHL007C	1,31			1,31				AQETVTTPTSKPA	ERK/MAPK;FHA KAPP;Proline-directed
STE2_YEAST	S366	YFL026W	1,31	1,57		1,31	1,68	1,08	1,30	SERTFVSETADDI	
STE12_YEAST	S226	YHR084W	0,52				0,52			TTKSDNSPPKLES	CDK1;CDK2;CK1;Proline-directed
STE12_YEAST	S400	YHR084W	0,94			1,07	0,81			NKEKLVSPSDPTS	CK2;Proline-directed
SSZ1_YEAST	S477	YHR064C	1,38	1,50	1,18	1,33	1,42	1,27	1,93	AEEDDESEWSDDE	
SSZ1_YEAST	S480	YHR064C	1,45	1,69	1,50	1,30	1,40	1,29	1,94	DDESEWSDDEPEV	CK1;CK2
SSN2_YEAST	S375	YDR443C	0,76			0,76	1,01	0,42		ISPKDFSPNFTGI	Proline-directed
SSN2_YEAST	S425	YDR443C	1,27			1,29	1,25			SNDLENSPLKTEL	CDK1;CDK2;NEK6;Proline-directed
SSN2_YEAST	S636	YDR443C	1,56	0,65		2,19	1,56			GGKFSFSPLQKEE	Proline-directed
SSD1_YEAST	S492	YDR293C	2,31			2,31				DSDSLSSPTKSGV	CDK1;CDK2;CK1;GSK3;Polo box;Proline-directed
SRP40_YEAST	S133	YKR092C	0,71	0,52	0,78	0,65	0,88	0,61	0,89	KKRARESDNEDAK	CK2;PKA
SRO9_YEAST	S148	YCL037C	0,74					0,74		KKDGFESAVGEED	
SPT8_YEAST	T85	YLR055C	1,24	0,62		1,35	1,24			RMDKTATPTNEHQ	CHK1;Proline-directed
SPT5_YEAST	S136	YML010W	2,61			3,49	1,73			EEDTKNSDGDTKD	CK2
SPT2_YEAST	S193	YER161C	0,27				0,27			SIKSSDSPKPVKL	CDK1;CK1;Proline-directed
SPP41_YEAST	S1014	YDR464W	1,80			1,80				LTKRAESVEPVEN	CAMK2;PKA
SPP41_YEAST	S1067	YDR464W	1,22			1,22				KRILIESPVEKTD	CK2;NEK6;Proline-directed
SPP1_YEAST	S87	YPL138C	1,27					1,27		IINGEGSLPKTLW	PLK1
SPB1_YEAST	T432	YCL054W	0,61	0,58	0,43	0,51	0,65	0,81	0,65	KKRMIFTDDELAK	CK2
SPB1_YEAST	S505	YCL054W	1,70			1,70				TGFNEGSLEKKEE	PLK1
SPB1_YEAST	S529	YCL054W	1,14				1,14	0,72	1,73	EGVEGDSDDDEAI	CK2
SPB1_YEAST	S765	YCL054W	1,29			1,29	1,04		1,78	GLINDDSDKTEKD	
SPA2_YEAST	S274	YLL021W	1,41			1,48	1,35			GPEQLKSPEVQRA	Proline-directed
SNX41_YEAST	S499	YDR425W	1,19	0,90		1,19	1,45			KDVRSLSKSSSNS	CAMK2;GSK3;PKA/AKT
SNU66_YEAST	S268	YOR308C	1,27			1,49	1,05			DSANNMSDEDGGD	CK2
SNT1_YEAST	T796	YCR033W	1,60			1,60				KGDPLGTPEKVEN	CDK1;CDK2;Proline-directed
SNF5_YEAST	S818	YBR289W	1,87			1,87				TNAMLPSPESLKT	Proline-directed
SNF2_YEAST	S358	YOR290C	0,93			0,93				ENFASVSPAGPSS	Proline-directed
SNC2_YEAST	T57	YOR327C	0,84	0,84						ERGERLTSIEDKA	CK2;PKA
SNC2_YEAST	S58	YOR327C	1,24	0,84		1,34	1,24			RGERLTSIEDKAD	CAMK2;CK2
SMD2_YEAST	S2	YLR275W	0,36			0,36				_____MSSQIIDR	
SMD2_YEAST	S3	YLR275W	0,65				0,54		0,76	____MSSQIIDRP	

Uniprot Name	Phosphosite	Protein ID	Ratio Ctk1/wt MV	Ratio Ctk1/wt 1	Ratio Ctk1/wt 2	Ratio Ctk1/wt 3	Ratio Ctk1/wt 4	Ratio Ctk1/wt 5	Ratio Ctk1/wt 6	Sequence Window	Kinase Motifs Matching
SLA1_YEAST	T818	YBL007C	2,48	2,59		2,14	2,37		6,60	KKAAASTPEPNLK	Polo box;Proline-directed
SKG1_YEAST	T273	YKR100C	1,46			1,46				LEDVFATPKSAAQ	CDK1;FHA KAPP;Proline-directed
SET2_YEAST	S10	YJL168C	0,59			0,63	0,55			NQSVSASEDEKEI	CK1;CK2
SET1_YEAST	S655	YHR119W	3,53	3,15		5,58	3,89	3,16		LNEETDSKETTPL	
SET1_YEAST	T659	YHR119W	3,82	2,36		4,46	3,18		6,71	TDSKETTPLNDEG	Proline-directed
SET1_YEAST	S701	YHR119W	1,60			1,68	1,52			KKFKSESEPTTPE	
SET1_YEAST	T705	YHR119W	1,60			1,68	1,52			SESEPTTPESDHL	ERK/MAPK;FHA KAPP;Proline-directed;WW GroupIV
SEC4_YEAST	S8	YFL005W	1,07				1,07			SGLRTVSASSGNG	CAMK2;PKA/AKT
SEC4_YEAST	S11	YFL005W	0,92			0,89	1,01	0,76	0,94	RTVSASSGNGKSY	CK1
SEC16_YEAST	S268	YPL085W	1,79	1,47	1,31	2,69	1,79		2,11	KLETHVSTEEKKQ	CK2
SEC16_YEAST	S483	YPL085W	0,86	0,76	0,68	1,28	0,96	0,67	1,48	KLPWEVSDGEVSS	CK2
SEC16_YEAST	S806	YPL085W	1,33	0,77	1,33	1,43	1,27		2,88	NKYAPVSPTVQQK	ERK/MAPK;Proline-directed;WW GroupIV
SDS23_YEAST	S42	YGL056C	1,55				1,55			NTEANKSDTESLH	CK2;GSK3
SDS23_YEAST	S46	YGL056C	1,55				1,55			NKSDTESLHKSIS	CK1;GSK3
SDA1_YEAST	S591	YGR245C	0,65	0,54	0,78	0,50	0,76	0,51	0,84	DVDMEDSDDEKDN	CK2
SCS2_YEAST	S106	YER120W	2,35			2,63	2,07			AVADVWSDLEAEF	CK2
SBE22_YEAST	S459	YHR103W	1,64			1,64				LSERTKSSDFLPI	CAMK2
SAS10_YEAST	S477	YDL153C	1,01					1,01		DDKDYGSEDEAVS	CK2
SAC7_YEAST	S16	YDR389W	1,66			1,80	1,44		1,66	SKIENVSPSKGHV	CDK1;CDK2;Proline-directed
SAC7_YEAST	S435	YDR389W	2,97			2,97				KITSSDSPPIVSS	CK1;Proline-directed
RT107_YEAST	S720	YHR154W	1,24	0,51		1,24	1,34			HLFEGLSDNDDHI	CK2
RT01_YEAST	T243	YDR347W	0,27		0,27	4,89	0,13	12,39	0,21	LEDSEMTAKQAKT	CK1
RSN1_YEAST	S949	YMR266W	0,75						0,75	KYKEEESRSAV__	
RSN1_YEAST	S951	YMR266W	0,79			0,83			0,75	KEEESRSAV____	
RSC7_YEAST	S2	YMR091C	1,07	0,95		2,64	1,07			_____MSDSEGGL	CK2
RSC4_YEAST	S406	YKR008W	0,84	0,32					1,36	NERSTTSDIEKTN	CK1;CK2
RS9B_YEAST	S9	YBR189W	0,61	0,58	0,70	0,57	0,64	0,58	0,64	RAPRTYSKTYSTP	CAMK2;GSK3;PKA/AKT
RS9B_YEAST	S21	YBR189W	1,26						1,26	PKRPYESSRLDAE	
RS9B_YEAST	S22	YBR189W	1,26						1,26	KRPYESSRLDAEL	CK2
RS9B_YEAST	S152	YBR189W	1,65	2,06		1,24				FMVRLDSEKHIDF	CAMK2;CHK1
RS8_YEAST	T132	YBL072C	0,58	1,02	0,58				0,53	NVKEEETVAKSKN	PLK1
RS7B_YEAST	S31	YNL096C	0,65	0,76			0,11	0,54	0,95	IDLESSSPELKAD	Polo box;Proline-directed
RS7A_YEAST	S115	YOR096W	0,23	0,23						VQKRPRSRTLTAV	CAMK2;PKA
RS7A_YEAST	S156	YOR096W	0,80			0,69	0,90			QKVLLDSKDVQQI	NEK6
RS6_YEAST	T163	YBR181C	0,57	0,59	0,58	0,53	0,53	0,57	0,57	VIRREVTKGEKTY	CAMK2;CHK1;CK2;PKD
RS6_YEAST	S232	YBR181C	1,27	1,20	1,34	0,73	0,83	1,54	1,43	IRKRRASSLKA__	CAMK2;PKA;PKA/AKT

Uniprot Name	Phosphosite	Protein ID	Ratio Ctk1/wt MV	Ratio Ctk1/wt 1	Ratio Ctk1/wt 2	Ratio Ctk1/wt 3	Ratio Ctk1/wt 4	Ratio Ctk1/wt 5	Ratio Ctk1/wt 6	Sequence Window	Kinase Motifs Matching
RS6_YEAST	S233	YBR181C	0,89	0,81	1,06	0,96	0,80	0,78	2,43	RKRRASSLKA___	CAMK2
RS5_YEAST	S2	YJR123W	1,10	1,03	1,40	0,85	1,05	1,35	1,15	_____MSDTEAPV	CK2
RS5_YEAST	S206	YJR123W	1,81						1,81	NAAKGSSTSYAIK	
RS3B_YEAST	S245	YML063W	0,87	0,88		0,80	0,83	0,87	0,92	EKGKKVSGFKDEV	
RS3B_YEAST	T254	YML063W	0,75	0,71		0,80	0,75	0,88	0,72	KDEVLETV_____	
RS3A_YEAST	S36	YLR441C	0,70			0,67	0,74			FDIKAPSTFENRN	CK2
RS3A_YEAST	S169	YLR441C	1,08	1,08	0,82	1,29	1,24		0,79	AIRKVISEILTKE	CHK1;PKD
RS3A_YEAST	S236	YLR441C	1,35	1,21	1,42	1,29	1,41	1,25	1,85	ALHGEGSGEEKGK	CK2
RS3A_YEAST	T254	YLR441C	0,98					0,98		KDEVLETV_____	
RS3_YEAST	T207	YNL178W	1,11	1,18	1,13	1,09	1,07	1,13	1,02	ALPDAVTIIEPKE	CK2
RS3_YEAST	S221	YNL178W	0,95	0,97	1,04	0,88	0,91	0,99	0,93	EPILAPSVKDYRP	CK2;NEK6
RS28B_YEAST	T5	YLR264W	1,43	1,43	1,43	1,51	0,98	1,48	1,06	__MDSKTPVTLAK	Proline-directed
RS28A_YEAST	T5	YOR167C	1,98	2,21	2,00	2,02	1,97	1,92	1,76	__MDNKTPVTLAK	Proline-directed
RS27B_YEAST	T11	YHR021C	0,75				0,75			QDLLHPTAASEAR	FHA KAPP;NEK6
RS27B_YEAST	S14	YHR021C	0,75				0,75			LHPTAASEARKHK	
RS25B_YEAST	S93	YLR333C	0,90	0,90		1,26	0,88			GIIKPISKHSKQA	CHK1;PKD
RS24_YEAST	S2	YER074W	1,30	1,25	1,37	1,18	1,31	1,67	1,29	_____MSDAVTIR	
RS24_YEAST	S14	YER074W	0,73	0,93	0,73				0,68	RTRKVISNPLLAR	
RS23_YEAST	S40	YGR118W	0,61					0,61		LGTAFKSSPFGGS	CK1
RS23_YEAST	S41	YGR118W	1,12	1,12		0,82			1,17	GTAFKSSPFGGSS	Polo box;Proline-directed
RS23_YEAST	S46	YGR118W	0,63	0,63						SSPFGGSSHAKGI	
RS2_YEAST	S2	YGL123W	1,19		1,05	1,23	1,22	1,19	0,90	_____MSAPEAQQ	CK2
RS19A_YEAST	S117	YOL121C	2,27	2,15	2,12	2,57	2,40	2,01	2,53	IGIVEISPKGGRR	CDK1;Proline-directed
RS18_YEAST	S107	YDR450W	0,82				0,64	0,82	0,87	LANNVESKLRDDL	
RS17B_YEAST	S70	YDR447C	0,59	0,69	0,61	0,55	0,63	0,56	0,56	GPVRGISFKLQEE	CAMK2
RS16_YEAST	S2	YDL083C	0,57			0,57	0,56	0,57	0,58	_____MSAVPSVQ	GSK3
RS16_YEAST	S6	YDL083C	0,64	0,64						_MSAVPSVQTFGK	CK1
RS16_YEAST	T17	YDL083C	1,02	1,02	1,20	0,96	1,02		1,10	GKKKSATAVAHVK	FHA KAPP
RS16_YEAST	S34	YDL083C	1,11	1,11		1,08			1,15	LIKVNGSPITLVE	Proline-directed
RS15_YEAST	S2	YOL040C	1,85	1,74					1,96	_____MSQAVNAK	
RS15_YEAST	S29	YOL040C	1,35	1,08		0,11	1,35	1,56	1,37	EKLLEMSTEDFVK	CK2;NEK6
RS15_YEAST	T30	YOL040C	0,80						0,80	KLLEMSTEDFVKL	
RS13_YEAST	S30	YDR064W	1,16				1,09	1,26	1,16	AWFKLSSESVIEQ	
RS13_YEAST	S32	YDR064W	1,36			1,36				FKLSSESVIEQIV	CK1;CK2
RS12_YEAST	S2	YOR369C	1,18	1,15	1,44	0,71	1,03	1,61	1,21	_____MSDVEEVV	CK2
RS11_YEAST	S2	YBR048W	1,40	1,40	1,78	1,38	1,41	1,37	1,44	_____MSTELTVQ	

Uniprot Name	Phosphosite	Protein ID	Ratio Ctk1/wt MV	Ratio Ctk1/wt 1	Ratio Ctk1/wt 2	Ratio Ctk1/wt 3	Ratio Ctk1/wt 4	Ratio Ctk1/wt 5	Ratio Ctk1/wt 6	Sequence Window	Kinase Motifs Matching
RS11_YEAST	T6	YBR048W	0,89						0,89	_MSTELTVQSERA	FHA KAPP;PLK1
RS11_YEAST	S9	YBR048W	0,86	0,85	1,05	0,72	0,85	0,87	0,89	TELTVQSERAFQK	
RS11_YEAST	T44	YBR048W	0,62	0,75		0,62	0,61	0,58	0,69	AGLGFKTPKTAIE	CDK1;Proline-directed
RS11_YEAST	S52	YBR048W	0,97			0,73	1,22	0,97		KTAIEGSYIDKKC	CK2;PLK1
RS10B_YEAST	S48	YMR230W	1,60	1,47		1,60	1,56	1,77	1,74	VIKALQSLTSKGY	
RRS1_YEAST	S41	YOR294W	1,46			1,46				DKNDLDSSNARRE	
RRS1_YEAST	S42	YOR294W	1,48			1,48				KNDLDSSNARREE	NEK6
RRP5_YEAST	S187	YMR229C	1,40				1,40	0,89	2,15	EDAEYESSDDEDE	CK2
RRP5_YEAST	S188	YMR229C	1,40				1,40	0,89	2,15	DAEYESSDDEDEK	CK2
RRP3_YEAST	S45	YHR065C	2,55			2,55				KEGGSESDSEEDA	CK2
RRP15_YEAST	S69	YPR143W	1,07	0,71	1,07	1,35	1,12	0,85		IIDNEQSDAEEDD	CK2
RPN8_YEAST	S317	YOR261C	1,35					1,35		SKVSDDSESESGD	CK1;CK2;GSK3
RPN8_YEAST	T327	YOR261C	8,40			8,40				SGDKEATAPLIQR	FHA2 Rad53p
RPN13_YEAST	S135	YLR421C	1,77	1,55		1,77	2,23	1,33	2,64	LNNSSESDEEESN	CK1;CK2
RPN13_YEAST	S140	YLR421C	1,51			1,71		1,31		ESDEEESNDEKQK	CK2
RPN1_YEAST	S19	YHR027C	1,72			1,72				DEQSQISPEKQTP	CDK1;CDK2;CK1;Proline-directed
RPN1_YEAST	S695	YHR027C	1,65			1,65				EKKNGESLEGEEI	
RPC7_YEAST	S189	YNL151C	0,99			0,99				EDVDDASTGDGAA	CK2
RPC4_YEAST	S119	YDL150W	2,28			2,28				FIKSEGSGSSLVQ	CK1
RPAC2_YEAST	T33	YNL113W	0,96			0,96				EQDVDMTGDEEQE	CK2
ROM2_YEAST	S628	YLR371W	2,51			2,51				GLKRNISMALDDD	CAMK2;CHK1;CHK1/2;PKA;PKD
ROD1_YEAST	S641	YOR018W	2,16				2,16			DLSRVPSYDKAMK	CAMK2;CHK1;CHK1/2;CK1;PKD
RNT1_YEAST	S468	YMR239C	1,13			1,15	1,13	0,47		NKKRKFSDTS___	CAMK2;PKA
RLM1_YEAST	S164	YPL089C	1,37	1,00		2,19	1,37			AHMKLLSPTALIS	Proline-directed
RLI1_YEAST	S6	YDR091C	4,89						4,89	_MSDKNSRIAIVS	CK1
RLA4_YEAST	S100	YDR382W	0,92	0,94	0,97	0,74	0,60	1,05	0,90	EEAKEESDDDMGF	CK2
RLA3_YEAST	S58	YDL130W	1,08		1,08					DLKEILSGFHNAG	
RLA3_YEAST	S96	YDL130W	1,17	1,12	1,09	1,19	1,16	1,36	1,27	EEAAEESDDDMGF	CK2
RLA2_YEAST	S40	YOL039W	0,69				0,69			EDEKVSSVLSALE	
RLA2_YEAST	S43	YOL039W	1,36	1,20		1,13	1,51		1,68	KVSSVLSALEGKS	CK1;CK2
RLA2_YEAST	S49	YOL039W	2,81	2,84	2,44	2,79	2,42	3,01	3,11	SALEGKSVDELIT	CK2
RLA2_YEAST	S71	YOL039W	3,47	2,98		2,94	3,52	3,47	3,83	PAAGPASAGGAAA	
RLA2_YEAST	S79	YOL039W	1,22	1,15	0,99	1,25	1,22	1,39		GGAAAASGDAAAE	
RLA2_YEAST	S96	YOL039W	1,25	1,20	1,10	1,18	1,30	1,98	1,39	EEAAEESDDDMGF	CK2
RLA1_YEAST	S96	YDL081C	0,91	0,91	0,90	0,83	0,92	1,42	1,02	EEAKEESDDDMGF	CK2
RL8B_YEAST	S29	YLL045C	0,88				1,00		0,77	KNPLTHSTPKNFG	NEK6

Uniprot Name	Phosphosite	Protein ID	Ratio Ctk1/wt MV	Ratio Ctk1/wt 1	Ratio Ctk1/wt 2	Ratio Ctk1/wt 3	Ratio Ctk1/wt 4	Ratio Ctk1/wt 5	Ratio Ctk1/wt 6	Sequence Window	Kinase Motifs Matching
RL8B_YEAST	S126	YLL045C	1,02	1,12	0,93	1,28	0,94		1,02	KSKQDASPKPYAV	CDK1;Proline-directed
RL8B_YEAST	S216	YLL045C	1,38	1,33	1,61	1,14	1,50	1,43	1,15	ALAKLVSTIDANF	CHK1;CK2;PKD
RL7B_YEAST	T8	YPL198W	2,13	2,14	2,07	2,20	2,13	2,02	2,45	AAEKILTPESQLK	FHA KAPP;Proline-directed
RL7B_YEAST	S11	YPL198W	2,07	2,53	2,06	1,99	2,20	2,08	1,91	KILTPESQLKKSK	
RL7B_YEAST	S228	YPL198W	0,56	0,56						HFIQGGSFGNREE	
RL6A_YEAST	S12	YML073C	5,26	5,26	5,02	10,57	5,64		4,77	APKWYPSEDVAAL	
RL4A_YEAST	S53	YBR031W	0,84		0,67	0,76	0,92		0,91	RQAYAVSEKAGHQ	
RL4A_YEAST	S158	YBR031W	1,52				1,52			VSTDLESIQKTKE	CK1
RL4A_YEAST	S176	YBR031W	1,08			1,08	1,16		1,02	KAVGAHSDLLKVL	
RL37A_YEAST	T5	YLR185W	0,60				0,64		0,56	__MGKGTPSFGKR	Proline-directed
RL37A_YEAST	S7	YLR185W	0,93	0,84	0,95	0,90	0,96	0,92	0,94	MGKGTPSFGKRHN	
RL37A_YEAST	S82	YLR185W	1,21			1,36	1,06			NGFQTGSASKASA	
RL37A_YEAST	S84	YLR185W	0,82						0,82	FQTGSASKASA__	CK1
RL36B_YEAST	S79	YPL249C-A	0,61	0,57	0,61	0,47	0,85		0,69	AKKRLGSFTRAKA	CAMK2;PKA
RL35_YEAST	S19	YDL136W	0,62					0,67	0,56	SKEQLASQLVDLK	
RL35_YEAST	S40	YDL136W	1,14	1,13		1,15	1,19		0,98	QKLSRPSLPKIKT	AURORA;CK1;PKA
RL35_YEAST	S98	YDL136W	0,57		0,66	0,57	0,67	0,57	0,55	LTKFEASQVTEKQ	
RL33A_YEAST	S4	YPL143W	0,82	0,94		0,70				___MAESHRLYVK	
RL33A_YEAST	S19	YPL143W	1,10	1,10						HLSYQRSKRVNNP	CK1
RL32_YEAST	S3	YBL092W	1,20	1,20		1,21	0,97			_____MASLPHPKI	
RL32_YEAST	S67	YBL092W	1,76	1,78	1,73	1,98	1,74	1,92	1,69	KKTKFLSPSGHKT	CK1;Proline-directed
RL32_YEAST	S69	YBL092W	1,06	1,12		1,26	1,00		0,98	TKFLSPSGHKTFL	NEK6
RL31A_YEAST	S100	YDL075W	1,05	1,27	1,01	0,98	1,07	1,02	1,13	EPVLVASAKGLQT	NEK6
RL3_YEAST	S24	YOR063W	0,61	0,62	0,61	0,79		0,60		PRKRAASIRARVK	CAMK2;PKA;PKA/AKT;PKC
RL3_YEAST	S65	YOR063W	0,77	0,77						DLDRPGSKFHKRE	CAMK2;CHK1;CHK1/2;PKD
RL3_YEAST	S187	YOR063W	1,17					1,17		IQLNGGSISEKVD	CK2
RL3_YEAST	S297	YOR063W	1,12	0,95	1,18		1,12	1,21	1,06	EANGATSFDRTKK	
RL3_YEAST	S355	YOR063W	1,25	1,31	1,27	1,32	1,18	1,23	1,23	KALEEVSLKWIDT	PLK1
RL27A_YEAST	S33	YHR010W	0,97	0,97	0,86	1,05	0,99		0,83	KPHDEGSKSHPFG	
RL27A_YEAST	S94	YHR010W	0,77	0,80		0,77			0,76	DVEAFKSVVSTET	
RL27A_YEAST	S105	YHR010W	0,80	0,89	0,76	0,76	0,83		0,80	ETFEQPSQREEAK	CK2
RL26B_YEAST	S5	YGR034W	0,83	0,99					0,66	__MAKQSLDVSSD	AURORA;GSK3
RL26B_YEAST	S10	YGR034W	0,99	0,90					1,08	QSLDVSSDRRKAR	
RL26B_YEAST	S62	YGR034W	1,76	1,49		2,91	1,76			VLVVRGSKKGQEG	PKA
RL24B_YEAST	S7	YGR148C	1,71	1,77	1,81	1,61	1,65	1,82	1,52	MKVEVDSFSGAKI	
RL24B_YEAST	S9	YGR148C	0,75	0,74	0,75	0,69	0,73	0,88	0,79	VEVDSFSGAKIYP	
RL24B_YEAST	S26	YGR148C	1,06	1,06						LFVRGDSKIFRFQ	CAMK2

Uniprot Name	Phosphosite	Protein ID	Ratio Ctk1/wt MV	Ratio Ctk1/wt 1	Ratio Ctk1/wt 2	Ratio Ctk1/wt 3	Ratio Ctk1/wt 4	Ratio Ctk1/wt 5	Ratio Ctk1/wt 6	Sequence Window	Kinase Motifs Matching
RL24B_YEAST	S36	YGR148C	0,49						0,49	RFQNSKSASLFKQ	
RL24B_YEAST	S38	YGR148C	0,45	0,45	0,44	0,48	0,46		0,42	QNSKSASLFKQRK	CK1
RL24B_YEAST	S86	YGR148C	0,91	0,95	0,96	0,82	0,97	0,78	0,88	RPITGASLDLIKE	
RL24A_YEAST	S7	YGL031C	1,59	1,71	1,64	1,48	1,50	1,75	1,53	MKVEIDSFSGAKI	
RL24A_YEAST	S9	YGL031C	0,78	0,83	0,87	0,67	0,73	0,81	0,75	VEIDSFSGAKIYP	
RL21A_YEAST	S70	YBR191W	1,07	1,07		0,93	1,07	1,09		VYNVTKSSVGVII	
RL2_YEAST	S52	YFR031C-A	0,96	0,87		1,05				KQIVHDSGRGAPL	
RL1D1_YEAST	S270	YKR060W	1,10			1,32	0,87			QKNEDLSDIKL__	
RL19_YEAST	T29	YBL027W	0,96	0,96						WLDPNETSEIAQA	FHA2 Rad53p
RL19_YEAST	S30	YBL027W	0,77				0,79		0,75	LDPNETSEIAQAN	
RL18_YEAST	S167	YNL301C	0,42	0,39	0,42	0,41	0,47		0,48	KAPRILSTGRKFE	CAMK2
RL17A_YEAST	S142	YKL180W	1,21	1,06		1,20		1,22	1,38	INKYESSPSHIEL	Polo box;Proline-directed
RL16B_YEAST	S2	YNL069C	0,71			0,71				_____MSQPVVVI	
RL16B_YEAST	S178	YNL069C	0,82	0,82						AFTKKVSSASAAA	CK1
RL16B_YEAST	S179	YNL069C	0,86	0,93		0,87		0,85	0,52	FTKKVSSASAAAS	
RL16B_YEAST	S181	YNL069C	0,83	0,81	1,38		0,81	0,84		KKVSSASAAASES	CK1;GSK3
RL16B_YEAST	S185	YNL069C	0,81	0,81	0,90	0,69	0,87	0,80	0,81	SASAAASESDVAK	CK1;CK2
RL16B_YEAST	S187	YNL069C	0,94	0,87	0,95	0,93	0,99	0,67	1,05	SAAASESDVAKQL	
RL16A_YEAST	S2	YIL133C	1,05				1,14	0,97		_____MSVEPVVV	
RL16A_YEAST	S163	YIL133C	0,29						0,29	EAKRKVSSAEYYA	CAMK2;CK2;PKA
RL16A_YEAST	S188	YIL133C	0,83					0,83		NATAAESDVAKQL	CK1
RL14B_YEAST	S2	YHL001W	1,44			1,44	1,50		0,89	_____MSTDSIVK	
RL14B_YEAST	S5	YHL001W	1,15	0,99	1,42	1,05	1,24	1,00	1,26	__MSTDSIVKASN	CK1
RL12_YEAST	S38	YDR418W	1,48	1,31	1,46	1,93	1,46	1,50	1,99	IGPLGLSPKKVGE	CDK1;CDK2;NEK6;Proline-directed
RL11B_YEAST	T44	YGR085C	0,91		0,91	1,67	0,85			EQLSGQTPVQSKA	CK1;Proline-directed
RL11B_YEAST	S161	YGR085C	0,93	0,87		0,85	1,08		0,98	TKEDTVSWFKQKY	
RL10_YEAST	S205	YLR075W	0,83			0,83	0,83		0,81	FLSKKGSLENNIR	AURORA;CHK1;CK1;PKD
RL1_YEAST	S6	YGL135W	0,73	0,73						_MSKITSSQVREH	CHK1;CK1
RL1_YEAST	S7	YGL135W	0,94	0,88	0,96	0,91	0,96	0,96	0,92	MSKITSSQVREHV	
RIR2_YEAST	S15	YJL026W	0,79			0,96			0,62	AAADALSDLEIKD	CK2
RFC1_YEAST	S80	YOR217W	3,15			3,15				AKRKASSPTVKPA	Polo box;Proline-directed
RFA1_YEAST	S178	YAR007C	0,84	0,63		1,35	0,84	0,51	0,87	ANENPNSQKTRPI	
REI1_YEAST	T111	YBR267W	0,64	0,51	0,77		0,68	0,64	0,58	KSQEGNTPDLSKL	FHA2 Rad53p;Proline-directed
REI1_YEAST	S118	YBR267W	1,86				1,21		2,50	PDLSKLSLQENEE	AURORA;CK1;CK2
RAS2_YEAST	T227	YNL098C	1,22			1,22				NVNSSTTVVNARN	CK1
RAS1_YEAST	S229	YOR101W	2,09				2,09			TGSSSKSAVNHNG	CK1

Uniprot Name	Phosphosite	Protein ID	Ratio Ctk1/wt MV	Ratio Ctk1/wt 1	Ratio Ctk1/wt 2	Ratio Ctk1/wt 3	Ratio Ctk1/wt 4	Ratio Ctk1/wt 5	Ratio Ctk1/wt 6	Sequence Window	Kinase Motifs Matching
RAEP_YEAST	S470	YOR370C	0,35			0,36	0,34	0,23	0,45	SVKLGQSFKEYVP	CK2;NEK6
RAD16_YEAST	S109	YBR114W	1,93			2,55	1,32			KEERDVSDDDEPL	CAMK2;CK2
Q05382_YEAST	S4555	YLR106C	0,68				0,68			DEEEMLSDIDAHD	CK2
PYR1_YEAST	S1857	YJL130C	3,54			1,91	4,59		3,54	SAKRRFSITEEAI	AURORA;AURORA-A;CAMK2;CK2;PKA;PKA/AKT
PXR1_YEAST	S159	YGR280C	0,67				0,67			KREGDDSEDEDDD	CK2
PWP2_YEAST	S232	YCR057C	1,39	1,24	1,58		1,39	1,26	2,47	DDDDNESEDDDKQ	CK2
PWP1_YEAST	S52	YLR196W	1,59	1,46	1,87	1,29	1,73	1,15	2,05	EEAEGESGVEDDA	CK2
PWP1_YEAST	S131	YLR196W	1,42			1,28	1,56			LPNQEDSQEEKQE	CK2
PVH1_YEAST	S212	YIR026C	1,07						1,07	MFKDSESSQDLDK	CK2
PUT4_YEAST	S96	YOR348C	1,37			1,92	0,81			DLEKSPSVDGDSE	CHK1;PKD
PUF6_YEAST	S34	YDR496C	1,08	0,88	1,11	1,04	1,11	1,00	1,82	PRISIDSSDEESE	CK1;CK2
PUF6_YEAST	S35	YDR496C	1,23	1,04	1,11	1,34	1,62	1,00	3,28	RISIDSSDEESEL	CK1;CK2;GSK3
PTR2_YEAST	S9	YKR093W	3,74	2,64		4,83				NHPSQGSDDAQDE	CK1
PSP2_YEAST	S238	YML017W	0,66	0,47		0,66	0,87			KTQRSKSNPFGSA	14-3-3 binding;CAMK2
PSP2_YEAST	S340	YML017W	2,60			2,60				PLSKLDSPALELQ	CHK1;CK1;PKD;Proline-directed
PSH1_YEAST	T382	YOL054W	1,91	1,91	2,07	1,20	1,92		0,90	DNNDDNTEELDDP	FHA2 Rad53p
PSA5_YEAST	T55	YGR253C	4,82			4,82				GVEKRATSPLLES	CHK1;FHA2 Rad53p;PKA;PKD
PSA5_YEAST	S56	YGR253C	4,17			4,17				VEKRATSPLLESD	CAMK2;PKA;Proline-directed
PRTB_YEAST	S58	YEL060C	4,28			5,10			3,46	DDDEEPSDSEDKE	CK2
PRS6B_YEAST	T8	YDR394W	2,28			1,74	2,28		2,86	EELGIVTPVEKAV	CK2;Proline-directed
PRP43_YEAST	S8	YGL120C	1,35			1,34	1,35			GSKRRFSSEHPDP	CAMK2;PKA
PRP43_YEAST	S9	YGL120C	1,34	0,89		1,34	1,35			SKRRFSSEHPDPV	CAMK2
PRP21_YEAST	S61	YJL203W	0,85			0,85				EPTDTVSGEDNDR	CK1;CK2
PRK1_YEAST	S484	YIL095W	6,08			6,08				VPNLKLSPTITSK	NEK6;Proline-directed
POP1_YEAST	T524	YNL221C	0,45				0,49		0,41	YKLLTATPNSINK	FHA KAPP;NEK6;Proline-directed
PLP2_YEAST	S35	YOR281C	1,25	1,25		1,25	0,67			IPERAPSPTAKLE	CAMK2;Proline-directed
PKH1_YEAST	S5	YDR490C	0,62	0,62						__MGNRSLTEADH	CK2
PHO84_YEAST	S15	YML123C	2,74	7,28		0,92	3,55	2,74	1,06	IHVAERSLHKEHL	PLK1
PHO4_YEAST	S242	YFR034C	1,73	1,33		2,13				SLSKRRSSGALVD	CHK1;CK1;PKA;PKD
PHO4_YEAST	S243	YFR034C	1,73	1,33		2,13				LSKRRSSGALVDD	CAMK2;PKA
PESC_YEAST	S288	YGR103W	1,07				1,38	0,75		EDVKVESLDASTL	GSK3
PESC_YEAST	S292	YGR103W	0,88			0,67	1,18	0,60	1,10	VESLDASTLKSAL	CK1;GSK3;NEK6
PEP3_YEAST	S907	YLR148W	1,04			1,06	1,02			KIDQPISIDETEL	CK2
PCY1_YEAST	T59	YGR202C	1,65	1,65		2,23	1,59			NKDTQLTPRKRRR	CDK1;CDK2;Proline-directed
PCY1_YEAST	S346	YGR202C	1,70	1,76		2,47	1,16		1,64	KLIREASPATEFA	CAMK2;CHK1;CHK1/2;PKD;Proline-directed
PBP2_YEAST	S20	YBR233W	1,87			2,08	1,65			PTTVLVSPNTLKR	CK1;Proline-directed

Uniprot Name	Phosphosite	Protein ID	Ratio Ctk1/wt MV	Ratio Ctk1/wt 1	Ratio Ctk1/wt 2	Ratio Ctk1/wt 3	Ratio Ctk1/wt 4	Ratio Ctk1/wt 5	Ratio Ctk1/wt 6	Sequence Window	Kinase Motifs Matching
PBP1_YEAST	S436	YGR178C	1,73				1,73			PSAKTVSPTTQIS	Proline-directed
PAT1_YEAST	S456	YCR077C	0,71	0,71						SKQRRRSSYAFNN	CAMK2;PKA
PAT1_YEAST	S457	YCR077C	0,71	0,71						KQRRRSSYAFNNG	CAMK2;PKA
PAT1_YEAST	Y458	YCR077C	0,71	0,71						QRRRSSYAFNNGN	
OTU2_YEAST	S96	YHL013C	1,86			1,86				LEQLSISRDEKEQ	CK2;NEK6
OSH2_YEAST	S825	YDL019C	2,12				2,12			EPKTDQSLKNFKA	PLK1
ORC6_YEAST	T114	YHR118C	1,65			1,65				MKQFAWTPSPKKN	Proline-directed
ORC6_YEAST	S116	YHR118C	1,65			1,65				QFAWTPSPKKNKR	CDK1;CDK2;Proline-directed
ORC6_YEAST	T146	YHR118C	1,33			1,69	0,96			RNQLFGTPTKVRK	CDK1;CDK2;NEK6;Proline-directed
ORC2_YEAST	S16	YBR060C	1,71			2,03	1,38			HNDILSSPAKSRN	CDK1;CDK2;GSK3;Polo box;Proline-directed
ORC2_YEAST	S61	YBR060C	2,50			1,88			3,12	NERKNTSPDPALK	Proline-directed
OM14_YEAST	S15	YBR230C	2,52			2,52				SNASPNSDSEDGH	CK1;CK2
ODPX_YEAST	S320	YGR193C	1,33	1,33						EDLVTLSPREPRF	CDK1;CK2;Proline-directed
ODPB_YEAST	T352	YBR221C	3,60				3,60			DFAFPDTPTIVKA	ERK/MAPK;FHA2 Rad53p;Proline-directed;WW GroupIV
NUP60_YEAST	S162	YAR002W	1,05			1,05				SEGEQKSAEGNNI	
NUP60_YEAST	S352	YAR002W	0,88				0,88			LNATKISPSAPSK	Proline-directed
NUP60_YEAST	S478	YAR002W	0,94			0,94				NSVQKKSRSNLSQ	
NSG2_YEAST	S49	YNL156C	1,41			1,63	1,20			ELKRSVSIDSTKY	CAMK2;CHK1;CHK1/2;PKA;PKD
NSG2_YEAST	S52	YNL156C	1,65			1,65				RSVSIDSTKYSRD	CK1;GSK3
NOT3_YEAST	S322	YIL038C	1,60			1,60				SKETERSPSSSPI	GSK3;Proline-directed
NOT3_YEAST	S344	YIL038C	1,69			2,02	1,40	1,02	1,99	VKTSIKSPRSSAD	CDK1;CK1;GSK3;Proline-directed
NOP8_YEAST	S268	YOL144W	0,99			1,21	0,77			PMTLNDSDEELLT	CK1;CK2;NEK6
NOP8_YEAST	S370	YOL144W	0,95	0,68	0,93	0,96	1,10	0,75	1,86	FKLIEDSDNDIDH	CK2
NOP4_YEAST	T657	YPL043W	0,77	0,52		1,01				KKEEATTPTNPDD	Proline-directed
NOP16_YEAST	T152	YER002W	0,58	0,44	0,92	0,55	0,61	0,40	1,11	EIKARDTTEETEV	CK2;PKA
NOP16_YEAST	S176	YER002W	0,52	0,37	0,40	0,53	0,52		0,70	VIRKERSQSEREE	CHK1;CK2;PKD
NOP13_YEAST	S2	YNL175C	0,56	0,35	0,72	0,64	0,49	0,42	0,75	_____MSETELSK	CK2
NOP13_YEAST	T4	YNL175C	0,74	0,49	0,63	0,80		0,74	1,72	___MSETELSKED	FHA KAPP
NOP12_YEAST	S65	YOL041C	3,60			3,54	3,67			QEEKEASKPDVSD	CK2
NOP12_YEAST	T181	YOL041C	1,76			1,95	1,57			TNPIAETEESGNE	FHA KAPP
NOP12_YEAST	S184	YOL041C	1,23	1,02	1,17	1,65	1,28	0,95	2,01	IAETEESGNEKEE	CK2
NOL10_YEAST	S529	YGR145W	1,55	1,15		1,88	1,55			LTAAEESDEERIA	CK2
NOC2_YEAST	S70	YOR206W	1,71	1,52	1,28	2,70	1,90	1,32	4,02	EVFKDMSVETFFE	CHK1;PKD;PLK1
NOC2_YEAST	S149	YOR206W	1,41			1,41	1,41			PLDGIDSQDEGED	CK2
NOC2_YEAST	S160	YOR206W	1,00			0,96	1,04			EDAERNSNIEEKS	CK2;PKA
NOC2_YEAST	S166	YOR206W	0,60	0,41	0,44	0,77	0,86	0,44	1,43	SNIEEKSEQMELE	

Uniprot Name	Phosphosite	Protein ID	Ratio Ctk1/wt MV	Ratio Ctk1/wt 1	Ratio Ctk1/wt 2	Ratio Ctk1/wt 3	Ratio Ctk1/wt 4	Ratio Ctk1/wt 5	Ratio Ctk1/wt 6	Sequence Window	Kinase Motifs Matching
NMD3_YEAST	S189	YHR170W	1,21			1,01	1,41			AHVDTISISEAKD	CK2
NEW1_YEAST	T1191	YPL226W	1,56	0,76	1,49	2,73	1,64	1,28	3,97	TPKPVDTDDEED_	CK2
NAT1_YEAST	S194	YDL040C	8,18	5,41		10,96				LAEGKISDSEKYE	CK2
NAP1_YEAST	S177	YKR048C	3,26			3,26				EKAQNDSEEEQVK	CK2
NACA_YEAST	S2	YHR193C	1,35					1,35		_____MSAIPENA	
NAB2_YEAST	S2	YGL122C	1,50			0,34			2,66	_____MSQEQYTE	
MTR4_YEAST	T34	YJL050W	1,31		1,31	1,18	1,53	1,14	3,09	DTNVGDTPDHTQD	Proline-directed
MSN4_YEAST	S446	YKL062W	1,83			1,83				FNILKSSPAQDQQ	NEK6;Polo box;Proline-directed
MSN4_YEAST	S558	YKL062W	2,13		1,16	3,10	1,05		6,42	QPRKRKSITTIDP	AURORA;AURORA-A;PKA
MRH1_YEAST	T295	YDR033W	0,60				0,60			SPRPAATPNLSKD	FHA2 Rad53p;Proline-directed
MRD1_YEAST	S264	YPR112C	1,73			1,81	1,66	1,15	2,71	VNDDANSDEKENE	
MRC1_YEAST	S605	YCL061C	2,32			2,32				KHIINESDSDTEV	CK2
MRC1_YEAST	S607	YCL061C	2,32			2,32				IINESDSDTEVEA	CK2
MPP6_YEAST	T148	YNR024W	1,65			2,50	0,80			AKDKEFTGSQDDG	
MPP6_YEAST	S150	YNR024W	1,65			2,50	0,80			DKEFTGSQDDGED	CK2
MPP10_YEAST	S176	YJR002W	1,61	1,46		1,91	1,61			GQDERHSSPDPYG	CK2;PKA
MPP10_YEAST	S177	YJR002W	1,61	1,46		1,91	1,61			QDERHSSPDPYGI	CAMK2;Polo box;Proline-directed
MFT1_YEAST	S266	YML062C	1,01				1,01			IDEDYESDEDEER	CK2
MEP2_YEAST	S460	YNL142W	2,98			2,98				PIRSKTSAQMPPP	CK1
MEP2_YEAST	T478	YNL142W	1,05			1,32			0,79	DKIVGNTDAEKNS	CK2
MEP2_YEAST	S491	YNL142W	1,38			0,87	1,90			TPSDASSTKNTDH	CK1
MED15_YEAST	S1034	YOL051W	1,45	0,77		1,52	1,37		2,71	KKIKVDSPDDPFM	CK2;ERK/MAPK;Proline-directed
MCM1_YEAST	S2	YMR043W	2,13			2,25	1,51		2,13	_____MSDIEEGT	CK2
MBP1_YEAST	S110	YDL056W	1,93			2,19	1,67			QTDGSASPPPAPK	Proline-directed
MAK5_YEAST	S678	YBR142W	1,22	0,83	1,18	1,25	1,43	0,95	2,92	LGIDVDSDEDDIS	CK2
MAK21_YEAST	S73	YDR060W	1,13	0,97	1,01	1,34	1,25	1,01	2,46	KLIQGLSDDDDAK	CK2
MAK21_YEAST	S80	YDR060W	0,84					0,84		DDDDAKSEQEFDA	CK2
MAK21_YEAST	S710	YDR060W	0,93	2,75				0,93	0,44	VDYEYESDAEEEQ	CK2
MAK21_YEAST	S878	YDR060W	1,15	0,95	1,10	1,19	1,35	0,95	2,58	KASNFDSDDEMDE	CK1;CK2
MAK11_YEAST	S430	YKL021C	1,64	0,90		1,64	1,82	0,54	2,43	ADIGDQSEVESDT	CK2;GSK3
MAK11_YEAST	S434	YKL021C	1,78	1,44	1,91	2,23	1,65	1,52	2,43	DQSEVESDTEELK	CK1;CK2
MAK11_YEAST	T436	YKL021C	1,96			1,96				SEVESDTEELKKI	FHA2 Rad53p
LTV1_YEAST	S281	YKL143W	0,63	0,47	0,70	0,49	0,84	0,56	0,94	RFQKDNSILEKHN	CK2;PLK;PLK1
LEUC_YEAST	S495	YGL009C	2,19	1,79		2,49		5,24	1,90	PKVEVTSEDEKEL	CK2
LEM3_YEAST	S36	YNL323W	1,73			1,90	1,55			EEDVDASEFEEDE	CK2
KIN2_YEAST	S146	YLR096W	2,46			2,46				KQHSLPSPKNESE	CDK1;CK1;Proline-directed

Uniprot Name	Phosphosite	Protein ID	Ratio Ctk1/wt MV	Ratio Ctk1/wt 1	Ratio Ctk1/wt 2	Ratio Ctk1/wt 3	Ratio Ctk1/wt 4	Ratio Ctk1/wt 5	Ratio Ctk1/wt 6	Sequence Window	Kinase Motifs Matching
KIN2_YEAST	S549	YLR096W	1,78			1,78				VALNNNSPDIMTK	Proline-directed
KEX1_YEAST	S660	YGL203C	1,06	0,64		1,06	1,06			NNRQHDSPNKTVS	CDK1;CDK2;Proline-directed
KEL3_YEAST	S47	YPL263C	0,93			1,15	0,71			GEEDDESDQDLDE	CK2
KCC4_YEAST	S894	YCL024W	1,56				1,30		1,82	KIAASLSDDDLKE	CK2
KBN8_YEAST	S505	YBR028C	1,36			1,49	1,22			INSVSKSPDMFKG	CK1;Proline-directed
KBN8_YEAST	S519	YBR028C	2,03	2,11		2,03	1,15			SYKASGSYLEKYF	CK2
K6PF2_YEAST	S163	YMR205C	2,37			2,04	2,70	1,94	2,80	PEASAESGLSSKV	CK1;GSK3
K6PF2_YEAST	S167	YMR205C	2,85			2,85	2,34		2,96	AESGLSSKVHSYT	CK1;GSK3
K6PF2_YEAST	S171	YMR205C	1,80	5,77			1,80		1,40	LSSKVHSYTDLAY	CK1;CK2
K6PF2_YEAST	Y172	YMR205C	1,01			1,01				SSKVHSYTDLAYR	ALK
JJJ1_YEAST	S386	YNL227C	0,79					0,79		LGLDNLSDLEKFD	CK2
JJJ1_YEAST	S393	YNL227C	0,83	0,83	0,85	0,83	0,80	0,80	1,01	DLEKFDSADESVK	CHK1;CK2;GSK3;PKD
JJJ1_YEAST	S397	YNL227C	1,01	0,82	0,82	0,89	1,13	1,22	1,34	FDSADESVKEKED	CK1;CK2;PLK;PLK1
JJJ1_YEAST	T504	YNL227C	0,77	0,76	0,83	0,78	0,76	0,75	0,93	GDKGLQTDDDEDW	CK2;FHA1 Rad53p
IWS1_YEAST	S89	YPR133C	2,11			2,74	1,49			HISTDFSDDDLEK	CK1;CK2
ITC1_YEAST	S332	YGL133W	1,26						1,26	NDSENNSSEEDKK	CK1;CK2
ITC1_YEAST	S333	YGL133W	1,26						1,26	DSENNSSEEDKKK	CK2
ISW1_YEAST	S846	YBR245C	3,59			3,59				AAYGDISDEEEKK	CK2
IST2_YEAST	S847	YBR086C	5,34			5,34				DNQSKVSVATEQT	AURORA;CK1
INP52_YEAST	S1005	YNL106C	0,59	0,55		0,59	0,59			PSSKLLSPTKEIS	CDK1;CDK2;CK1;Proline-directed
IFH1_YEAST	S972	YLR223C	0,73	0,62	0,73	0,73	0,63		1,22	RKNSTKSVGLDEI	CK1
IF5A2_YEAST	S2	YEL034W	1,23	1,19	1,22	1,19	1,23	1,23	1,28	_____MSDEEHTF	CK2
IF5A2_YEAST	T7	YEL034W	1,24				1,31	1,18		MSDEEHTFETADA	PLK1
IF4F2_YEAST	T196	YGL049C	1,93	1,93		4,37	1,93	1,86	4,66	PFEKEATPVLPAN	FHA2 Rad53p;Proline-directed
IF4F1_YEAST	S163	YGR162W	1,30	1,05	1,51	1,39	1,30		1,26	QERSTVSPQPESK	CK1;Proline-directed
IF4F1_YEAST	S195	YGR162W	2,46			2,46				NDSKASSEENISE	CK1
IF2B_YEAST	S2	YPL237W	1,76			1,76				_____MSSDLAAE	
IF2B_YEAST	S40	YPL237W	1,16	0,63	1,09	1,83	1,23	0,74	4,36	NGKENGSGDDLFA	CK2
IF2B_YEAST	S92	YPL237W	2,26	1,42	1,99	4,48	2,54	1,54	11,33	KKTKDSSVDAFEK	CK1;PLK1
IF2B_YEAST	S112	YPL237W	3,75	2,28	3,15	3,55	3,95	3,94	16,55	DNVDAESKEGTPS	
IBD2_YEAST	S106	YNL164C	1,36	0,88		1,36	1,44	0,76	2,69	SAYHIDSAEEKET	CK2
HXT2_YEAST	T29	YMR011W	4,49	7,67		3,84	4,49	5,53	2,16	IVQKLETDESPIQ	CHK1;FHA KAPP;PKD
HXT2_YEAST	S32	YMR011W	6,70	8,99		6,70	8,39	4,50	3,30	KLETDESPIQTKS	Proline-directed
HXT1_YEAST	S3	YHR094C	1,01			1,01	1,26		0,88	____MNSTPDLIS	CK2
HXT1_YEAST	S9	YHR094C	1,59			1,59				STPDLISPQKSNS	CDK1;CDK2;GSK3;Proline-directed
HXKG_YEAST	S2	YCL040W	5,15			5,15				_____MSFDDLHK	CK2

Uniprot Name	Phosphosite	Protein ID	Ratio Ctk1/wt MV	Ratio Ctk1/wt 1	Ratio Ctk1/wt 2	Ratio Ctk1/wt 3	Ratio Ctk1/wt 4	Ratio Ctk1/wt 5	Ratio Ctk1/wt 6	Sequence Window	Kinase Motifs Matching
HSL1_YEAST	S57	YKL101W	1,63			1,63				DATKRLSQPDSTV	CK1;CK2;GSK3;PKA
HPR1_YEAST	S673	YDR138W	0,48	0,48						KSQRINSASQTEG	CAMK2
HPC2_YEAST	S47	YBR215W	0,61				0,61			IKKETGSDSEDLF	CK2
HPC2_YEAST	S435	YBR215W	1,04			1,04				VAAPTVSPPKILQ	CDK1;CDK2;Proline-directed
HOSM_YEAST	S409	YDL131W	0,38						0,38	DFHAELSTPLLKP	
HOSM_YEAST	T410	YDL131W	0,72			1,05			0,38	FHAELSTPLLKPV	FHA2 Rad53p;Polo box;Proline-directed
HOS4_YEAST	T192	YIL112W	2,12			2,12				VLEKNTTEPENVE	CHK1;CK2;PKD
HOS3_YEAST	S629	YPL116W	2,35			3,44	1,25			KKGDEDSDHELKE	CK2
HFI1_YEAST	S6	YPL254W	0,99			0,99				_MSAIQSPAPKPL	CK1;Proline-directed
HFI1_YEAST	S387	YPL254W	1,49			1,49				GDISMSSITKAGE	CK1
HAS1_YEAST	S9	YMR290C	0,62	0,62						TPSNKRSRDSEST	CK1
HAS1_YEAST	S12	YMR290C	3,71			6,81		0,62		NKRSRDSESTEEP	CK1;PKA
H2A2_YEAST	S129	YBL003C	0,78		0,61	0,78			1,07	AKTAKASQEL___	CK1
H2A1_YEAST	S129	YDR225W	0,50	0,48				0,52		AKATKASQEL___	
H1_YEAST	S130	YPL127C	3,49	3,49	2,46	6,31	2,71		6,53	KKEKEVSPKPKQA	CDK1;Proline-directed
H1_YEAST	S174	YPL127C	2,73				2,70	2,73	6,50	TAKKASSPSSLTY	Polo box;Proline-directed
H1_YEAST	S176	YPL127C	3,77	2,91		4,63				KKASSPSSLTYKE	CK1
GPD1_YEAST	S24	YDL022W	0,84			1,10	0,58			GRKRSSSSVSLKA	CAMK2;PKA;PKA/AKT
GPD1_YEAST	S27	YDL022W	0,91			1,10	0,58	0,91		RSSSSVSLKAAEK	CK1
GNP1_YEAST	S111	YDR508C	1,64			1,54	1,74			PISTKDSSSQLDN	CK1
GNP1_YEAST	S113	YDR508C	1,21	1,17		1,25	1,50		1,17	STKDSSSQLDNEL	CK2
GIN4_YEAST	S930	YDR507C	1,44	1,10		1,44			2,40	ELRKQNSQEGDQA	CHK1;PKD
GFD1_YEAST	S106	YMR255W	3,53			3,53				QKATEISPPPVSP	Proline-directed
GFD1_YEAST	S111	YMR255W	1,84	0,72		2,75	0,93		3,63	ISPPPVSPSKMKT	CDK1;CDK2;ERK/MAPK;Proline-directed;WW GroupIV
GBLP_YEAST	S120	YMR116C	1,15	0,96	1,19	1,11	0,62	1,22	1,19	DIDKKASMIISGS	CHK1;GSK3;PKD
GBLP_YEAST	S166	YMR116C	1,26	1,12	1,29	1,19	1,28	1,24	1,39	EKADDDSVTIISA	PLK1
GBLP_YEAST	T168	YMR116C	1,37	1,29	1,43		1,50	1,28	1,37	ADDDSVTIISAGN	FHA KAPP
GAT1_YEAST	S288	YFL021W	4,83			4,83				ALKKIKSSTSVQS	CHK1;PKD
GAT1_YEAST	T369	YFL021W	3,82			3,82				KINNNITPPPSSS	Proline-directed
GAP1_YEAST	S5	YKR039W	0,84			0,84				__MSNTSSYEKNN	CK1;CK2
FUI1_YEAST	S4	YBL042C	0,74			0,42	1,05			___MPVSDSGFDN	
FUI1_YEAST	S12	YBL042C	0,51						0,51	SGFDNSSKTMKDD	
FMP42_YEAST	S269	YMR221C	0,91			0,91				RPQRRKSVLETYV	AURORA;AURORA-A;CAMK2;CK2;PKA
FKBP4_YEAST	S80	YLR449W	1,02				1,02			GLEEDESESEQEA	CK2
FKBP4_YEAST	S82	YLR449W	1,02				1,02			EEDESESEQEADV	CK2
FHL1_YEAST	S40	YPR104C	1,04			1,04				DQETKESITNSPT	AURORA;GSK3

Uniprot Name	Phosphosite	Protein ID	Ratio Ctk1/wt MV	Ratio Ctk1/wt 1	Ratio Ctk1/wt 2	Ratio Ctk1/wt 3	Ratio Ctk1/wt 4	Ratio Ctk1/wt 5	Ratio Ctk1/wt 6	Sequence Window	Kinase Motifs Matching
FHL1_YEAST	S44	YPR104C	0,88				0,88			KESITNSPTSEVP	CK1;Proline-directed
FCY2_YEAST	S18	YER056C	0,94	0,74		0,85	1,13	0,94	1,03	QDLEKRSPVIGSS	Proline-directed
FAS2_YEAST	S180	YPL231W	1,32	1,17		1,20	1,54		1,44	DLVGGKSTVQNEI	
FAS2_YEAST	S615	YPL231W	1,64			1,26	1,82	1,45	1,84	STKEVASLPNKST	
FAS2_YEAST	S958	YPL231W	1,40	1,61		1,20				EVRKAVSIETALE	CHK1;PKD
FAS2_YEAST	S1440	YPL231W	1,03	0,89		1,04		1,03	1,26	SSVKYASPNLNMK	Proline-directed
FAS1_YEAST	S1121	YKL182W	1,97			1,87	2,06			VDSSSVSEDSAVF	CK1
FAS1_YEAST	S1525	YKL182W	1,37	1,13		1,37	1,85			FLKRNGSTLEQKV	CAMK2;CHK1;CHK1/2;CK2;PKA;PKD
ESF2_YEAST	S47	YNR054C	1,02				1,02			KVEDIESENESDI	CK2;GSK3
ESF2_YEAST	S51	YNR054C	1,05				1,05			IESENESDIEEEQ	CK1;CK2
ESF1_YEAST	S86	YDR365C	0,83	0,64	0,83	1,35	1,14	0,82		AENDEDSEVNAKT	
ESF1_YEAST	S225	YDR365C	1,69			1,69				KTDDSDSDMDIGI	CK2
ERB1_YEAST	S20	YMR049C	1,34	0,94	1,41	1,28	1,44	0,86	2,25	SKKRAASEESDVE	CAMK2;PKA
ERB1_YEAST	S23	YMR049C	1,15	0,89	1,18	1,12	1,27	0,79	1,82	RAASEESDVEEDE	CK1;CK2
ERB1_YEAST	S72	YMR049C	1,15		1,36	0,94	1,55	0,76		KEAQDDSDDDSDA	CK2;GSK3
ERB1_YEAST	S76	YMR049C	1,15		1,36	0,94	1,41	0,76		DDSDDDSDAELNK	CK1;CK2
ERB1_YEAST	S149	YMR049C	0,91					0,91		VYDSDDSDAETQN	CK1;CK2
ERB1_YEAST	T153	YMR049C	0,91					0,91		DDSDAETQNTIGN	
ERB1_YEAST	S212	YMR049C	1,71				1,71	0,73	3,67	LDKNSGSSLNLTK	
ERB1_YEAST	S418	YMR049C	1,38			1,38	1,01		3,11	LIPELPSPKDLRP	CDK1;CK2;Proline-directed
EIF3J_YEAST	S65	YLR192C	3,88	3,23	3,46	4,60	4,29	3,25	8,30	KKGKESSADRALL	
EIF3J_YEAST	T162	YLR192C	1,80			2,41			1,19	ALTAAITPMNKKS	Proline-directed
EIF3B_YEAST	S61	YOR361C	1,79			2,10	1,48			VDDIDFSDLEEQY	CK2
EIF3A_YEAST	S504	YBR079C	6,66			6,66				IFASTASKEVSEE	CK1;GSK3
EIF3A_YEAST	S893	YBR079C	2,25			2,48	2,03			LPKATVSPDKAKL	CDK1;CDK2;Proline-directed
EIF2A_YEAST	S560	YGR054W	8,21			8,21				RRANKKSSETSPD	GSK3
EIF2A_YEAST	S564	YGR054W	2,69		2,30	4,27	2,69			KKSSETSPDSTPA	CK1;Proline-directed
EI2BG_YEAST	S296	YOR260W	0,80	0,60		0,57	0,99		1,13	LGPQSMSRQASFK	GSK3
EI2BE_YEAST	S435	YDR211W	1,00	1,00		0,98	1,39			NTKISASPLKNAG	CDK1;CDK2;Proline-directed
EFR3_YEAST	S771	YMR212C	1,23			1,20	1,26			ANEDLHSLSSRGK	
EFR3_YEAST	S773	YMR212C	1,07				1,07			EDLHSLSSRGKIF	
EFR3_YEAST	S774	YMR212C	1,14			1,20	1,07			DLHSLSSRGKIFS	CK1
EFG1P_YEAST	S29	YGR271C-A	2,20			2,20				SIGLTLSPDKDHE	CDK1;CDK2;NEK6;Proline-directed
EFG1P_YEAST	S41	YGR271C-A	1,56		1,00	1,84	1,28		2,31	EDGSQVSPTQDRK	CK1;Proline-directed
EDC1_YEAST	S82	YGL222C	0,62	0,64	0,59	0,64	0,68	0,45	0,49	FNQKKHSPPSSPS	GSK3;Proline-directed
EDC1_YEAST	S85	YGL222C	0,45		0,59			0,31		KKHSPPSSPSSTT	CK1;GSK3

Uniprot Name	Phosphosite	Protein ID	Ratio Ctk1/wt MV	Ratio Ctk1/wt 1	Ratio Ctk1/wt 2	Ratio Ctk1/wt 3	Ratio Ctk1/wt 4	Ratio Ctk1/wt 5	Ratio Ctk1/wt 6	Sequence Window	Kinase Motifs Matching
EDC1_YEAST	S86	YGL222C	0,55	0,64		0,57	0,54		0,49	KHSPPSSPSSTTT	CK1;ERK/MAPK;Polo box;Proline-directed;WW GroupIV
EDC1_YEAST	S117	YGL222C	0,22						0,22	DDTRLLSQNLKNL	CAMK2;CK1
EBP2_YEAST	S177	YKL172W	1,30	1,03	1,27	1,33	1,38	0,99	1,89	EQDVPLSDVEFDS	CK2
EBP2_YEAST	S183	YKL172W	1,27	1,03	1,27	1,26	1,38	0,99	1,96	SDVEFDSDADVVP	CK2
DRS1_YEAST	S208	YLL008W	2,20	1,71	2,05	2,34	2,75	1,84	3,67	IDEEDDSEEAKAD	
DPOA_YEAST	S170	YNL102W	1,21				1,21			RENLNSSPTSEFK	NEK6;Polo box;Proline-directed
DIG1_YEAST	S45	YPL049C	1,40			1,65	1,16			DSNIKNSPGGNSV	Proline-directed
DEP1_YEAST	S120	YAL013W	2,10			2,10				SKEEEKSQELEEA	
DBP9_YEAST	S356	YLR276C	1,11			1,07	1,15	0,87	2,06	ENQEEKSLEGEPE	PLK1
DBP4_YEAST	S692	YJL033W	1,69			1,69				AMEEEISGDEEEG	CK2
DBP10_YEAST	S101	YDL031W	0,94	0,83		0,94	1,05	0,76	1,56	FPMLEMSDDENNA	CK2;NEK6
DBP10_YEAST	S392	YDL031W	1,76						1,76	LQKLQNSNNEADS	CK2;NEK6
DBP10_YEAST	S398	YDL031W	1,30	0,85					1,76	SNNEADSDSDDEN	CK2
DBP10_YEAST	S400	YDL031W	1,30	0,85					1,76	NEADSDSDDENDR	CK2
CYC8_YEAST	S741	YBR112C	1,05			1,03	1,08			KKQKLNSPNSNIN	Proline-directed
CWC24_YEAST	S33	YLR323C	0,71	0,60		0,62	0,80		1,03	EEKLVASDEEKGS	CK2;NEK6
CUS1_YEAST	S114	YMR240C	1,38	1,37		1,38				ELEDTPSDGIEEH	
CSI2_YEAST	S330	YOL007C	0,89	0,89		0,83	1,05			KKYRPPSVHLDQL	CAMK2
COS6_YEAST	S16	YGR295C	2,85			2,85				KSVDVLSVKQLES	
COS5_YEAST	S16	YJR161C	3,07	2,76		2,33	3,38		3,68	KSVDVLSFKQLES	
CMS1_YEAST	S59	YLR003C	0,90	0,63	0,90	0,92	0,90	0,62	1,88	KKEERNSEDDSNR	CK2;GSK3;PKA
CIC1_YEAST	T11	YHR052W	0,70	0,75	0,64	0,66	0,99	0,67	0,72	SNSKKSTPVSTPS	FHA KAPP;Polo box;Proline-directed
CIC1_YEAST	T15	YHR052W	0,66				0,66			KSTPVSTPSKEKK	CDK1;CDK2;ERK/MAPK;Polo box;Proline-directed
CIC1_YEAST	S17	YHR052W	0,63	0,56	0,64	0,62	0,64	0,60	0,72	TPVSTPSKEKKKV	CK1
CIC1_YEAST	S357	YHR052W	2,16		0,75				3,58	NNAKKRSSSELEK	CK2
CIC1_YEAST	S358	YHR052W	7,03			7,03				NAKKRSSSELEKE	PKA
CIC1_YEAST	S359	YHR052W	0,66	0,55	0,66	0,63	0,83		1,03	AKKRSSSELEKES	CAMK2;CK2;PKA
CIC1_YEAST	S366	YHR052W	0,77		0,72	0,77	0,96	0,52	1,19	ELEKESSESEAVK	CHK1;CK2;PKD
CHS5_YEAST	S318	YLR330W	4,47			4,47				SPNDNESNPSEAK	
CHS5_YEAST	S579	YLR330W	3,18			3,18				SVAVEPSNEDVKP	CK2
CHS5_YEAST	S590	YLR330W	1,46			1,42	1,49			KPEEKGSEAEDDI	CK2
CF130_YEAST	S1042	YGR134W	1,17			1,17				LNAKPASELNLKL	
CDC45_YEAST	T453	YLR103C	1,67			1,67				NDNNDDTDGEEEE	CK2
CDC28_YEAST	Y19	YBR160W	1,76			1,76				KVGEGTYGVVYKA	ALK
CDC15_YEAST	S309	YAR019C	1,53			1,86	1,20			EEKLNISPSKFSL	CDK1;CDK2;NEK6;Proline-directed
CBF5_YEAST	T378	YLR175W	2,44	2,00		2,56	2,31		2,65	GRVNENTPEQWKK	Proline-directed

Uniprot Name	Phosphosite	Protein ID	Ratio Ctk1/wt MV	Ratio Ctk1/wt 1	Ratio Ctk1/wt 2	Ratio Ctk1/wt 3	Ratio Ctk1/wt 4	Ratio Ctk1/wt 5	Ratio Ctk1/wt 6	Sequence Window	Kinase Motifs Matching
CBF5_YEAST	S399	YLR175W	0,42					0,42		EQSTSSSQETKET	CK1
CBF5_YEAST	S416	YLR175W	1,55	0,97	1,22	1,70	1,55		2,86	KKAKEDSLIKEVE	PLK1
CBF5_YEAST	T423	YLR175W	0,55	0,32	0,38	0,59	0,55		0,69	LIKEVETEKEEVK	CK2
CASP_YEAST	S364	YKL179C	1,83			1,83	1,51		2,13	GVNEDDSDNDIRS	CK2
BUR1_YEAST	S417	YPR161C	0,77	0,62	0,73	0,95	0,77		1,31	IVEKGESPVVKNL	CHK1;PKD;Proline-directed
BUD3_YEAST	S10	YCL014W	2,78			2,78				DLSSLYSEKKDKE	CK1
BUD3_YEAST	S903	YCL014W	1,30	1,12			1,48			PKRAVVSSPKIKK	
BUD3_YEAST	S904	YCL014W	1,48	1,12		2,28	1,48			KRAVVSSPKIKKK	CDK1;ERK/MAPK;Polo box;Proline-directed
BUD3_YEAST	T1157	YCL014W	3,84			3,84				QASKVLTENSNEL	FHA KAPP
BUD3_YEAST	S1160	YCL014W	2,03	1,62		2,03	4,66			KVLTENSNELKDT	
BUD3_YEAST	S1183	YCL014W	2,85			2,85				KLGDDYSDKETAK	CK2
BUD3_YEAST	S1501	YCL014W	2,01			1,74	2,28			ISSDLSSNKTVLG	CK1
BUD22_YEAST	S285	YMR014W	0,87	0,85			1,27	0,87		SNKETTSDNEDLL	CK2
BUD21_YEAST	S144	YOR078W	1,45	1,17	1,44	1,61	1,45	1,27	2,63	FDKLDESDENEEA	NEK6
BUD2_YEAST	S854	YKL092C	4,88			4,88				DKKDLDSPIEVKP	CK2;Proline-directed
BRX1_YEAST	S285	YOL077C	2,31	1,98		2,60	2,31			LAADPLSNDALFK	
BRR2_YEAST	S403	YER172C	0,77			0,77	1,20	0,76		SKRELDSGDDQPQ	CK2
BRL1_YEAST	S397	YHR036W	1,83						1,83	FGDIINSFIDPLN	CK2
BRE5_YEAST	S176	YNR051C	1,09				1,09			DKIRHESGVEKEK	CAMK2;CK2;PIM1/2
BRE5_YEAST	S187	YNR051C	3,00	2,84		5,06	3,15	1,36		EKEKEKSPEISKP	GSK3;Proline-directed
BRE5_YEAST	S282	YNR051C	5,40			5,40				IKTKEGSVEAINA	CK1;PLK1
BRE5_YEAST	S398	YNR051C	2,92			1,45	4,39			NRRDNASANSKNK	
BOI2_YEAST	S519	YER114C	2,31			3,42	1,20			GGGKALSPIPSPT	GSK3;Proline-directed
BOI2_YEAST	S523	YER114C	2,31			3,42	1,20			ALSPIPSPTRNSV	CDK1;CDK2;CK1;Proline-directed
BOB1_YEAST	S209	YBL085W	1,18			1,30	1,07			SNISTKSLEPSSE	CK1;GSK3
BOB1_YEAST	S655	YBL085W	1,85			1,85				PLKTSLSPINSKS	GSK3;Proline-directed
BMS1_YEAST	S578	YPL217C	1,34	1,24	1,42	1,28	1,39	1,15	2,07	DDSKDESDIEEDV	CK1;CK2
BFR2_YEAST	S44	YDR299W	1,12			1,12				NGESDLSDYGNSN	CK1
BFR2_YEAST	S379	YDR299W	1,66	1,16	1,73	2,17	1,59	1,14	3,53	VDDNENSDDGLDI	
BFR1_YEAST	S260	YOR198C	2,06	2,24		2,22	1,90	1,63		EEEQRLSKLLEQK	PKA
BFR1_YEAST	T336	YOR198C	1,80				1,80			DDLVLVTPKKDDF	CDK1;CDK2;Proline-directed
BEM2_YEAST	S141	YER155C	3,21			3,21				NSSSQKSNAQDET	CK1
BEM1_YEAST	S458	YBR200W	1,83			2,82	0,84			KLNKKLSDLSLSG	CHK1;PKD
BBP_YEAST	S95	YLR116W	0,78	0,74		0,97	0,83	0,73		RKNRSPSPPPVYD	14-3-3 binding;CAMK2;Proline-directed
BBC1_YEAST	S103	YJL020C	0,97				0,97			DLPEPISPETKKE	ERK/MAPK;Proline-directed;WW GroupIV
BAP2_YEAST	S3	YBR068C	4,24			4,24				_____MLSSEDFGS	CK2

Uniprot Name	Phosphosite	Protein ID	Ratio Ctk1/wt MV	Ratio Ctk1/wt 1	Ratio Ctk1/wt 2	Ratio Ctk1/wt 3	Ratio Ctk1/wt 4	Ratio Ctk1/wt 5	Ratio Ctk1/wt 6	Sequence Window	Kinase Motifs Matching
BAP2_YEAST	S4	YBR068C	3,04				3,04			___MLSSEDFGSS	
BAP2_YEAST	S9	YBR068C	2,32			2,04	2,61			SSEDFGSSGKKET	
AVT1_YEAST	S8	YJR001W	1,33				1,33			PEQEPLSPNGRKR	ERK/MAPK;Proline-directed;WW GroupIV
ATN5_YEAST	S516	YDR038C	2,88			2,88				NENDQSSLSQHNE	
ATC3_YEAST	T7	YAL026C	1,85	1,35		2,37	1,56		2,15	MNDDRETPPKRKP	CDK1;CDK2;PKA;Proline-directed
ASK1_YEAST	S250	YKL052C	0,42			0,42				SNNIESSPLKQGH	CDK1;CDK2;Polo box;Proline-directed
ARE2_YEAST	S175	YNR019W	1,93			1,11	1,93		2,73	NLHHRKSSPDAVD	CK2;PKA
ARE1_YEAST	S21	YCR048W	1,36	1,50		1,21				KIRRLNSAEANKR	CAMK2;CHK1;PKD
ARB1_YEAST	S43	YER036C	0,93			0,92	0,95			EAAAEESEVDAAA	CK2
APN1_YEAST	S297	YKL114C	2,42			2,42				EWLESKSESELLE	CK2
AP3D_YEAST	S918	YPL195W	7,39						7,39	KTKAKNSPEPNEF	Proline-directed
AMPM2_YEAST	T2	YBL091C	0,73	0,59	0,80	0,70	0,73	0,72	0,94	_____MTDAEIEN	CK2
AMPM2_YEAST	S9	YBL091C	1,12	1,13	1,12	1,04	1,12	1,09		DAEIENSPASDLK	Proline-directed
AMPM2_YEAST	S35	YBL091C	1,04	0,87	1,07	1,04	1,04	0,91	1,39	QAKADESDPVESK	
AIR2_YEAST	T16	YDL175C	0,79	0,71			0,86	0,72	1,69	VDTAPTTPPDKLV	CK2;ERK/MAPK;FHA1 Rad53p;Proline-directed;WW GroupIV
AIR1_YEAST	S2	YIL079C	0,73				0,73			_____MSTLLSEV	GSK3
AIR1_YEAST	S6	YIL079C	0,50			0,56			0,44	_MSTLLSEVESID	CK1;CK2;GSK3
AIR1_YEAST	T21	YIL079C	1,73	1,66	1,67	2,07	1,80	1,53	2,44	PYVKDTTPTGSDS	Proline-directed
AGP1_YEAST	S6	YCL025C	0,53				0,57	0,51	0,53	_MSSSKSLYELKD	CK1;CK2
AGP1_YEAST	S101	YCL025C	1,11	0,63	0,57	1,32	1,11		1,35	ELEKNESSDNIGA	CHK1;PKD
ADR1_YEAST	S212	YDR216W	6,11			6,11				NTRRKASPEANVK	CAMK2;PKA;Proline-directed
ADR1_YEAST	T259	YDR216W	8,22	4,60		11,32	5,12		12,03	DRVKFSTPELVPL	FHA2 Rad53p;Polo box;Proline-directed
ACF4_YEAST	S44	YJR083C	1,83	1,82		1,83	2,49			VQPESKSPRVTTP	CDK1;Proline-directed
ACF4_YEAST	T49	YJR083C	1,83	1,82		1,83	2,49			KSPRVTTPLKPKR	CAMK2;CDK1;CDK2;ERK/MAPK;Proline-directed
ACE2_YEAST	S709	YLR131C	1,42			1,82	1,01			KKSLLDSPHDTSP	CK1;CK2;NEK6;Proline-directed
ACE2_YEAST	T713	YLR131C	3,13			4,90	1,35			LDSPHDTSPVKET	
ACE2_YEAST	S714	YLR131C	4,90			4,90				DSPHDTSPVKETI	CDK1;CDK2;Proline-directed
ACAC_YEAST	S2	YNR016C	0,71			0,71				_____MSEESLFE	
ACAC_YEAST	S10	YNR016C	0,75					0,75		ESLFESSPQKMEY	CDK1;CDK2;Polo box;Proline-directed

*MV – mean value